

Oji International
Conference on
Spin Chemistry

Spin Polarization and Magnetic Field Effects
in Photochemical Reactions

Abstract

Y. Fujiwara

July 15~18, 1991

Tomakomai, Japan

Organization

CONFERENCE ORGANIZER

Yasumasa J. I'Haya
University of Electro-Communications

ORGANIZING COMMITTEE

Saburo Nagakura	(Yokohama)	Honorary Chairman
Yasumasa J. I'Haya	(Tokyo)	Chairman
Hisaharu Hayashi	(Wako)	Secretary
Jiro Higuchi	(Yokohama)	
Noboru Hirota	(Kyoto)	
Yusaku Ikegami	(Sendai)	
Keiji Kuwata	(Osaka)	
Kin-ichi Obi	(Tokyo)	
Yoshifumi Tanimoto	(Hiroshima)	
Hiroshi Yoshida	(Sapporo)	

SPONSORS

The Japan Society for the Promotion of Science
The Fujihara Foundation of Science

July 14 (Sunday)

- 15:00~20:00 **Registration** (Front)
18:00~20:00 **Reception** (Aoi Room)

July 15 (Monday)

- 9:00~ 9:30 **Opening Session** (Wakakusa Room)
presided by H. Hayashi (Inst. Phys. Chem. Res.)
Welcome Address Y. J. I'Haya, Organizer
Address G. L. Closs (Chicago)
- Theoretical and experimental aspects of spin polarization*
presided by P. W. Atkins (Oxford Univ.)
- 9:30~10:15 Mo-1 F. J. Adrian (Johns Hopkins Univ.)
Theoretical aspects of chemically induced magnetic polarization
- 10:30~11:15 Mo-2 K. A. McLauchlan (Oxford Univ.)
Departures from simple CIDEP behavior
- 11:30~13:30 **Lunch Break**

presided by K. Obi (Tokyo Inst. Tech.)
- 13:30~14:00 Mo-3 R. W. Fessenden (Univ. of Notre Dame)
CIDEP in the photolysis of benzoic acid derivatives
- 14:15~14:45 Mo-4 H. Paul (Zurich Univ.)
Electron spin polarization by a radical-triplet pair mechanism
- 15:00~15:20 Mo-5 H. Murai (Osaka Univ.)
Formation mechanism of spin polarized solvated electron in photoionization
- 15:30~16:00 **Coffee Break**

presided by Y. Ikegami (Tohoku Univ.)
- 16:00~16:30 Mo-6 J. B. Pedersen (Odense Univ.)
Diffusional aspects of CIDNP and CIDEP
- 16:45~17:15 Mo-7 R. Z. Sagdeev (Inst. Chem. Kinet. Comb.)
Stimulated nuclear polarization and related phenomena

- 17:30~17:50 Mo-8 M. Terazima (Kyoto Univ.)
CIDEP measurement in the L band microwave frequency region

- 18:00~20:00 **Dinner**

- 20:00~22:00 **Poster Session A** (Wakakusa Room)

Triplet states and polarization transfer

- (A1) K. Akiyama, S. Tero-Kubota, and Y. Ikegami (Tohoku Univ.)
Spin polarization transfer during the intramolecular triplet-triplet energy transfer in a rigid matrix as studied by time-resolved EPR spectroscopy.
- (A2) T. Ikoma, K. Akiyama, S. Tero-Kubota, and Y. Ikegami (Tohoku Univ.)
Time-resolved EPR studies on the excited triplet states of non phosphorescent troponoid compounds.
- (A3) K. Obi and A. Kawai (Tokyo Inst. Tech.)
Electron spin polarization generated in singlet-doublet and triplet-doublet systems.
- (A4) S. Tero-Kubota, T. Noguchi, K. Akiyama, and Y. Ikegami (Tohoku Univ.)
Time-resolved EPR studies on the short-lived triplet states generated from the intramolecular proton transfer.

Chemical reactions studied by magnetic resonance

- (A5) T. Aizawa, T. Sakata, K. Maeda, and T. Azumi (Tohoku Univ.)
Effect of Coulomb force on diffusion as studied by CIDNP intensities of photo-induced electron transfer reactions of *trans*-stilbene.
- (A6) H. Hayashi, M. Igarashi, Y. Sakaguchi (Inst. Chem. Phys. Res.), and Y. J. I'Haya (Univ. Elect. Comm.)
Formation of novel radicals from the $\pi\pi^*$ triplet states of aromatic ketones.
- (A7) K. Maeda, N. Suzuki, Q. X. Meng, K. Suzuki, M. Terazima, T. Azumi (Tohoku Univ.), and Y. Tanimoto (Hiroshima Univ.)
CIDNP and CIDEP studies on intramolecular hydrogen abstraction reaction of polymethylene linked system.
- (A8) K. Makino, A. Hagi, H. Ide, A. Murakami (Kyoto Inst. Tech.), and M. Nishi (Setsunan Univ.)
On the formation of aminoxyl radicals from 5,5-dimethyl-1-pyrroline-*N*-oxide and implications to its biological applications.
- (A9) M. Mukai, S. Yamauchi, and N. Hirota (Kyoto Univ.)
CIDEP of benzil.

(A10) H. Murai, Hidekazu Honma, Natsuo Ishiwata, and Keiji Kuwata (Osaka Univ.)

Investigation of novel radical pair interaction: ionic system and micellar system.

(A11) N. Suzuki, K. Maeda, Q.-X. Meng, K. Suzuki, M. Terazima, and T. Azumi (Tohoku Univ.)

Temperature dependence of the magnetic field effect of the CIDNP in the photocleavage of cycloalkanone.

(A12) M. Wakasa, M. Igarashi, Y. Sakaguchi, and H. Hayashi (Inst. Phys. Chem. Res.)

Photo-induced electron transfer reaction between hexamethyldisilane and quinones as studied by CIDNP technique.

July 16 (Tuesday)

Theoretical and experimental aspects of spin polarization

presided by N. Hirota (Kyoto Univ.)

9:00~9:45 Tu-1 G. L. Closs (Univ. of Chicago)

EPR spectroscopy of biradical in liquid solution

10:00~10:30 Tu-2 K. M. Salikhov (Kazan Phys. Tech. Inst.)

Quantum beating of ESR line intensities of spin-correlated radical pairs

10:45~11:15 Tu-3 T. Azumi (Tohoku Univ.)

Determination of the enhancement factor of CIDNP in the photochemical α -cleavage of ketones

11:30~13:30 **Lunch Break**

Magnetic field effects on chemical reactions

presided by U. E. Steiner (Konstanz Univ.)

13:30~14:15 Tu-4 S. Nagakura (Grad. Univ. for Adv. Stud.)

Magnetic field effects on photophysical and photochemical processes of excited molecules

14:30~14:50 Tu-5 M. M. Triebel (Inst. Energetic Prob. of Chem. Phys.)

Phase shift of the magnetic field effects in luminol chemiluminescence in water solution as the new method of intermediate species lifetime determination

15:00~15:20 Tu-6 Y. Tanimoto (Hiroshima Univ.)

Temperature dependence of lifetime of chain-linked biradicals in the absence and presence of a magnetic field

15:30~16:00 **Coffee Break**

presided by K. A. McLauchlan (Oxford Univ.)

16:00~16:30 Tu-7 U. E. Steiner (Konstanz Univ.)

Mechanism of spin-orbit coupling dependent magnetic field effects in chemical kinetics

16:45~17:15 Tu-8 A. I. Shushin (Inst. Chem. Phys.)

Recent theory of magnetic effects in radical pair recombination in viscous solution

17:30~17:50 Tu-9 Y. Sakaguchi (Inst. Phys. Chem. Res.)

Paramagnetic ion quenching of the magnetic field effect in the photochemical reaction of naphthoquinone in micelles

18:00~20:00 **Dinner**

20:00~22:00 **Poster Session B** (Wakakusa Room)

Magnetic field effects on chemical reactions

(B1) Y. Kuriyama, T. Arai, H. Sakuragi, and K. Tokumaru (Univ. of Tsukuba)

Heavy atom effect on magnetic field effect on isomerization of stilbene.

(B2) T. Matsuo, H. Nakamura, and H. Yonemura (Kyushu Univ.)

Magnetic field effects in photoinduced electron-transfer in phenothiazine-viologen systems.

(B3) T. Matsuo, H. Nakamura, and H. Yonemura (Kyushu Univ.)

Magnetic field effects in photoinduced electron-transfer in porphyrin-viologen systems.

(B4) R. Nakagaki (Kanazawa Univ.)

External magnetic field effects on bichromophoric photochemistry.

(B5) H. Ohnishi, H. Sasaki, and M. Ipponmatsu (Osaka Gas Co. Ltd.)

External magnetic field effect on the H_2 - O_2 reaction on SnO_2 surface.

(B6) H. Sakuragi, K. Naitoh, T. Oguchi, T. Arai, K. Tokumaru (Univ. of Tsukuba), R. Nakagaki, and S. Nagakura (Inst. Mol. Sci.)

Solvent dependence of magnetic field effects on photoisomerization of a butenyl naphthalene in the presence of electron acceptor.

(B7) Y. Tanimoto, Y. Fujiwara, A. Saegusa, and M. Hayashi (Hiroshima Univ.)

Laser flash photolysis studies of magnetic field effects on the bifunctional chain molecules containing benzophenone and *N,N*-diethylaniline.

Pulse techniques and ODESR

- (B8) T. Ichikawa and H. Yoshida (Hokkaido Univ.)
Application of pulsed EPR spectroscopy to the study of radical reactions.
- (B9) V. Kurshev and T. Ichikawa (Hokkaido Univ.)
Effect of electron spin diffusion on electron spin echo decay.
- (B10) Y. Ohba, Y. Yoshida, and M. Iwaizumi (Tohoku Univ.)
ESEEM of copper (II) complexes coordinated by imidazole containing ligands.
- (B11) Y. Tai, M. Okazaki, and K. Toriyama (Govt. Indus. Res. Inst. Nagoya)
An ODESR study on charge recombination process in polymers.
- (B12) M. Yagi (Yokohama Natl. Univ.), B. D. Schlyer, and A. H. Maki (Univ. Calif. Davis)
EPR and ODMR studies of the phosphorescent states of *trans*-2,2'-bipyridine, metal-free *cis*-2,2'-bipyridine and [Zn(bpy)]²⁺

July 17 (Wednesday)

Magnetic field effects on chemical reactions

presided by J. Higuchi (Yokohama Natl. Univ.)

- 9:00~ 9:30 We-1 O. A. Anisimov (Inst. Chem. Kinet. Comb.)
Spin dependent phenomena in radical spur recombination
- 9:45~10:15 We-2 P. Levin (Inst. Chem. Phys.)
Magnetic field effects on the decay kinetics of triplet radical pairs in homogeneous and organized systems.
- 10:30~11:00 We-3 M. Chowdhury (Indian Association for Cult. Sci.)
Magnetic field effect on exciplex luminescence
- 11:15~11:30 **Photograph**
- 11:30~13:00 **Lunch Break**
- 13:30~17:30 **Excursion**
- 19:00~21:00 **Banquet** (Botan Room)
after dinner talk P. W. Atkins (Oxford Univ.)

July 18 (Thursday)

Novel instrumentation in the time domain electron and nuclear spin resonance experiments

presided by H. Yoshida (Hokkaido Univ.)

- 9:00~ 9:30 Th-1 L. Kevan (Univ. Houston)
Application of electron spin echo spectroscopy to location control of electron donors in photoinduced charge separation across vesicle, micelle and reverse micelle interfaces
- 9:45~10:15 Th-2 K. P. Dinse (Univ. Dortmund)
New aspects of photo-induced electron reactions studied by FT-EPR
- 10:30~10:50 Th-3 K. Kuwata (Osaka Univ.)
Pulsed ESR study on electron spin relaxation of free radical intermediates in photoreduction
- 11:00~11:20 Th-4 M. Okazaki (Gov. Indus. Res. Inst. Nagoya)
An application of spin trapping to the study of magnetic field dependent chemical reactions
- 11:30~13:30 **Lunch Break**
- presided by J. R. Norris (Argonne Natl. Lab.)
- 13:30~13:50 Th-5 Yu. N. Molin (Inst. Chem. Kinet. Combs.)
Electron spin echo study of cross relaxation in free radicals with CIDEP
- Biological applications*
- 14:00~14:45 Th-6 A. J. Hoff (Leiden Univ.)
Spin-polarization in photosynthetic reaction center: Applications of ESE to unravel polarized EPR spectra
- 15:00~15:20 Th-7 S. Yamauchi (Tohoku Univ.)
CIDEP studies on the photoinduced electron transfer reactions from metalloporphyrins to quinone
- 15:30~16:00 **Coffee Break**
- presided by A. J. Hoff (Leiden Univ.)
- 16:00~16:30 Th-8 P. J. Hore (Oxford Univ.)
Electron spin polarization in photosynthetic bacteria
- 16:45~17:15 Th-9 J. R. Norris (Argonne Natl. Lab.)
The role of spin chemistry in the primary events of photosynthesis
- presided by H. Hayashi (Inst. Phys. Chem. Res.)
- 17:30~ **Closing Address** F. J. Adrian (Johns Hopkins Univ.)

Mo-1

9:30

~10:15

Theoretical Aspects of Chemically Induced Magnetic Polarization

Frank J. Adrian

Applied Physics Laboratory, The Johns Hopkins University

Laurel, Maryland 20723, USA

Recent experimental advances in high energy, pulsed, excimer lasers operating at photochemically important wavelengths, and in time-resolved detection of transient paramagnetic species by pulsed and direct-detection electron spin resonance (ESR) spectrometers, offer exciting new possibilities for investigating the reaction dynamics of rapid chemical reactions involving free radical intermediates. Of special interest are those reactions involving electron-spin-dependent processes with consequent magnetic-field-dependent effects, of which chemically induced electron spin polarization (CIDEP) of the radical intermediates is arguably the most striking and informative. Since the interpretation of these experiments usually involves determining the parameters of a theoretical model from the experimental data, it is likely that refinement of various aspects of these models will be helpful in realizing the full capabilities of the new experimental techniques. This talk will review some of the more important theoretical problems arising in fast photochemically-induced reactions, with emphasis on CIDEP mechanisms, and will suggest some approaches to them.

The CIDEP mechanisms themselves are obviously important, but there are also significant problems connected with the kinetics of the polarization-producing reactions. Polarization-destroying processes such as radical recombination, spin exchange, and spin-lattice relaxation are of special interest because they not only play a role in determining the conditions under which the polarizations can be observed, but it is often possible to determine their rates from the observed polarization decay. However, these rate determinations are complicated by the fact that these processes have quite similar effects on some polarizations but dissimilar effects on others. For example, bimolecular radical recombination, spin exchange, and spin-lattice relaxation all reduce the spin-segregation

or "entropy" type polarization produced by the $S-T_0$ mixing part of the Radical Pair Mechanism (RPM), but only relaxation, and possibly bimolecular reaction of different radicals, affect the absolute polarization produced by the Triplet Mechanism (TM) or the $S-T_{-}$ mixing part of the RPM.

Kinetic models involving simple radicals such as the H atom (i.e., a single, spin 1/2, magnetic nucleus) adequately illustrate the key problems and suggest useful approximations without the complications posed by multinuclear radicals. One such approximation for treating the combined effects of bimolecular recombination and spin exchange is to use the theoretical result that spin-exchange is composed of a short-range part, which is approximately the same as the bimolecular reaction rate except that spin exchange acts directly on the $S-T_0$ polarization whereas the reactive process acts indirectly by removing the singlet component of the pair, and a long-range part which is obtained by solution of the Stochastic-Liouville equation for spin evolution of a diffusing, fully-polarized, radical pair at a given initial separation [1,2]. The correct weight factors for these spin exchange terms, which is the subject of some confusion, are obtained by recognizing that the short-range spin-exchange term affects only those radicals which survive the reactive encounter, whereas the long-range spin-exchange term affects all encountering pairs. The random, or F-pair, $S-T_0$ polarization process also results from these short range encounters; its effect is to favor one of the two otherwise equally likely spin distributions resulting from the spin-exchange part of the encounter.

Another useful simplification is to assume pure electron spin-lattice relaxation (no accompanying nuclear spin transitions) with equal rates for the longitudinal and transverse processes (i.e., $T_1=T_2$). This assumption usually is valid if the dominant spin relaxation mechanism is spin-rotation, as found experimentally for many small free radicals [3]. Whether spin-rotation relaxation is dominant in a particular system may be ascertained by using the Curl relation $\gamma=-2A\Delta g/\hbar$ [4] to estimate the spin-rotation interaction (γ) from the electron g-factor shift (Δg) and the rotational constant (A), and estimating the rotational angular momentum correlation time (τ_N) from the rotational correlation time (τ_2) by the relation $\tau_N\tau_2=I/6kT$ [5], where I is the moment of inertia and τ_2 is calculated

using a slipping model of rotational diffusion [6] rather than the commonly used sticking model. Usually, $\omega_Z \tau_N \ll 1$, where ω_Z is the Zeeman energy, so that $T_1 = T_2$.

The $S-T_0$ and $S-T_-$ radical pair polarization processes, and other level-crossing processes like $S-T_+$, may be qualitatively envisioned by vector models which give considerable insight into the physical factors involved in these processes and the time scales involved [7,8]. More quantitative treatments require solution of the Stochastic-Liouville equation, in which the diffusion of the radicals determines the time dependence of the separation-dependent exchange interaction that combines with the internal magnetic interactions of the radicals to produce the polarized electron spin states of the pair [9]. A particularly promising approach to solutions of this equation lies in the application of various Green's-function techniques. Sushin has recently obtained analytic formulas for $S-T_0$ CIDEP and other effects over a wide range of conditions by dividing the problem into regions of strong and weak exchange [10]. An earlier treatment by Monchick and Adrian yielded single integral equations for both $S-T_0$ [7] and $S-T_-$ [8] radical pair CIDEP. Although the $S-T_0$ equation can be solved only under limited conditions, it is also useful for obtaining a qualitative picture of the CIDEP process, and its range of solvability can be extended by variational techniques [11]. Some applications of this equation are: Estimating the rate at which $S-T_0$ CIDEP develops and CIDEP in a confined region such as a micelle.

A Monte-Carlo calculation of $S-T_0$ CIDEP will be described in which the diffusive evolution of the radical pair, and the corresponding spin evolution under the resulting exchange and magnetic interactions, is determined by a computer-generated random number sequence. The polarization for a given set of exchange and magnetic parameters is the average over a large number of runs, typically 10^4 , which required run times of 15 to 45 min on a 25 MHz, 386 personal computer. Within the rather larger error limits indicated by their standard deviations the results generally agree with other numerical calculations and analytic formulas. It remains, however, to examine possible dependences on diffusion step length which presently is approximately 1 Å in the strong to moderate exchange region and 4 Å outside this region. Although a considerably larger, albeit computationally

feasible, number of runs (at least 10^6) would be required to reduce the error to the point where the calculated $S-T_0$ polarizations are more semiquantitative, it should be noted that $S-T_0$ CIDEP in an unrestricted three-dimensional environment is an especially challenging case because this polarization is the small difference between relative large positive and negative polarizations produced by different diffusive trajectories. In this case the method is probably more useful as another way of visualizing the polarization process than for quantitative calculation. The method may, however, be useful for more complex cases where analytic treatments are harder, especially in situations where the polarization or other magnetic field effect always has the same sign. Possible applications are diffusion in confined systems or in solids, or situations where the time evolution of the phenomena is important.

References.

- [1] F. J. Adrian, J. Chem. Phys. 88, 3216 (1988).
- [2] A. I. Sushin, Chem. Phys. 144, 223 (1990).
- [3] D. M. Bartels, R. G. Lawler, and A. D. Trifunac, J. Chem. Phys. 83, 2686 (1985).
- [4] R. F. Curl, Mol. Phys. 9, 585, (1965).
- [5] G. Nyberg, Mol. Phys. 12, 69 (1967).
- [6] C.-M. Hu and R. Zwanzig, J. Chem. Phys. 60, 4354 (1974).
- [7] L. Monchick and F. J. Adrian, J. Chem. Phys. 68, 4376 (1978)
- [8] F. J. Adrian and L. Monchick, J. Chem. Phys. 71, 2600 (1979); J. Chem. Phys. 72, 5786 (1980).
- [9] J. H. Freed and J. B. Pedersen, in *Advances in Magnetic Resonance*, edited by J. S. Waugh (Academic, New York, 1975), Vol. 8.
- [10] A. I. Sushin, Chem. Phys. 144, 201 (1990).
- [11] F. J. Adrian, Chem. Phys. Letters 80, 106 (1981).

Mo-2

10:30

~11:15

Departures from simple CIDEP behaviour.

K.A. McLauchlan, N.J.K. Simpson and P.D. Smith.

Physical Chemistry Laboratory, South Parks Rd.,

Oxford OX1 3QZ, U.K.

It has long been apparent that at least two different processes contribute to the polarization observed in the spectra of small free radicals in low-viscosity solutions. This led to the recognition of the radical pair mechanism (RPM) and of the triplet mechanism (TM), and spectra could be reproduced by adding contributions from the two different sources of polarization in empirically-adjusted proportions [1,2]. There has been little questioning of whether the polarization origins are correctly attributed. The operation of the TM has rarely been demonstrated in an unequivocal fashion, for the interpretations of experimental spectra show only that they can be reproduced by addition of a calculated RPM pattern to another with no hyperfine intensity distortion.

The TM was first thought to be an unlikely source of spin polarization in the liquid state [3], but this was overcome by the recognition of the rôle of rapid triplet reaction [4]. There seems little doubt that emissive single-phase, hyperfine-undistorted, polarisation does have this origin. Other sources of absorptive single phase hyperfine-independent contributions come from reaction of equilibrated triplets [5] and from radicals which have undergone rapid relaxation. There is some evidence that these are inadequate to account for all observations.

Firstly, we review the evidence that the TM exists at all. Most spectra reported wholly in one phase (emission), and without hyperfine intensity distortion, are from radical ions. It was a puzzle why these did not also exhibit a RPM contribution, but this was understood by the realisation that this was averaged out over the ensemble by degenerate electron exchange processes involving the parent molecule [6]. Undistorted spectra from neutral radicals may indicate that radical-ions are involved in the reaction pathway. It has not been demonstrated directly that the TM occurs, and it is possible that the chemistry of the systems is not sufficiently well established to conclude that the source of polarization is

not the RPM, originating between radicals of different g -value, and re-distributed by electron exchange. It is likely, however that the TM is the source of the polarization, but no attention has been given to why the signals are unusually strong; no accurate method for measuring the magnitude of polarization yet exists.

Direct evidence that the TM does occur was first obtained from observations of radicals formed from by hydrogen addition to nitrogen heterocyclics, which exhibit intensity-distorted spectra demonstrating the occurrence of both polarization processes. The sense of the single phase contribution was shown to be predictable from the group theoretical arguments applied to the inter-system crossing step in the triplet, and to vary as both the symmetry [7] and the sign of the zero-field coupling constant [8] was varied. An suggestion that the operation of the TM could be demonstrated by producing radicals by photolysis with plane-polarized light [9] was shown, to yield effects below the detection level for a variety of systems [10], despite some initial claims to the contrary [11]. Finally, recent Fourier-transform experiments have demonstrated the growth of the single phase polarization in real time, and it correlates with polarization via the triplet mechanism [12]. Nevertheless, it is remarkable that so long after the mechanism was proposed, its theory has not been verified in any detail.

The phase of the single-phase contribution to the CIDEP spectrum has been used to determine the sign of the zero-field coupling constant in the triplet states of aliphatic and aromatic ketones, for all non-cyclic ones yield radicals which exhibit mixed polarization behaviour [13,14]. It is well known, for instance, that the ketyl radical formed by photolysis of acetone in propan-2-ol, in a symmetric radical pair, exhibits a spectrum with excess absorption. We remarked some years ago [15] that it seemed unlikely that this originated in the TM, due to the rate of hydrogen abstraction being too low for radical formation to compete with relaxation in the triplet. Further evidence will be presented to show that this is indeed so. In the reaction with tri-ethylamine, the radicals are formed largely (perhaps predominantly) via a singlet route, yet the single-phase absorptive contribution is as evident as ever [16]. Direct observation of the polarised triplet of acetone showed it to be emissively, not absorptively, polarised [17]. A recent Fourier transform study of the

deuterated species has shown independently and unequivocally that the single-phase signal does not arise from the TM [18]. It was said rather to arise in the reaction of equilibrated triplet. This explanation appears inconsistent with our own results and leads to values of various rate constants which are incompatible with their literature values [19]. It seems therefore, that the single-phase contribution does not arise from the reaction of either spin-polarised or spin-equilibrated triplet. It appears to be a property more of the polarised radical itself than of the way it is produced. We are unable at present to suggest any convincing origin for it.

The common appearance of CIDEP spectra is for them to be in one phase at low field, and in the other phase at high. We now turn to situations in which the appearance of the spectrum differs from this standard form, whilst still dealing with effects due to the mixing of only the S and T₀ levels of the radical pair. There are three separate situations known in which the smooth progression, for example, from emission to absorption is interrupted, and every line apparently shows an E/A antiphase signal, or an emission line intercedes in an otherwise absorptive region of the spectrum. The initial case is observed with radicals present in micellar systems [20,21], or in high viscosity solutions [22], and originates in the direct observation of the spin-correlated radical pair [22,23]. The second has been reported in radicals undergoing chemical exchange, in particular the chair-to-chair interconversion of derivatives of cyclohexyl radicals [6]. This is a special case of the third instance, that of secondary radical formation in processes involving the formation of radicals in which the electron is coupled to the same nucleus as it was in the first [24]. In both, the mixed-phase nature of the spectrum arises in polarization transfer processes. In the most extreme case, a change in the sign of the coupling constant between the primary and secondary species can cause a complete phase inversion of the spectrum, and primary radicals formed with E/A polarization from triplet precursors can yield secondaries with A/E polarization [25]. This accentuates the need to determine the whole time-dependence of a system studied using CIDEP techniques.

References

1. A.J.Dobbs, Molec. Phys., 30 (1975) 1073.
2. S.Basu, K.A.McLauchlan and A.J.D.Ritchie, Chem.Phys., 79 (1983) 904.
3. P.W.Atkins and K.A.McLauchlan in "Chemically Induced Magnetic Polarization", ed: A.R.Lepley and G.L.Closs, Wiley, New York (1973) p68.
4. J.K.S.Wan, S.K.Wong and D.A.Hutchinson, J.Chem.Phys., 58 (1973) 985.
5. H.Paul, Chem.Phys., 40 (1979) 265.
6. K.A.McLauchlan and D.G.Stevens, J.Chem.Phys., 87 (1987) 4399.
7. S.Basu, K.A.McLauchlan and G.R.Sealy, Chem.Phys.Letts., 88 (1982) 84.
8. C.D.Buckley and K.A.McLauchlan, Chem.Phys., 86 (1984) 323.
9. F.J.Adrian, J.Chem.Phys., 61 (1974) 4875.
10. K.A.McLauchlan and D.G.Stevens, Molec.Phys., 60 (1987) 1159.
11. e.g. S.Yamauchi, K.Tominaga and N.Hirota, J.Phys.Chem., 90 (1986) 2367.
12. M.Plüschau, A.Zahl, K.P.Dinse and H.van Willigen. J.Chem.Phys., 90 (1989) 3153.
13. A.I.Grant and K.A.McLauchlan, Chem.Phys.letts., 108 (1983) 120.
14. S.Yamauchi and N.Hirota, J.Phys.Chem., 88 (1984) 4361.
15. S.Basu, A.I.Grant and K.A.McLauchlan, Chem.Phys.Letts., 94 (1983) 517.
16. K.Tominaga, S.Yamauchi and N.Hirota, J.Phys.Chem., 92 (1988) 5160.
17. S.Yamauchi, K.Tominaga and N.Hirota, 5th Nodzu Memorial Lectures, (1985) 24.
18. P.R.Levstein and H.van Willigen, J.Phys.Chem., in the press. I am most grateful for a preprint of this paper.
19. H.Paul and C.Segaud, Intern.J.Chem.Kinet., 12 (1980) 637.
20. Y.Sakaguchi, H.Hayashi, H.Murai and Y.J.I'Haya, Chem.Phys.Letts., 110 (1984) 75.
21. H.Murai, Y.Sakaguchi, H.Hayashi and Y.J.I'Haya, J.Phys.Chem., 90 (1986) 113.
22. C.D.Buckley, D.A.Hunter, P.J.Hore and K.A.McLauchlan, Chem.Phys.Letts., 135 (1987) 307.
23. G.L.Closs, M.D.E.Forbes and J.R.Norris, J.Phys.Chem., 91 (1987) 3592.
24. K.A.McLauchlan and N.J.K.Simpson, Chem. Phys.letts., 154 (1989) 550.
25. K.A.McLauchlan and N.J.K.Simpson, J.Chem.Soc. Perkin Trans.II (1990) 1371.

Mo-3

13:30

~14:00

CIDEP in the Photolysis of Benzoic Acid
Derivatives

A. S. Jeevarajan and R. W. Fessenden

Radiation Laboratory and Department of
Chemistry and Biochemistry, University of
Notre Dame, Notre Dame, IN 46556, USA

ESR spectra of basic aqueous solutions of a wide variety of benzoic acid derivatives during steady-state photolysis show that two types of radicals are formed in the presence of a hydrogen donor (such as 2-propanol): anion radicals and cyclohexadienyl radicals. A typical system is 1,4-benzenedicarboxylic acid (terephthalic acid). The anion radical (a trianion in basic solution) is well known, is long-lived, and its concentration is high. The cyclohexadienyl radical is that formed by net hydrogen atom addition (transfer from the donor) at the position opposite one carboxyl group. Addition of acetone as sensitizer increases the yield substantially. The spectrum of this radical is notable in that the low-field half of the spectrum is in emission as a result of CIDEP. Part of the reason for the large polarization is the long relaxation time for the radical ~ 10 μ s. However, the radicals involved all bear multiple negative charges so it is surprising that the reaction rate is fast enough to produce such a polarization. The purpose of the work reported here is to better understand the origins of the polarization.

The reaction mechanism involves reaction of the triplet state of the acid anion as shown by optical laser photolysis studies on terephthalic acid [1]. The triplet has a strong

absorption at 320 nm and an unquenched lifetime of at least 40 μ s. The spectrum remains the same from pH 6.7 to 13. The terephthalate triplet lifetime in the presence of 10% 2-propanol by volume is about 6 μ s at pH 13. The optical absorption by the cyclohexadienyl radical is not evident because it absorbs near 350 nm with a much weaker absorption ($\epsilon \sim 3000$ M^{-1} cm^{-1}) than the anion radical ($\epsilon=30000$). The formation of two products from these acids is interpreted in terms of the spin densities of the triplet state which, for the dimethyl ester, has been shown to have a quinoid structure [2]. In terephthalate triplet, there will be spin density mainly on the oxygens and the 1 and 4 carbons of the ring. Addition of hydrogen from the donor can occur at those positions. There must be parallel reactions of the triplet because radiolysis studies show that the anion radical does not protonate on carbon. Reaction at the oxygen will be like that in typical ketones. The reaction at a ring carbon is like that seen by Saguchi et al. [3] for xanthone.

To further understand the observed behavior, time-resolved ESR studies were carried out using a Lumonics HyperEX-400 laser at 308 nm and the direct detection ESR spectrometer previously used for pulse radiolysis experiments. Large signals of the cyclohexadienyl radical were found with terephthalate only when alcohols such as ethanol and 2-propanol were used as hydrogen donors and then only in basic solution above about pH 12. If tetrahydrofuran or sodium borohydride were the donors, little if any cyclohexadienyl radical was formed. At neutral pH, where the acid is still present as the dianion, little cyclohexadienyl radical is found. Typical curves are shown in figure 1. The growth and decay of the ESR signal for the cyclohexadienyl

radical follow a typical pattern for a radical polarized in random encounters.

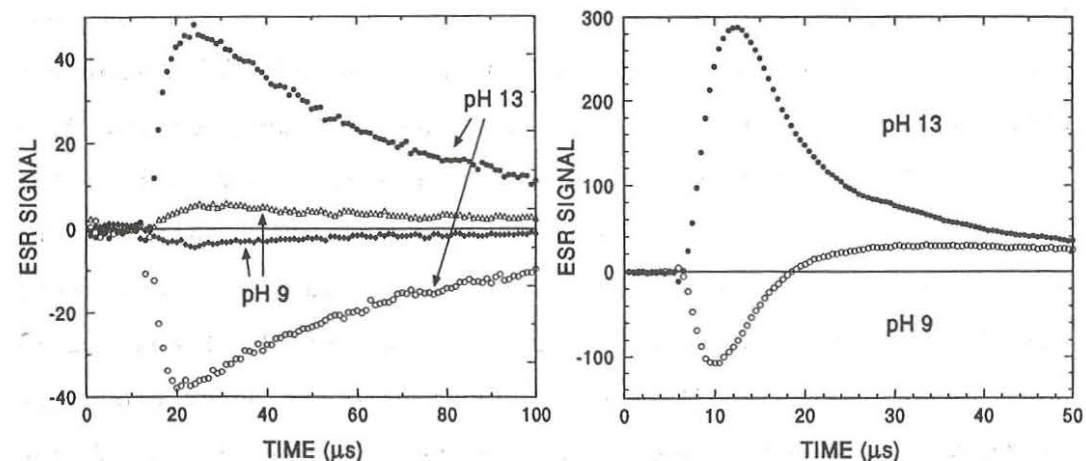


Figure 1. Time profiles of the lines at the centers of the low- and high-field subgroups of the cyclohexadienyl radical spectrum.

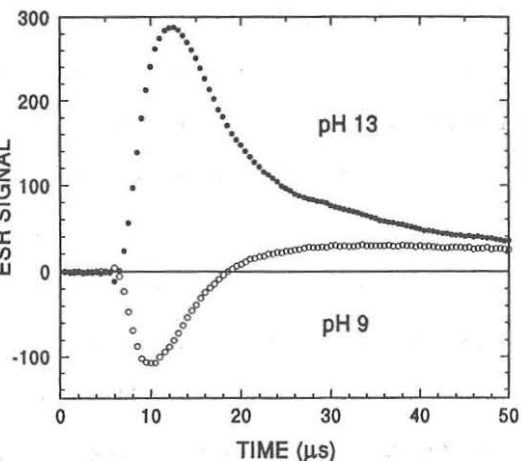


Figure 2. Time profiles of the central line of the anion radical.

The time-resolved ESR signal of the anion radical showed very unusual behavior. At neutral pH (monoanion radical) the ESR line at the center of the spectrum showed an emission which lasted for about 10 μs and then converted to absorption as shown in figure 2. At pH 13, the anion radical (trianion here) showed an initial excess positive amplitude which lasted a similar short time. Experiments were then carried out in which the physical quencher β -hydromuconic acid at mM was added. The ESR signals for the anion at both pH values clearly were separated into an initial part which decayed faster (5 μs) and a long time part with a slow decay. The initial part of the signal clearly depends on the triplet lifetime. Two explanations are possible. The initial magnetization of the anion radical may be that trans-

ferred from the triplet when the anion is formed. Because the triplet lifetime is $\sim 6 \mu\text{s}$ as shown from the optical experiments, it is hard to understand how the triplet can have other than equilibrium magnetization. The other, and preferred, explanation is that the polarization is the result of anion radical-terephthalate triplet encounters as described by Blattler et al. [4]. It remains to explain why the sense of the polarization changes between neutral and basic solution. In the theory, the sign of the effect depends on the sign of the exchange interaction. The only change in the species is the state of ionization. It is not clear whether changes in the charge on the species could invert the ordering of the doublet and quartet states. Further studies with terephthalate and other benzoic acid derivatives are under way to further understand the origins of the polarizations.

References

- [1] Studies done in conjunction with D. Weir.
- [2] D. R. Arnold, J. R. Bolton, and J. A. Pederson, *J. Am. Chem. Soc.*, 94 (1972), 2872.
- [3] Y. Saguchi, H. Hayashi, H. Murai, and Y. J. I'Haya, *J. Am. Chem. Soc.*, 110 (1988), 7479.
- [4] C. Blattler, F. Jent, and H. Paul, *Chem. Phys. Lett.*, 166 (1990), 375.

Mo-4

14:15

~14:45

Electron Spin Polarization by a Radical-Triplet
Pair Mechanism

Cyrill Blättler and Henning Paul

Physikalisch-Chemisches Institut, Universität Zürich
CH-8057 Zürich, Switzerland

Experimental evidence is presented for a spin polarization mechanism of transient radicals in solution, which occurs if the radical sample contains triplet state molecules. It resembles the wellknown radical pair mechanism (RPM) for radical F-pairs but is built up during encounters of triplets and radicals and therefore, is termed radical-triplet pair mechanism (RTPM). The RTPM seems to generate a net polarization of the entire ESR spectrum of the radicals. It probably results from quartet-doublet mixing and splitting due to the zero-field splitting and the exchange interaction, respectively. In addition, doublet pair spin states are filtered out by triplet quenching. In fact, the ESR polarization thus created is just the counterpart of the magnetic field dependent component of triplet quenching by radicals [1].

Figure 1 on the next page gives an example [2]. The upper part of that figure shows a steady state ESR spectrum of benzyl radicals recorded during continuous UV irradiation of a dibenzylketone solution. The slight increase of intensities from left to right indicates an E/A multiplet polarization due to the RPM. Two arrows mark a high-field (h) and low-field line (l) positioned symmetrically to the centre of the spectrum. They have been investigated by time-resolved ESR (TRESR), i.e. their intensities have been recorded in dependence on time after laser-flash photolytic radical generation. The result is given in fig. 1a which also displays the time profile of the sum $s = h + l$. Since summing h and

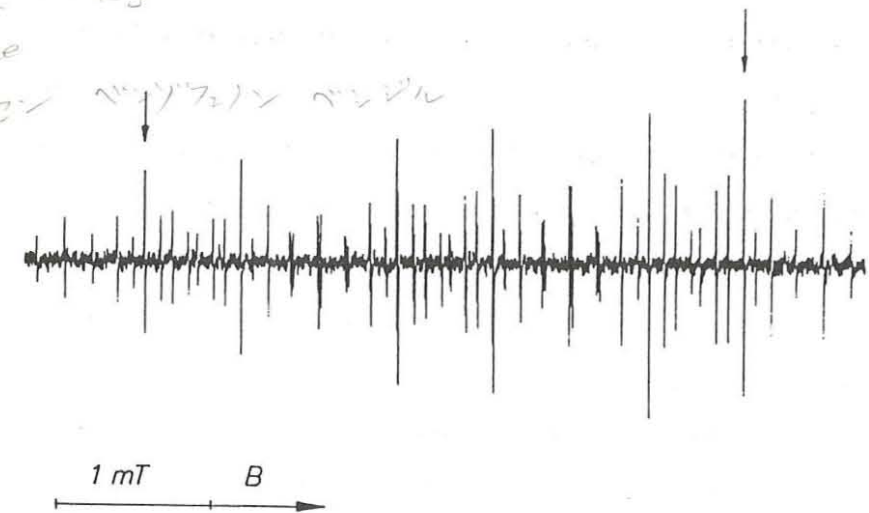
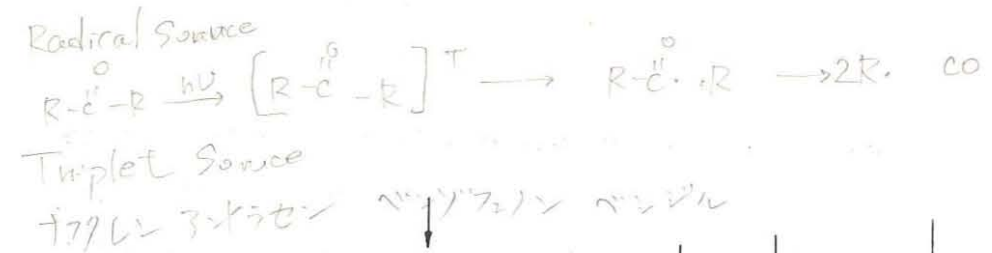
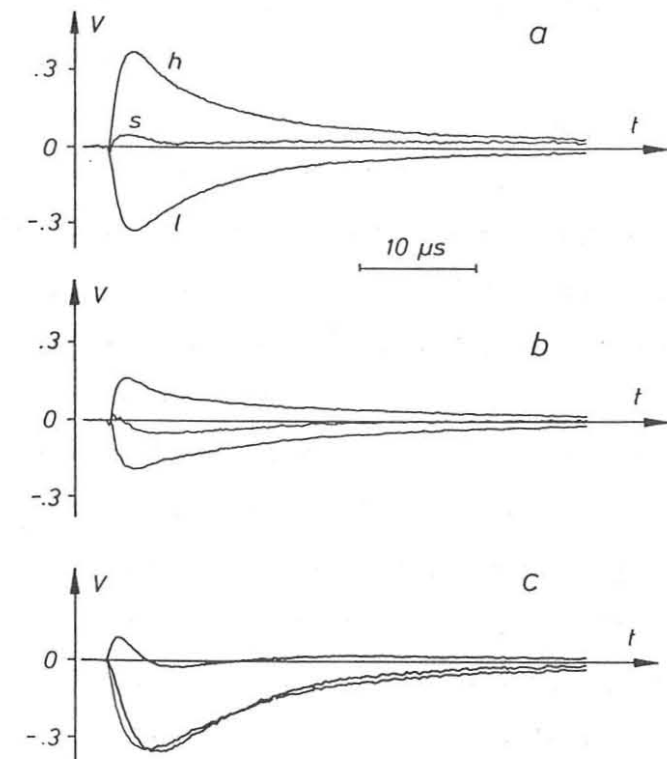


Figure 1

Upper part:
Steady state ESR spectrum of benzyl radicals.

Lower part:
Time profiles of a benzyl radical high-field (h) and low-field (l) resonance and sum $s = h + l$. Irradiation of solutions containing only dibenzylketone (a) and added anthracene (b) or benzil (c).



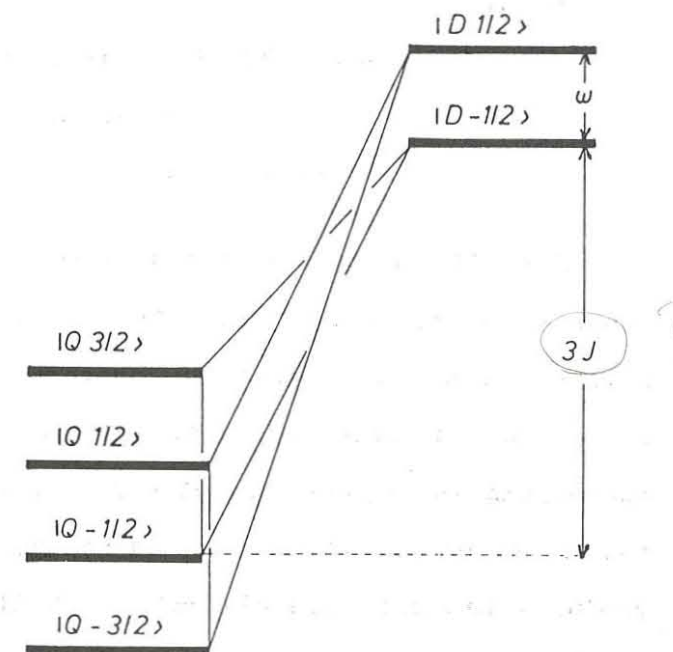
l cancels the antisymmetric E/A multiplet polarization, s reflects twice the net polarization. Obviously, this is a weak absorption whose origin is no matter of concern here. Figs. 1b and 1c give time profiles of the same resonances as well as their sum, which are observed for solutions containing in addition anthracene (1b) or benzil (1c) in amounts resulting in optical densities of 0.6 in the additive. Clearly, the net polarization changes to weak and strong emission, if anthracene and benzil, respectively, are present. Investigation of several other benzyl radical resonances indicates, that the additives induce net emission only and no additional multiplet polarization.

The same phenomenon is observed with other radicals and additives which, like anthracene and benzil, form long-lived triplet states upon irradiation. Since the size of the polarization in most cases increases with the zero-field splitting (ZFS) parameter D of the triplet state, we suppose that the emissive electron spin polarization originates from encounters of radicals with those triplet state molecules. Upon collision they can form a doublet or quartet pair spin state.

The overall doublet states will lead to triplet quenching [3,4], thus destroying the radical-triplet pair. The remaining quartet states experience radical-triplet interactions altering the spin state populations with time. The ZFS, for example, mixes quartet and doublet states as depicted in fig. 2. Treating ZFS as perturbation in the high-field spin Hamiltonian of the radical-triplet pair indeed shows that the combined action of ZFS and exchange interaction induces an electron spin polarization of the radicals leaving those pairs. Its sign depends on the sign of J , and emission indicates the quartet to be lower in energy than the doublet pair state.

Figure 2

Energy level diagram of a radical-triplet pair with exchange ($3J$) and Zeeman (ω) splitting. States connected with each other are mixed by ZFS.



References

- [1] U.E. Steiner and T. Ulrich, Chem. Rev. **89** (1989) 51, and references cited therein.
- [2] C. Blättler, F. Jent and H. Paul, Chem. Phys. Letters **166** (1990) 375.
- [3] O.L.J. Gijzeman, F. Kaufman and G. Porter, J. Chem. Soc. Faraday Trans. II **69** (1973) 727.
- [4] H. Hiratsuka, S. Rajadurai, P.K. Das, G.L. Hug and R.W. Fessenden, Chem. Phys. Letters **137** (1987) 255, and references cited therein.

Mo-5
15:00
~15:20

Formation Mechanism of Spin Polarized Solvated Electron in Photoionization.

Hisao Murai and Keiji Kuwata,

Department of Chemistry, Faculty of Science
Osaka University, Toyonaka, Osaka 560, Japan.

Most ESR studies on the solvated electron are limited to the reports of radiation chemistry. Only a few reports on the solvated electron formed in photoionization are available^{1,2}). Concerning the spin polarized solvated electron, the study on the radiolysis of aqueous solutions containing several ion species has reported in which the quenching to the triplet state of products has been postulated³). In the present talk, new CIDEP studies on photoionization of organic compounds and the formation of the spin polarized solvated electron concerning two different systems will be given.

An X-band ESR spectrometer was modified for the time-resolved ESR measurements. Both a transient memory with computer and a boxcar integrator were used to observe the CIDEP signals. In the first system, a nitrogen-gas laser ($\lambda = 337$ nm) was used for the excitation. Throughout the experiment, the concentration of TMPD was between 5.0×10^{-3} and 2.0×10^{-2} M (mol dm^{-3}), and 2-propanol was mainly used as the solvent. In the second system, an excimer laser ($\lambda = 308$ nm) was used for the excitation. The concentrations of xanthone (or other carbonyls) and SDS in distilled water were 2.0×10^{-3} and 1.0×10^{-1} M, respectively.

1) TMPD in alcohols²⁾ Fig. 1. shows the time-resolved ESR spectra of some paramagnetic species at several observation times

after laser excitation at -2°C . Immediately after a laser pulse, a broad E/A polarized spectral pattern appeared. This E/A pattern gradually became narrower and some strong total absorptive component grew up along with the disappearance of the E/A pattern component. Finally, the absorptive peak reached to $g = 2.0020$

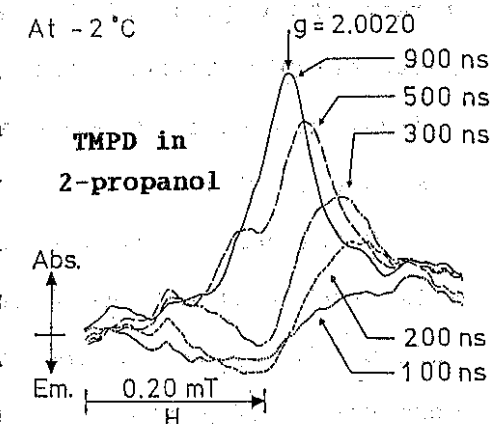


Fig. 1. trESR spectra of e_{solv}^- .

position which was almost identical with that of the solvated electron reported in the radiolysis of methanol.

The rise and the decay of the total absorptive signal strongly depend upon the microwave power (Fig. 2). This indicates that the absorptive signal is mainly due to the spin polarization induced probably by the S-T₀ mixing as a geminate pair of the solvated electron and the TMPD cation radical. Since the photoejection of an electron from TMPD in 2-propanol takes place from the excited singlet state⁴) and the isotropic g-tensor of TMPD cation ($g = 2.0034$) is a bit larger than that of solvated electron, the total absorption spectrum leads to the postulation of a positive value of

At -5°C exchange interaction (J). The contribution of the excited triplet state of TMPD to the spin polarization is excluded by careful examination.

The E/A pattern observed immediately after laser excitation is explained by the

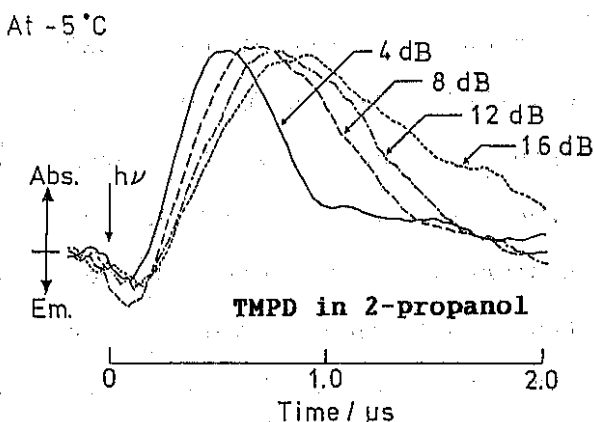


Fig. 2. Time-profiles of CIDEP signals of e_{solv}^- .

direct observation of the radical ion pair showing the exchange interaction⁵⁾ between the radical ions. This spectrum of the radical ion pair is also explained by a singlet precursor with positive J value.

These data indicate that the transient time region of the S-T₀ mixing after the decrease of the exchange interaction of radical ion pair is observed in this particular system. The observation of a positive J value is not surprising in the system of ionic radical pair in which the situation is quite different from that of the ordinary neutral radical pairs.

The addition of water to the solution drastically changed the spin polarization from enhanced absorption to net emission. This may be explained by the increase of the contribution of TM (triplet mechanism).

2) Xanthone in SDS micellar solution

Fig. 3. shows the time-resolved ESR spectrum observed in the laser photolysis of xanthone in the SDS micellar solution at the observation time of 0.2 to 0.4 μ s at room temperature. The g-factor of this sharp emissive signal is 2.0003 which is identical with that of the hydrated electron reported previously. Some other CIDEP signals superposed on the spectrum of the solvated electron are too weak to be assigned. This indicates that the hydrogen abstraction reaction from a SDS molecule which occurs in other carbonyls such as benzophenone

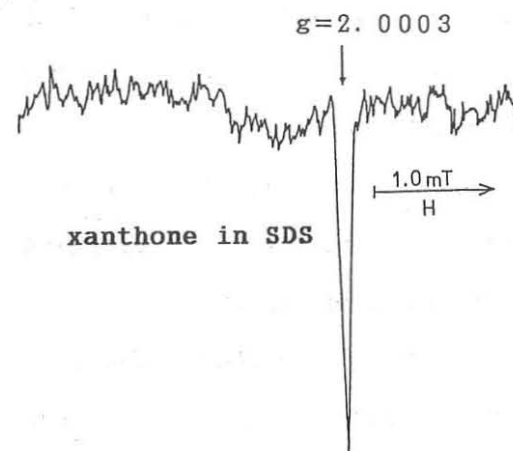
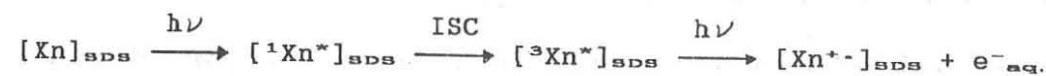


Fig. 3. trESR spectrum of e⁻ aq.

is very slow. According to the light intensity dependence of the ESR signal, the hydrated electron is produced through biphotonic process. The signal of the hydrated electron easily quenched by the addition of Cu²⁺ ion and the quenching rate ($3 \times 10^{10} \text{ M}^{-1}\text{s}^{-1}$) was in good agreement with that reported in the transient optical absorption method.

These results lead to the conclusion that xanthone is photoionized through the two photon processes in an SDS micelle and the electron is quickly ejected to the aqueous circumstance through the interface of the micelle. The cause of the emissive spin polarization may be explained by the fast intersystem crossing followed by photoionization in the second excitation of the spin polarized triplet state.



Further detailed information of these two systems will be given in this talk.

References

- [1] A. S. Jeevarajan and R. W. Fessenden, *J. Phys. Chem.*, **93** (1989) 3511.
- [2] Preliminary report; H. Murai and K. Kuwata, *Chem. Phys. Letters*, **164**(1989) 567.
- [3] R. W. Fessenden and N. C. Verma, *J. Am. Chem. Soc.*, **98** (1976) 243.
- [4] Y. Hirata and N. Mataga, *J. Phys. Chem.*, **89** (1985) 4031.
- [5] G. L. Closs, M. D. E. Forbes and J. R. Norris, Jr., *J. Phys. Chem.*, **91** (1987) 3592; C. D. Buckley, D. A. Hunter, P. J. Hore and K. A. McLauchlan, *Chem. Phys. Letters*, **135** (1987) 307.

Mo-6

16:00

~16:30

Diffusional Aspects of CIDNP and CIDEP;

Fundamental Quantities and Relations.

J. Boiden Pedersen

Fysisk Institut, Odense Universitet,

DK-5230 Odense M, Denmark

The description of radical reactions in media where the diffusive motion of the radicals is an important or even controlling factor may be quite complicated and involve a large number of seemingly unrelated quantities. Furthermore these quantities are often difficult to calculate. The magnetic field dependence of the reaction yield and the spin polarization phenomena CIDNP and CIDEP increase the complication of the description but add valuable and sometimes detailed information about the diffusive process. There are, however, several general relations which facilitate both the understanding and the description. For sufficiently diluted systems all information on the diffusion process is contained in the rate of first encounter at a separation d starting from an initially separation $r_0 > d$. This fundamental quantity is denoted $R(t, d | r_0)$ and may equivalently be interpreted as the probability density for the first arrival (or first passage) time at d starting from r_0 . Several accurate expression for this fundamental quantity and their implications on the observable quantities will be discussed.

The kinetic equation for a recombination reaction of "classical" particles is

$$\frac{dn}{dt} = -R(t)n - K(t)n^2$$

The first term describes the rate of disappearance of initially correlated pairs and the second term describes the bulk recombination of initially uncorrelated pairs. This equation implies that $R(t)$ and $K(t)$ varies on a short time scale and $n(t)$ on a long time scale. On the short time scale $R(t) \rightarrow 0$, as $t^{3/2}$ in 3-d, and $K(t) \rightarrow K$, the steady state constant, for $t \rightarrow \infty$. For

21

3-dimensional continuous diffusion $K(t)$ can be calculated from $R(t)$ as [1,2]

$$K(t) = -4\pi D(d)d^2 e^{\beta V(d)} R'(t, d)$$

where $R'(t, d)$ is the partial derivative of R with respect to the initial separation r_0 evaluated at the reaction distance d .

In general both $R(t)$ and $K(t)$ depend on the rate by which the radicals form a product when they encounter. This is usually described by a microscopic rate constant h . This extra complication can be eliminated by the use of the following general relations [2] that show that the general case can be calculated from the diffusion controlled quantity:

$$\tilde{R}(s, x, h) = \frac{\tilde{R}(s, x)}{1 - \tilde{R}'(s)D(d)/h}$$
$$\tilde{K}(s, h) = \frac{\tilde{K}(s)}{1 - \tilde{R}'(s)D(d)/h}$$

where $\tilde{R}'(s) = (\partial \tilde{R}(s, r)/\partial r)_{r=d}$ and tilde indicates the Laplace transformed quantity with variable s . The steady state rate constant can be written as

$$K = \lim_{s \rightarrow 0} s \tilde{K}(s, h) = K_D \Lambda$$

where K_D is the diffusion controlled rate constant. This equation can be interpreted as the rate of which the members of a pair meet for the first time multiplied by the total probability that they react either during this encounter or during one of the subsequent reencounters before they diffuse apart never to meet again.

For 3-d continuous diffusion in an interradical potential $V(r)$ these quantities are equal to

$$K_D = \left(\int_d^\infty \frac{\exp(\beta V(x))}{4\pi D(x)x^2} dx \right)^{-1} = 4\pi D(d)df^*(d)$$

$$\Lambda = \frac{h\tau}{1 + h\tau}$$

22

where $\tau^{-1} = -\tilde{R}'(s)D(d)$. In the reencounter picture one would write

$$\Lambda = \frac{\lambda}{1 - p(1 - \lambda)}$$

where λ is the probability of reaction during a single encounter and p is the probability that two particles separating after an encounter will later reencounter. The two descriptions are related by $p = \tilde{R}(s = 0)$.

For a spin system the probability of reaction Λ depends on the spin states and on the magnetic interactions. In order to distinguish it from the classical quantity we call it F . The reencounter calculation scheme, initiated by Pedersen [3] and Salikhov [4], gives the following formal expression

$$F = \text{Tr} \left[(1 - M_i) \frac{1}{1 - M_o M_i} \rho(0) \right]$$

where M_i and M_o are the quantum mechanical propagators for the spin system, averaged respectively over the time duration of an encounter and the time between two consecutive encounters. The probability density of the latter time is given by the diffusion controlled $R(t)$. By diagonalizing the propagator M_o one then finds that the diagonal elements are simply equal to $\tilde{R}(i\omega_{ij})$ where the frequencies ω_{ij} are differences between the eigenvalues of the free pair Hamiltonian.

The effect of the diffusion in varying potentials is conveniently studied using the reencounter formalism which allows one to separate the treatment of the microscopic reaction, the quantum mechanical evolution, and the diffusion process. Furthermore this approach often leads to analytically or easily applicable formulae. For example for a triplet precursor in high magnetic fields [5]

$$F(T_0) = \frac{\Lambda F^*}{1 + F^*(1 - \Lambda)}$$

where the quantity F^* measures the efficiency of the S - T₀ mixing and

$$F^* = \frac{p(1 - c) + p^2[(1 - c) - (1 - s^2 - c^2)]}{2(1 - p)^2 + 3p(1 - c) - p^2[(1 - c) + (1 - s^2 - c^2)]}$$

with c and s equal to the real and imaginary parts of $\tilde{R}(iQ)$, respectively. Similar expressions can be derived for an arbitrary field strength [6].

The most accurate expression for long times and for 3-d continuous diffusion is [7]

$$\tilde{R}(s, r) = \exp \left(-\sqrt{\frac{s}{D}}(r - d) \right) \frac{df^*(d)}{rf^*(r)} \left\{ 1 + \sqrt{\frac{s}{D}} [r - rf^*(r) - d - df^*(d)] \right\}$$

There are several other expressions for 2-d and 3-d diffusion and a recent one [8] for jump diffusion on almost 2-dimensional lattices such as anthracene crystal.

References

1. V.Gösele, Chem. Phys. Lett., 69 (1980) 332.
2. J.B.Pedersen, J. Chem. Phys., 72 (1980) 3904.
3. J.B.Pedersen, Chem. Phys. Lett., 52 (1977) 333.
4. K.M.Salikhov, Theor. Exp. Chem. 13 (1977) 551.
5. J.B.Pedersen, J. Chem. Phys., 67 (1977) 4097.
6. J.B.Pedersen and L.Lolle, in preparation.
7. J.B.Pedersen and P.Sibani, J. Chem. Phys., 75 (1981) 5368.
8. L.Lolle and J.B.Pedersen, in preparation.

Mo-8

17:30

~17:30

CIDEP measurement in the L band microwave frequency region

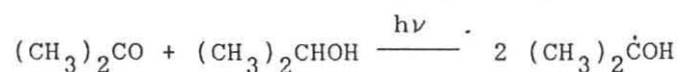
Masahide Terazima*, Shin-ichi Hayakashi, and Tohru Azumi

Department of Chemistry, Faculty of Science, Tohoku University, Aoba-ku, Sendai 980, Japan

*) present address; Department of Chemistry, Faculty of Science, Kyoto University, Kyoto, 606, Japan

CIDEP created by RPM (radical pair mechanism) and TM (triplet mechanism) appears frequently during photochemical reactions in homogeneous solution and have specially interested many investigators. CIDEP due to RPM arises by the S-T interaction of the intermediate radical pairs. This mechanism consists of ST_0M and ST_M (in many cases, the exchange interaction is negative and ST_M is preferable than ST_+M). Usually, CIDEP is created under the resonance magnetic field of the X band microwave ($B_0 \sim 330$ mT) and under this field, the large Zeeman splitting severely restricts the mixing between the S and T_- states.¹ Therefore, although ST_0M has been extensively studied, the effect of the S- T_- mixing has been observed only under very limited conditions and the experimental study on the mechanism of ST_M is rare. We investigate the mechanisms of CIDEP (especially ST_M) at low magnetic field by using an L band EPR spectrometer.

We choose acetone in 2-propanol photochemical reaction.



The reaction scheme and the polarization mechanism of this system at the X band region has been extensively studied.²

Fig.1 depicts the CIDEP spectrum observed at 1.5 μ s after the laser irradiation in the X band region ($\omega \sim 9.18$ GHz, $B_0 \sim 330$ mT) at room temperature. The CIDEP spectrum shows emission in the low field side and enhanced absorption in the high field side with net absorptive character (E/A^* pattern). The E/A polarization comes from the ST_0M and the net absorptive polarization is explained by TM .²

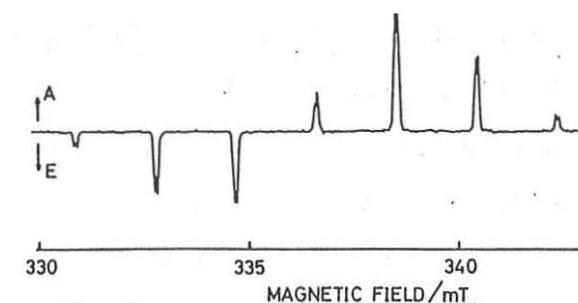


Fig.1

Fig.2 depicts the CIDEP spectrum in the L band region ($\omega \sim 1.44$ GHz, $B_0 \sim 50$ mT) under the same conditions as those of the X band CIDEP measurement.

There are two distinguished features compared with the X band CIDEP spectrum. First, the dominant polarization is still E/A pattern but the net polarization is emission at this magnetic field. Second, each hfs due to the methyl protons splits clearly to several peaks besides the splitting due to the hydroxyl proton.

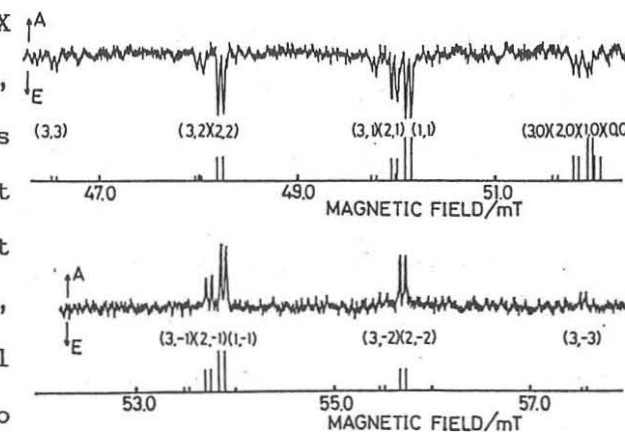


Fig.2

The further splitting can be explained by the second-order hyperfine splittings of the methyl protons. (The stick spectrum at the lower part of the CIDEP spectrum (Fig.2) depicts the calculated hfs.) Based on theoretical consideration, the opposite net

polarization in the X and L band regions is interpreted as the decrease of the TM polarization and the increase of the ST_M polarization by changing the magnetic field from 330 mT to 50 mT.

Recently, Buckley and McLauchlan have separated the ST_M into two parts; ^{2-d} hyperfine dependent (ST_{M-d}) and hyperfine independent (ST_{M-i}) parts. ST_M polarization arises from the mutual flip-flop of electron spin and nuclear spin through the non-zero matrix element

$$| \langle S, I, m-1 | AS_+ I_- | T_-, I, m \rangle |^2 = A^2 [I(I+1) - m(m-1)] \quad (1)$$

where A denotes hfcc. In this matrix element, the nuclear spin which plays a role in the S-T₋ interaction can belong to either the observed radical or the counter radical. The hyperfine dependent part of the ST₋ polarization appears when the nuclear spin which participates in the S-T₋ interaction belongs to the observed radical. In this case, the efficiency of the ST_M is determined by the magnitude of the non-zero matrix element (eq.(1)) and it depends on the set (I,m) of each hyperfine lines. While, the hyperfine independent part comes from the S-T₋ interaction using the nuclear spin of the observed and the counter radicals. The clear distinction of ST_{M-d} and ST_{M-i} in the X band CIDEP spectrum seems to be difficult because each hfs of the same m are mixed together. On the other hand, the hyperfine lines of different (I,m) are expected to show very different polarization pattern depending upon the mechanism. Thus, the L band CIDEP spectrum is expected to be suitable to distinguish ST_{M-d} and ST_{M-i}.

The observed L band CIDEP spectrum is tried to reproduce by using the polarization due to ST₀, TM, and ST_{M-d}, or ST_{M-i} for ST_M.

$$P = a P_{ST_0} + b P_{TM} + c P_{ST_-} \quad (2)$$

First, we neglect the contribution of TM (b=0). Fig.4 shows the observed and calculated spectrum based on eq.(2) with ST_{M-d} and ST_{M-i} for P_{ST₋}, and b=0. When ST_{M-d} is used for P_{ST₋}, the observed spectrum can be reproduced with a:c=1:0.20~0.25. When ST_{M-i} is the origin of the ST_M polarization, the calculated spectrum with a:c=1:0.15~0.2 is reasonably similar to the observed CIDEP spectrum (Fig.3). Although, at the first glance, both of the calculated spectra seem to reproduce the observed one well, there are several differences which support the preference of ST_{M-d} as ST_M polarization. We conclude that the ST_{M-d} for ST_M polarization is more reasonable to explain the observed CIDEP spectrum.

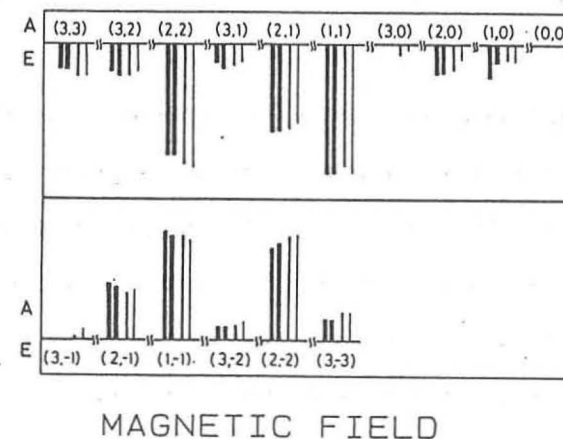


Fig.3 observed CIDEP spectrum (thick bars), the calculated ones by using eq.(2) and ST_{M-d} for ST_M (middle thick bars), and ST_{M-i} for ST_M (thin bars).

references

- Adrian, F.J.; Monchick, L.J. *Chem. Phys.*, 1979, 71, 2600.
- a) Wong, S.K.; Chui, T.M.; Bolton, J.R. *J. Phys. Chem.*, 1981, 85, 12.
b) Basu, S.; Grant, A.J.; McLauchlan, K.A. *Chem. Phys. Lett.*, 1983, 94, 517.
c) Thurnaner, M.C.; Chui, T.M.; Trifunac, A.D. *Chem. Phys. Lett.*, 1985, 116, 543.
d) Buckley, C.D.; McLauchlan, K.A. *Chem. Phys. Lett.*, 1987, 137, 86.
e) Tominaga, K.; Yamauchi, S.; Hirota, N. *J. Phys. Chem.*, 1986, 90, 2367; *J. Chem. Phys.*, 1988, 88, 553.
- Fessenden, R.W. *J. chem. Phys.*, 1962, 37, 747.

A1
20:00
~22:00

Spin Polarization Transfer during the Intramolecular
Triplet-Triplet Energy Transfer in a Rigid Matrix as
Studied by Time-Resolved EPR Spectroscopy

Kimio AKIYAMA, Shozo TERO-KUBOTA, and Yusaku IKEGAMI
Institute for Chemical Reaction Science, Tohoku
University, 2-1-1 Katahira, Aoba-ku, Sendai 980, Japan

There has been little study on the spin dynamics for the case of intramolecular energy transfer, while an efficient energy transfer has been reported in many systems. In the present study, we report the spin polarization conservation during the intramolecular energy transfer under the external magnetic field by using time-resolved EPR (TREPR) technique. If the spin angular momentum is conserved during the energy transfer process, the population differences among the three sublevels of the acceptor triplet state depends on the direction of the principal magnetic axes between the donor and the acceptor. We select the spiran systems, spiro (9,10-dihydro-9-oxoanthracene-10,2',5',6',-benzidan) (1) and spiro(9,10-dihydro-9-oxoanthracene-10,2'-(3H)phenalene) (2), to confirm the above possibility. Their structures and coordination axes are shown in Figure 1.

The rigid spiran, 1 and 2, were prepared according to the procedure reported previously.¹ The samples were purified by recrystallizations

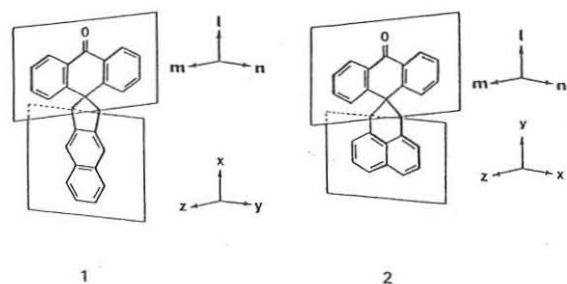


Figure 1. Structure and coordination systems of the rigid spirans (1 and 2)

from pyridine-water and from light petroleum and sublimation. For steady-state and TREPR measurements a concentration of $1 \times 10^{-3}M$ was used and degassed by using three freeze-thaw cycles. Solvents were purified by distillation after dehydration by the methods

reported previously. Time-resolved EPR spectra were observed with a Varian E-109E X-band EPR spectrometer without field modulation.

Since the energy level of T_1 state of anthrone is higher of 3100 cm^{-1} than that of naphthalene can be caused an efficient T-T excitation energy transfer. It was confirmed for the present samples by measuring the phosphorescence spectra. Excitation of 1 and 2 by the light with the wavelengths longer than 300 nm gave the phosphorescence due to the naphthalene moiety as reported previously.¹

Steady state EPR measurements also support the high efficiency of the energy transfer. Figure 2a shows the conventional EPR spectrum of 3*1 generated from the N_2 laser (337.1 nm, 10 Hz repetition rates) photolysis, which corresponds to the excitation of an anthrone moiety, in toluene matrix at 77 K. The spectrum easily assigned to the T_1 state of naphthalene moiety from the zero-field splitting (ZFS) parameters ($|D| = 0.0952$ and $|E| = 0.0137 \text{ cm}^{-1}$). Each value is nearly identical to that of T_1 state of naphthalene. The similar results were also observed for 2.

In Figure 2b and 2c are shown the transient EPR spectra of 1 and 2 in toluene matrix observed at 500 ns after the N_2 -laser pulse irradiation. They presented polarization patterns of E EEA/A AE and E EAE/A EA for 1 and 2, respectively (E denotes the emission and A the absorption of the microwave radiation). The ZFS parameters determined from the canonical points well coincided with those of the T_1 state of naphthalene. Since both polarization patterns obtained are clearly different from that of the direct excitation of naphthalene by XeCl excimer laser (308 nm) excitation, they certainly result from spin polarization transfer during the intramolecular T-T energy transfer. The reasoning is supported from the facts that the polarization pattern depends on the relative orientation between the donor and acceptor, while the ISC always takes place on the ketone and is the step where spin polarization is created for both molecules.

High field approximation cannot explain these spectral pattern, be-

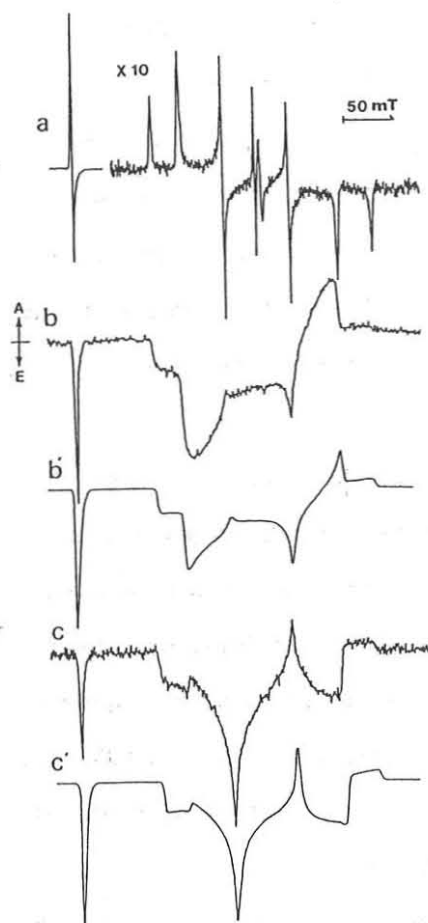


Figure 2. Steady-state(a) and TREPR (b) spectra of 1 and TREPR (c) spectrum of 2 in toluene at 77 K. Computer simulated spectra (b' and c') obtained by taking into account of intramolecular spin polarization transfer.

where C_{ih} are the components of the unitary transformation diagonalizing the spin Hamiltonian and P_h^D are the populating ratios for the donor sublevels in a molecular frame providing $\sum P_h^D = 1$. It can be expected that the spin alignment is conserved during the T-T energy transfer, because the operator containing in the exchange mechanism is independent of electron spin. Thus, we can assume, $\langle \chi_h^D | \chi_k^A \rangle \sim \cos \theta_{hk}$ where, θ_{hk} is the mutual angle between the directions of the principal axes h of the donor and k ($k = x, y, \text{ and } z$) of the acceptor and $|\chi_h^D\rangle$ and $|\chi_k^A\rangle$ are

cause the spectral intensities were significantly distorted with the spectral center. Therefore, general expression for the spin polarization transfer under the finite external magnetic field was attempted. The TREPR signal, $I(\theta, \phi)$, with the polar angle θ and ϕ of the applied field with respect to the principal molecular axes is given by

$$I(\theta, \phi) = B_{i,j}(P_i^A - P_j^A) G(\theta, \phi)$$

where, $B_{i,j}$ is the transition probability between the i and j sublevels in the acceptor, P_i^A and P_j^A are the populating ratios for the corresponding sublevels, and $G(\theta, \phi)$ is the Gaussian function. During the anisotropic ISC, each sublevel of the donor moiety is populated with a different rate. The populating probability (P_i^D) for the donor sublevel under the applied field becomes

$$P_i^D = \sum_h |C_{ih}^D|^2 P_h^D \quad (h = 1, m, n)$$

the zero field spin functions of the donor and acceptor, respectively.

The probability (P_j^A) finding for acceptor sublevel is written as

$$P_j^A = \sum_i \sum_h \sum_k |C_{ih}^D|^2 |C_{jk}^A|^2 \langle \chi_h^D | \chi_k^A \rangle^2 P_i^D$$

It is well known for the donor anthrone that the preferential ISC occurs to the highest l sublevel ($l // C=O$).² For 1, the direction of l is parallel to the x axis of the acceptor naphthalene leading to the relation of $\cos \theta_{lx} = 1.0$. On the other hand, $\cos \theta_{ly}$ is unity for 2 ($l // y$). The ZFS parameters of the donor anthrone, as well as the acceptor, are required to calculate the line shape, because their eigenfunctions depend on the relative magnitude between the ZFS parameters and the applied field. Unfortunately, the exact ZFS parameters of anthrone are uncertain. Therefore, the D and E values of the donor triplet state, which is invisible state under the X-band EPR experiments, were adjustable parameters for the simulation. The simulated spectrum was not appreciably altered by the change of E value between 0.05 to 0.01 cm^{-1} , but affected by D value. When the values of $D = -0.5$ and $E = 0.02 \text{ cm}^{-1}$ is used for simulation, the results well reproduced the observed spectra both 1 and 2 as shown in Figure 2b' and c'.

The present results clearly show the spin polarization conservation in the molecular frame during the T-T energy transfer under the external magnetic field. This phenomenon will be useful to clarify the mutual orientation between the donor and the acceptor as well as the relaxation path of excited states.

References

- 1) R. A. Keller, J. Am. Chem. Soc. 1968, 90, 1940.
- 2) S. Dym and R. M. Hochstrasser, J. Chem. Phys. 1969, 51, 2458.

A2

20:00
~22:00

Time-Resolved EPR Studies on the Excited Triplet States of Nonphosphorescent Troponoid Compounds

Tadaaki Ikoma, Kimio Akiyama, Shozo Tero-Kubota, and Yusaku Ikegami

Institute for Chemical Reaction Science,
Tohoku University,
Katahira 2-1-1, Sendai 980, Japan

Time-resolved EPR (TREPR) technique has made a significant contribution to our understanding of the short-lived and nonphosphorescent triplet (T_1) states of various molecules. Since troponone (1) is a typical nonbenzenoid aromatic molecule, the electronic structure in the ground state and assignment of the absorption spectrum have been the subject of much interest. However, the nonphosphorescent character has prevented the investigation of electronic structure in the T_1 state of 1. In the present study, we have succeeded to detect the T_1 state of 1 and related compounds in rigid glassy matrices.

Troponoid compounds were purified by distillation under reduced pressure and/or recrystallization from cyclohexane before use. The sample solutions (0.01 mol dm^{-3}) were degassed by freeze-pump-thaw cycles and sealed in a quartz tube. A XeCl excimer laser and a dye laser pumped by the excimer laser were used as the light source.

The TREPR spectrum of the T_1 state of 1 was clearly observed in a toluene glassy matrix by the excimer laser irradiation at 77 K as shown in Figure 1a. The spectrum was obtained $0.5 \mu\text{s}$ after the laser pulse. A weak emissive signal at 0.15 T corresponds to

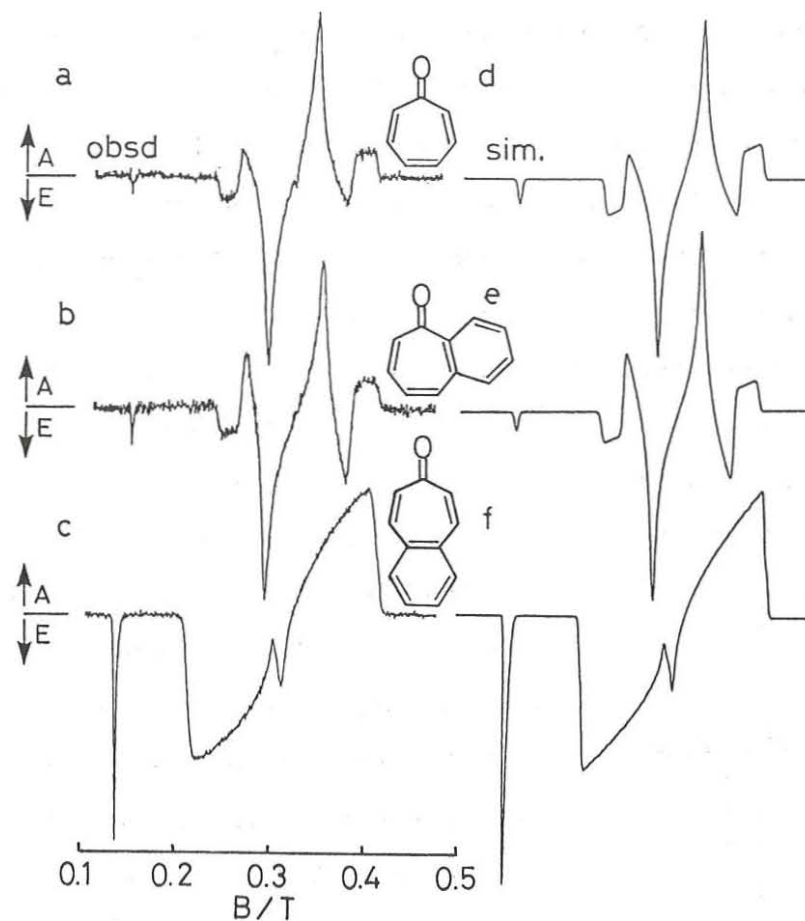


Figure 1. Observed (a-c) and simulated (d-f) TREPR spectra for the T_1 states of 1, 2 and 3 irradiated with 308 nm in a toluene glassy matrix at 77 K.

the $|\Delta M_S| = 2$ transition. The $|\Delta M_S| = 1$ transitions show the spin polarization of EAE at the low field half and of AEA at the high-field half, where E is emission and A is enhanced absorption of microwave. The spectrum was reproduced by computer simulation (Figure 1d) resulting in the zfs parameters of $|D| = 0.077 \text{ cm}^{-1}$ and $|E| = 0.011 \text{ cm}^{-1}$. In various glassy matrices of 2-methyltetrahydrofuran, ethanol, and 2,2,2-trifluoroethanol, similar TREPR spectra were observed, whereas a conventional EPR spectrum and luminescence were never detected even at 4.2 K in any matrices. As is distinct from simple ${}^3n\pi^*$ carbonyl molecules, little matrix dependence of the zfs parameters was observed and suggesting the T_1 state of 1 has nearly pure $\pi\pi^*$ character. Relatively small $|D|$ value and the narrow width (2 mT) of the spectral component support the assignment.

The TREPR spectra of 2,3-benzotropone (2) and 4,5-benzotropone (3) were shown in Figure 1b and 1c. The T_1 state character of 2 is considered to be very similar to that of 1, since both molecules show similar TREPR spectrum (Figure 1b) and nonphosphorescence. On the other hand, spectrum (Figure 1c) of 3 showed a very different canonical points and polarities from those of other two molecules. Furthermore, phosphorescence with some vibronic progressions and decay rate constant of 30 s^{-1} was observed. Both TREPR spectra of 2 and 3 exhibited little solvent dependence and suggested that the T_1 states of these molecules are pure $\pi\pi^*$.

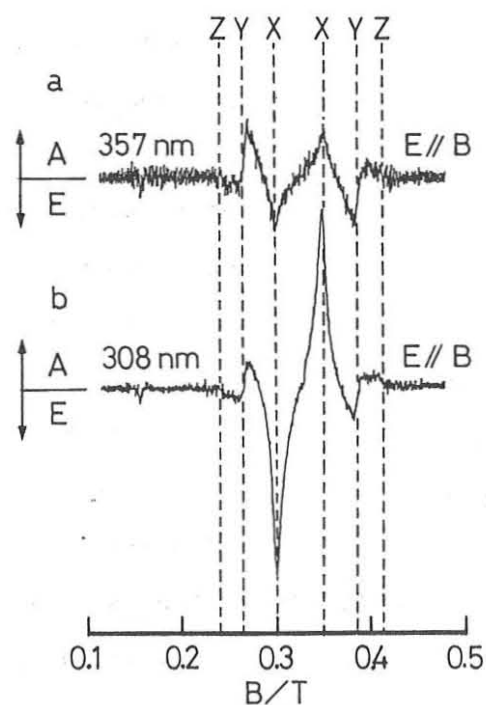


Figure 2. TREPR spectra of the T_1 state of 1 in a toluene glassy matrix excited with linearly polarized laser lights of 357 nm with $E // B$ (a) and of 308 nm with $E // B$ (b)

From the theoretical calculations and the dichromism of the spectrum induced by the external electric field, it has been clarified that the absorption band in the region of 250 to 370 nm of 1 consists of two types of $\pi\pi^*$ transitions with different transition dipole moment. Therefore, we can selectively excite these states by using the wavelengths of 357 and 308 nm. Figure 2 shows time-resolved magnetophotoselection (MPS) spectra obtained from the irradiation of 1 with these wavelengths. When the electric vector (E) of the light with 357 nm was parallel to the static magnetic field (B), the intermedi-

ate signals of the canonical orientations gained in intensity relative to the other signals (Figure 2a). In the excitation with 308 nm polarized by Glan-Thomson prism, the intensities of the innermost pair increased with $E // B$ (Figure 2b). Intermediate signals increased in the excitation by 357 nm with the light of $E // B$ correspond to those from the molecules aligned as $Y // B$. Innermost signals are due to those from the molecules aligned as $X // B$, since they are intensified in the excitation by 308 nm with $E // B$. It can be assumed that the energy level of the out-of-plane T_z sublevel locates at the lowest position in analogy with many $\pi\pi^*$ states. Therefore, we can determine the order of the triplet sublevels of 1 as shown in Figure 3, if the deviation of the structure is relatively small in the T_1 state. In the case of other compounds, MPS experiment with appropriate wavelength laser could determine zfs axes as shown in Figure 3. The polarization patterns of the TREPR spectra indicate that preferential population occurs at the T_x sublevel during the intersystem crossing process in all molecules. The reason for the nonphosphorescent character in the T_1 states of 1 and 2 will be discussed in comparison with MO calculations and decay kinetics.

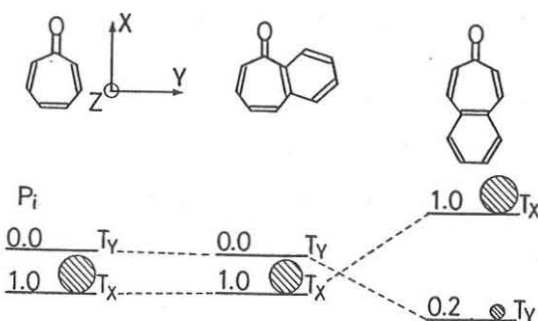


Figure 3. Molecular axes and zero-field sublevel schemes and relative population difference (P_i) of 1, 2 and 3.

	0.0 T_z	0.14 T_z	0.0 T_z
IDI	0.077 cm^{-1}	0.077 cm^{-1}	0.092 cm^{-1}
IEI	0.011 cm^{-1}	0.010 cm^{-1}	0.028 cm^{-1}

A3
20:00
~22:00

Electron Spin Polarization
Generated in Singlet-Doublet and Triplet-Doublet Systems

Kinichi Obi and Akio Kawai
Department of Chemistry, Tokyo Institute of Technology,
Ohokayama, Meguroku, Tokyo 152, Japan

1. INTRODUCTION

Just after the pulsed photoirradiation, many kinds of short lived excited molecules and intermediate species coexist interacting with each other and play an obscure but important role in photophysical and photochemical processes. Several kinetic studies have been reported on the quenching of the lowest excited singlet (S_1) or triplet (T_1) state with free radicals, but its detail is not revealed yet. ESR method has an advantage to investigate the paramagnetic species but is not applied the excited state quenching with free radical except for a few works.^{1,2)} Time resolved ESR detects CIDEP which is generated through the magnetic interaction between paramagnetic species. We applied the CIDEP studies to the quenching process of excited molecules with radicals and found out new mechanisms of CIDEP generation in the excited molecule-radical interaction.

2. RESULTS AND DISCUSSION

Fig.1 shows the time resolved ESR spectra of various molecule-TEMPO (2,2,6,6-tetramethyl-1-piperidinyloxy) systems. Spin polarized TEMPO was observed with E+E/A pattern in benzophenone and acetone systems. On the contrary, A+A/E pattern was observed in the coronene and fluoranthene systems. E and A mean emission and absorption, respectively. Paul and his coworkers reported²⁾ the net emissive CIDEP on radicals by Radical Triplet Pair Mechanism (RTPM), but in our

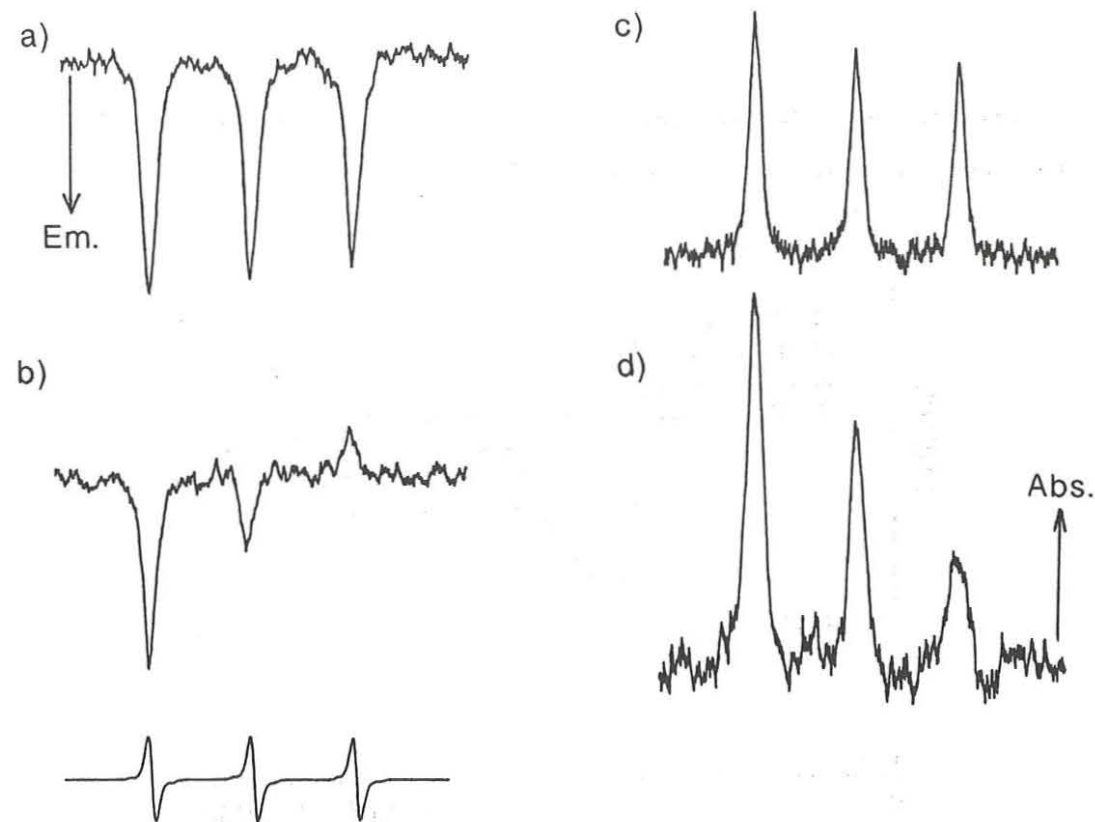


Fig.1 Time resolved ESR spectra obtained in TEMPO and a) bezophenone, b) acetone, c) coronene, d) fluoranthene mixture. Spectra were observed at 1 μ s after 308 nm laser excitation.

systems, not only net emissive CIDEP but also E/A, A and A/E patterns of CIDEP were obtained. We observed CIDEP in many excited molecule-TEMPO systems and summarized the results as follows.

	<Systems>	<CIDEP pattern>
Case 1.	molecules with long lived S_1 state and radical	A + A/E
Case 2.	molecules with high yield of T_1 state and radical	E + E/A

To explain the CIDEP generation, we consider the triplet-radical pair potential assuming $J < 0$ as shown in fig.2.

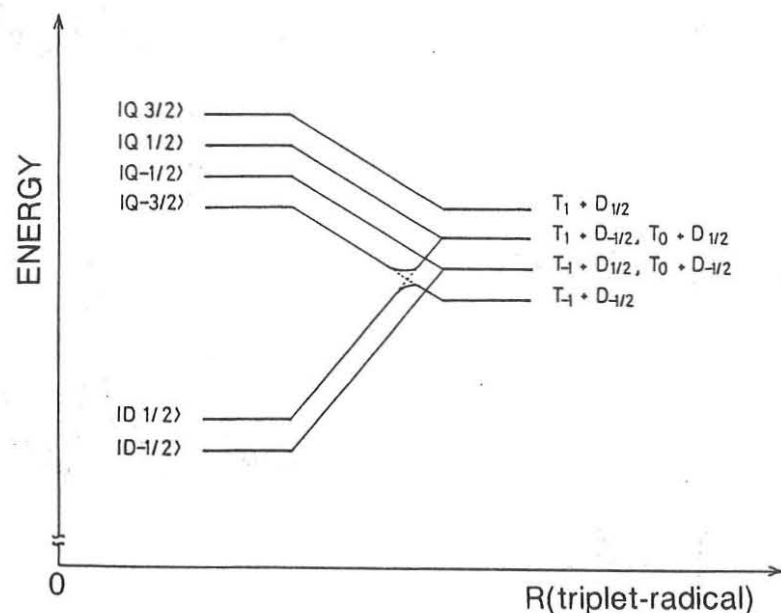


Fig.2 potential of triplet molecule and radical pair.

First, we discuss the net polarization. The $|Q-3/2\rangle$ and $|D1/2\rangle$ states show avoided crossing due to the zfs interaction of triplet molecule. As Paul suggested, doublet states of triplet-radical pair vanished owing to the quenching of T_1 state with radicals. Hence, during the course of dissociation of the pair, net emissive CIDEP is generated on radical, which is observed as the case 2 signal. On the other hand, if the radical quenches the S_1 state molecule, doublet states of T_1 -radical pair are generated due to S_1-T_1 enhanced intersystem crossing. This initial condition of T_1 -radical pair is opposite to that in above mechanism, and hence produces the net absorptive CIDEP on radical with the same mechanism. This is consistent with experimental results in case 1.

Secondly, we interpret the hyperfine dependence of CIDEP in the

T_1 -radical pair. Hyperfine dependence of CIDEP is explained by the $|Q1/2\rangle-|D1/2\rangle$ mixing in the none J region due to hyperfine interaction followed by reencounter of the pair, which is the similar to $S-T_0$ mixing mechanism of Radical Pair Mechanism. We simulated the spectra assuming initial state of the pair is quartet in T_1 quenching whereas doublet state in S_1 quenching, and $J < 0$. Obtained results showed E/A pattern in T_1 quenching and A/E pattern in S_1 quenching, which are consistent with the experimental results.

According to the above discussion, we concluded the general rule of CIDEP generation in the excited molecule-radical interaction as follows.

<Process>	<CIDEP pattern>
(1) S_1 quenching (doublet precursor RTPM)	A + A/E
(2) T_1 quenching (quartet precursor RTPM)	E + E/A

<REFERENCES>

- 1) T. Imamura, O. Onitsuka, and K. Obi, J. Phys. Chem. **90**, 6741 (1986).
- 2) C. Blattler, F. Jent, and H. Paul, Chem. Phys. Lett. **166**, 375 (1990).

A4

20:00
~22:00

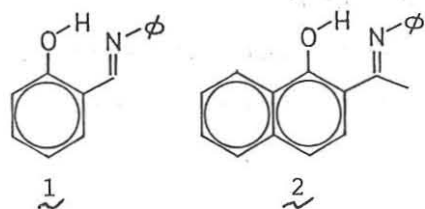
Time-resolved EPR Studies on the Short-lived
Triplet States Generated from the Intramolecular
Proton Transfer

Shozo Tero-Kubota, Tetsuji Noguchi, Kimio Akiyama,
and Yusaku Ikegami

Institute for Chemical Reaction Science,
Tohoku University, Katahira 2-1-1, Sendai 980,
Japan

Although much attention has been paid to study the intermediates in the excited state intramolecular proton transfer (ESIPT) of photochromic free Schiff bases, there has been little investigation on the triplet states generated during the process. This is attributed to the non or very weak phosphorescence and the short lifetime. In the present paper, we detected the short-lived excited triplet (T_1) states of phenylsalicylideneaniline (1) and 2-(N-phenylacetimidoyl)-1-naphthol (2) in glassy matrices using a time-resolved EPR (TREPR) method. The observed spectra were assigned to be the T_1 states of the corresponding keto tautomer. Direct excitation with a dye laser of the keto tautomer of 2 was also examined obtaining clear magnetophotoselection spectra (MPS). The principal axes of the zero-field splitting (ZFS) tensor was determined from the results of the MPS measurements and semi-empirical PPP SCF-MO calculations.

TREPR measurements were carried out by using an X-band EPR spectrometer (Varian E-109E) without field modulation at 77 K.



An excimer laser (Lumonics HE-420, XeCl 308 nm) and a dye laser (Lumonics HD-300) pumped by the excimer laser were used as the light source.

Figure 1a shows the TREPR spectrum obtained from the photolysis (308 nm) of 1 in an MCH glassy matrix at 77 K. The spectrum was observed 0.5 μ s after the laser pulse. The zfs parameters $|D| = 0.072$ and $|E| =$

0.016 cm^{-1} were determined from the spectral simulation (Fig. 1b). The polarization pattern and the zfs parameters were similar to those of the related molecules.¹ The transient spectrum can be assigned to the $T_1(\pi\pi^*)$ state of the keto tautomer generated by ESIPT.

Direct excitation measurement of the keto tautomer of 2 was examined to determine the direction of the principal axes of the zfs tensor. The presence of the keto tautomer of 2 in protic solvents was revealed by the appearance of a long wavelength absorption in the region of 410 - 460 nm. The clear magnetophotoselection (MPS) spectra were obtained by the dye laser photolysis with 442 nm in an EPA glassy matrix at 77 K as shown in Fig. 2. When the electric vector (E) of the light was perpendicular to the static magnetic field (B), the innermost (Y) and intermediate (Z) pairs were measured. On the other hand, only outermost (X) signals were detected with E // B. The results indicate that the direction of the transition moment for the

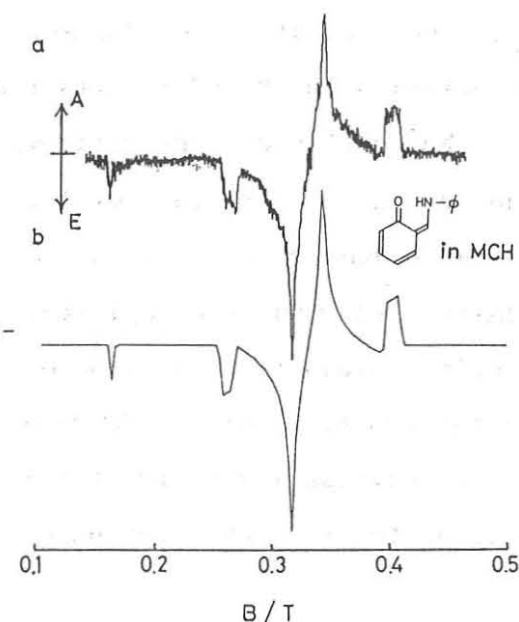


Fig.1 Observed(a) and simulated(b) TREPR spectra generated from the ESIPT in 1 in a methylcyclohexane glassy matrix at 77 K.

$S_1(\pi\pi^*)$ excitation of the keto form is parallel to one of the principal axis (X) of the zfs tensor.

We carried out the semi-empirical SCF-MO calculations, since the definite directions of the zfs principal axes cannot be assigned basing upon the above results. Wave functions were constructed from semiempirical PPP type LCAO MOs by including configurations arising from all the singlet excitations relative to the ground state. The result suggests that the direction of the transition moment for the S_1 excitation deviates $30^\circ \pm 5^\circ$ from that of the long axis for naphthalene moiety. Zfs sublevels

and the spin polarization are depicted in Scheme I.

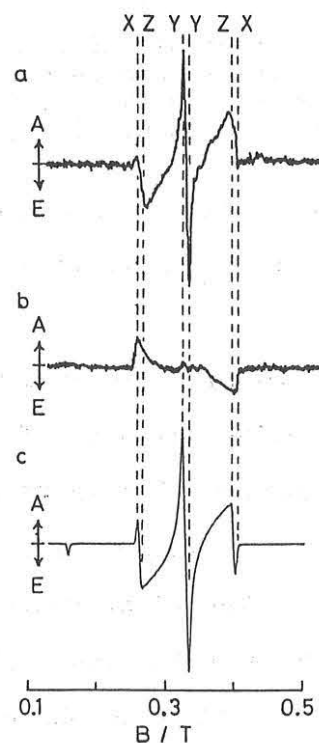


Fig. 2 Triplet TREPR spectra generated by the direct excitation with the polarized light (442 nm) of the keto tautomer of 2 in EPA matrix at 77 K: (a) $E \perp B$ and (b) $E // B$. (c) The simulated spectrum for the randomly oriented sample.

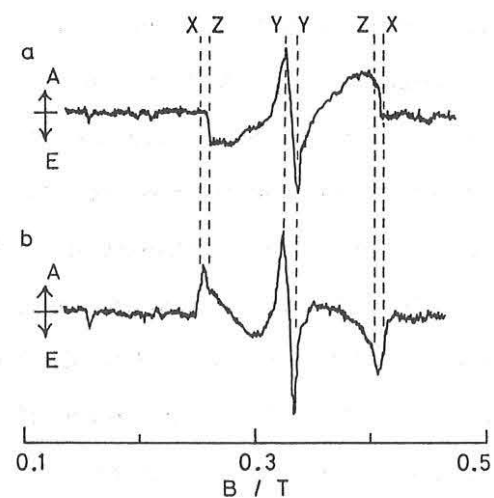
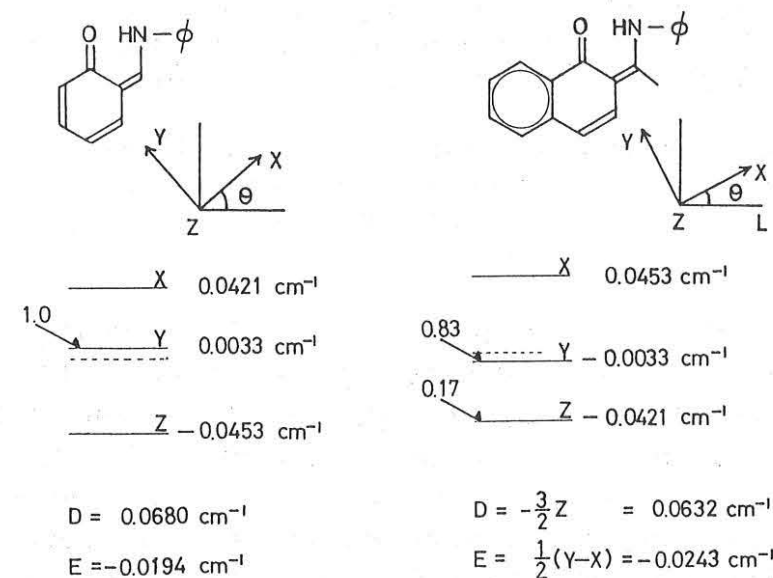


Fig.3 Triplet TREPR spectra obtained by the excitation with the polarized light (384 nm) of the enol form of 2 in a methylcyclohexane glassy matrix at 77 K: (a) $E \perp B$ and (b) $E // B$.



Scheme I

Since the keto-enol equilibrium lies in favor of the enol form in nonpolar solvents, the T_1 state generated from the ESIPT in 2 was also detected by the irradiation with 384 nm (Fig. 3). The intensities of the outermost and innermost pairs increased by the excitation with the polarized light $E // B$ (Fig. 3). The result suggests that the direction of the transition moment of the $S_1(\pi\pi^*)$ state in the enol tautomer deviates from the X axis in the keto form. It is obtained from the semiempirical PPP calculations that the S_1 transition moment of the enol form is nearly parallel to the long axis of the naphthalene moiety.

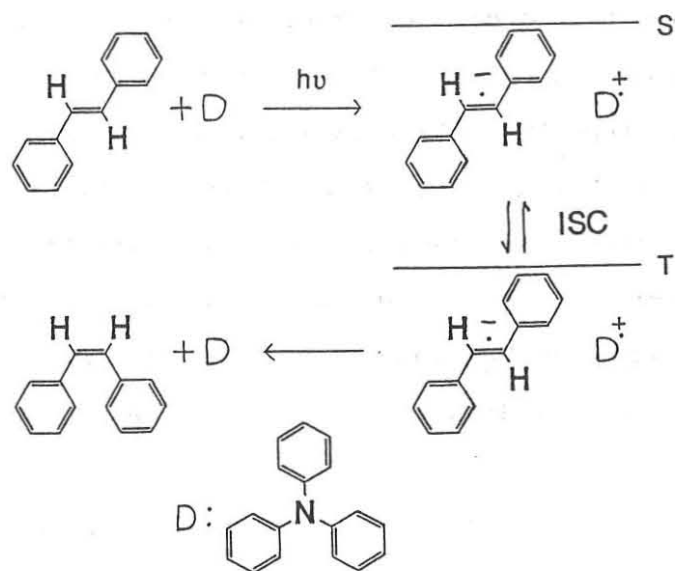
- 1) S.Tero-Kubota, K.Migita, K.Akiyama, and Y.Ikegami, J.Chem.Soc. Chem.Commun. (1988) 1067.

A-5
20:00
~22:00

Effect of Coulomb Force on Diffusion as Studied by CIDNP Intensities of Photo-Induced Electron Transfer Reactions of trans-Stilbene

Takafumi Aizawa, Tomonori Sakata, Kiminori Maeda, Tohru Azumi
Department of Chemistry, Faculty of Science, Tohoku University,
Sendai 980, Japan

The CIDNP intensity of triphenylamine-sensitized isomerization of trans-stilbene is measured. The CIDNP studies carried out by Kruppa et al. show that this reaction takes place via a radical ion pair.^{1,2} (Scheme 1) In this case, the effect of Coulomb force between the positive and negative radical components of each radical pair is important in the diffusional motion of radicals. In order to examine the effect of Coulomb force in the diffusional motion of radicals, the solvent polarity effect of the CIDNP intensity is measured. Theoretical analysis using a stochastic Liouville equation including the effect of Coulomb force in the diffusional motion is carried out.



Scheme 1 Reaction scheme of photo-induced electron transfer reactions of trans-stilbene. Triphenylamine is used as a donor. ISC, intersystem crossing, depends on the nuclear spin, so CIDNP is observed at the peak of cis-stilbene.

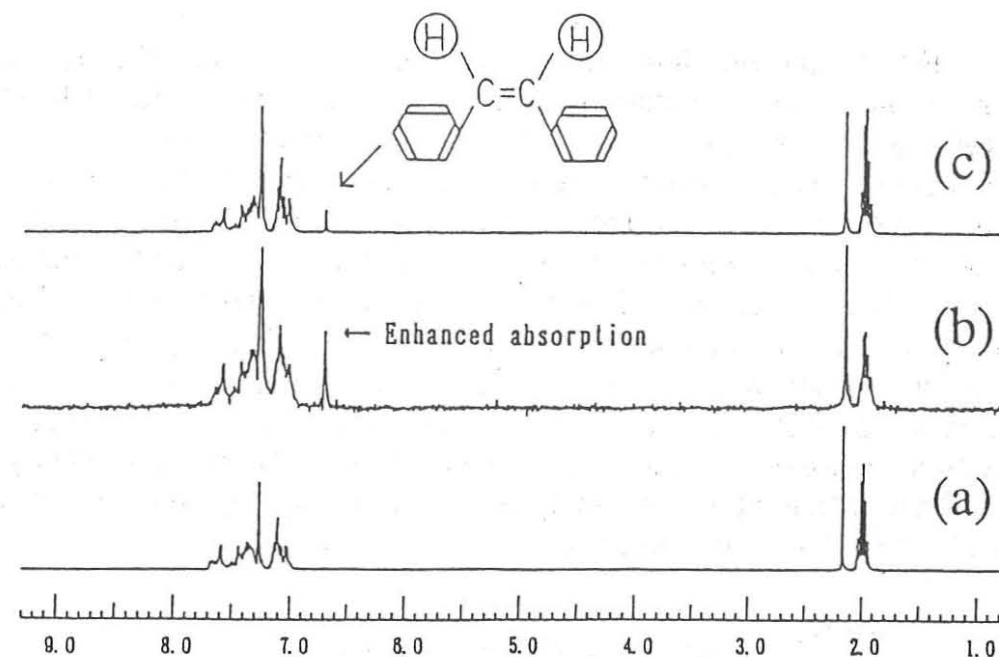


Fig. 1 ¹H CIDNP in trans-cis isomerization of stilbene in the presence of triphenylamine. The enhanced absorption is measured at the peak of cis-stilbene. (a) before irradiation, (b) in the presence of light, (c) after irradiation.

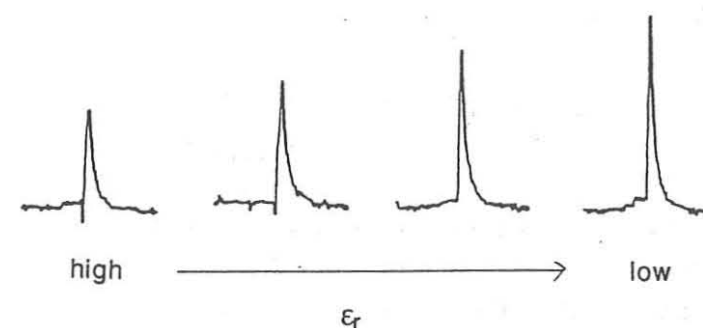


Fig. 2 CIDNP intensities at the peak of cis-stilbene. The CIDNP intensity gets large as the solvent permittivity decreases.

The CIDNP intensities (enhanced absorption for cis-stilbene, see Fig. 1) are measured in solvents of various permittivities. The sample is mixture of 0.02M trans-stilbene and 0.02M triphenylamine. We change the solvent permittivity by varying the mixing ratio of acetonitrile-d₃ ($\epsilon_r=37.5$) and benzene-d₆ ($\epsilon_r=2.28$).

Fig. 2 shows the effect of the solvent permittivity on the proton of cis-stilbene. It is clear that the CIDNP intensity increases as the permittivity of solvent decreases. The CIDNP intensities are determined by both the amount of product and the enhancement factor; however, this experiment is not capable of distinguishing these two factors. Therefore, another experiment was designed to discriminate the two effects. The results show that the enhancement factor is almost independent of the solvent permittivity and only the yield of the reaction product increases with decreasing the solvent permittivity.

This observation is analyzed theoretically by means of a stochastic Liouville equation,

$$\frac{\partial \rho(t)}{\partial t} = -iH^X \rho(t) + D\Gamma \rho(t) + K\rho(t)$$

where $\rho(t)$ is the spin density matrix of the radical pair, H^X is the spin Hamiltonian, K is the reaction operator, and Γ is the diffusion operator. The diffusion operator is expressed as follows:

$$\Gamma = \nabla^2 + \nabla^2 \left(\frac{1}{kT} \right) U \quad U = - \frac{e^2}{4\pi\epsilon_0\epsilon_r r}$$

The second term is added in order to include the effect of Coulomb force.

The results of the calculation are shown in Fig. 3. As the solvent permittivity decreases, the yield of the reaction product first increases (higher permittivity region), and then decreases (lower permittivity region). As the solvent permittivity decreases, the effect of Coulomb attractive force increases. In higher permittivity region as the solvent permittivity decreases the probability of reencounter increases. As a result the yield increases. In lower permittivity region as the solvent permittivity decreases the probability of intersystem crossing decreases. So the yield decreases.

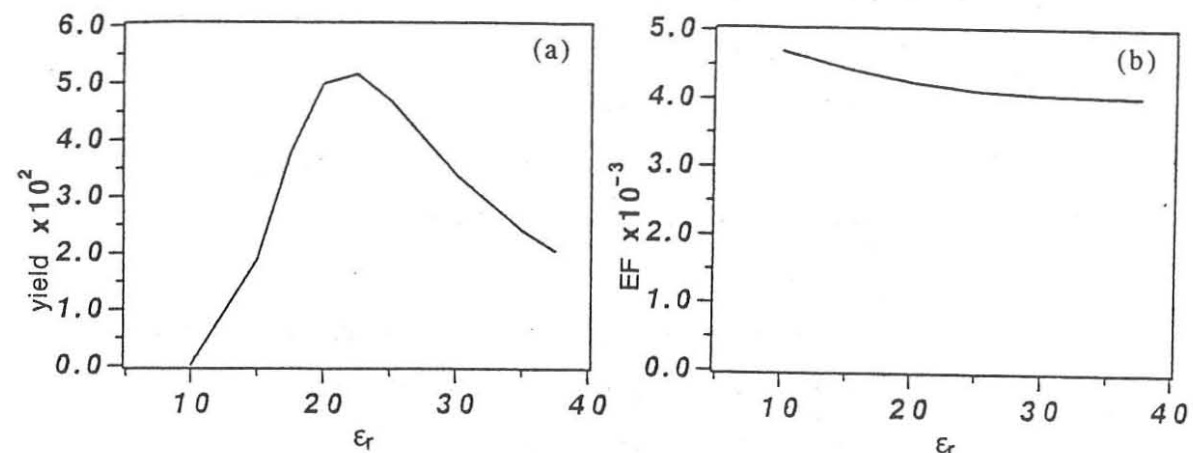


Fig. 3 The results of the calculation. (a) the yield of the reaction product, (b) enhancement factor

The behavior observed experimentally is in accord with theoretical calculations in higher permittivity region. In this region the increase of the probability of reencounter at higher permittivity is more important than the suppression of the probability of intersystem crossing. The Coulomb force affects more to increase the probability of reencounter than to suppress the probability of intersystem crossing.

In conclusion Coulomb force between radicals affects the diffusional motion of radicals. In the present system by the effect of Coulomb force the yield of the reaction product increases as the permittivity of solvent decreases.

References

- 1) T. V. Leshina, S. C. Belyaeva, V. I. Maryasova, R. Z. Sagdeev and Yu. N. Molin, Chem. Phys. Lett., 75, 438(1980).
- 2) A. I. Kruppa, O. I. Mikhailova and T. V. Leshina, Chem. Phys. Lett., 147, 65(1988).

A6
20:00
~22:00

Formation of Novel Radicals from the $\pi\pi^*$ Triplet States of Aromatic Ketones

H. Hayashi, M. Igarashi, Y. Sakaguchi,

The Institute of Physical and Chemical Research,
Wako, Saitama 351-01, Japan

and Y. J. I'Haya

Department of Applied Physics and Chemistry,
The University of Electro-Communication,
Chofu, Tokyo 182, Japan

In the course of the studies of magnetic field effects on photochemical reactions in solution [1, 2], we have carried out CIDEP and CIDNP studies on such reactions as to be influenced by external magnetic fields. In 1985, we found a peculiar CIDEP spectrum due to a cyclohexadienyl-type radical in the reaction of

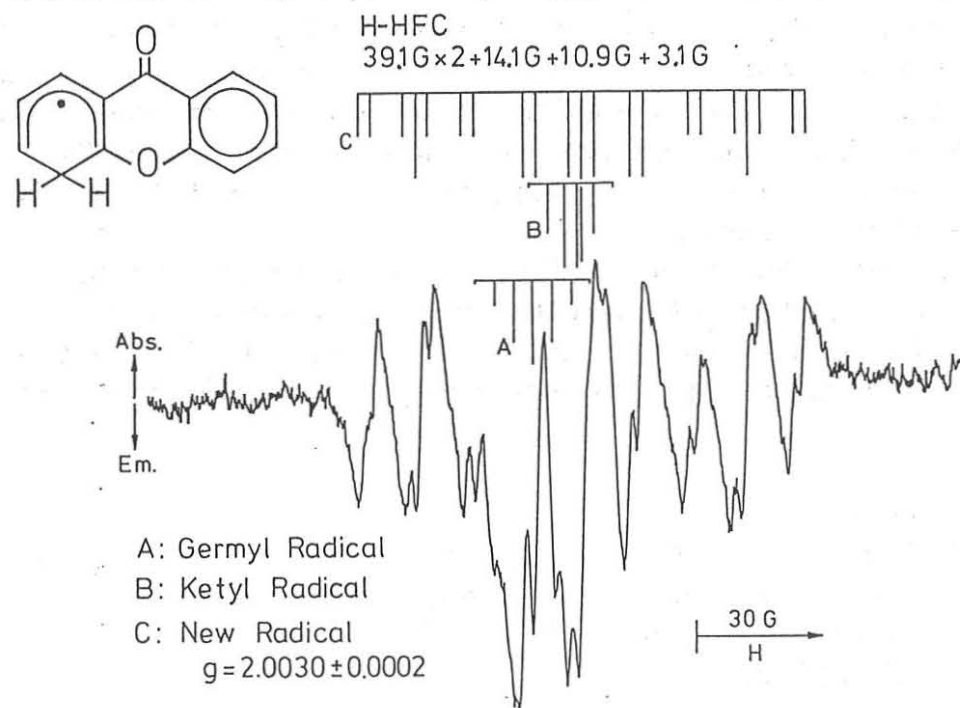


Fig. 1. CIDEP spectrum observed at 1.5 μ s after excitation of the SDS micellar solution containing xanthone and Et_3GeH [3].

triplet xanthone with triethylgermane (Et_3GeH) in an SDS micelle as shown in Fig. 1 [3]. This was not only one of the earliest observation of spin-correlated radical pairs but also the first report on the formation of non-ketyl radicals in the hydrogen abstraction reactions of triplet ketones.

We have also found the formation of cyclohexadienyl-type radicals in the reactions of acetophenone and 2-acetonaphthone [4] and that of benzyl-type radicals in those of flavones [5]. We have found that these novel radicals can be formed with hydride-type hydrogen-donors such as Et_3GeH and tri-n-butylstannane (Bu_3SnH) through the $\pi\pi^*$ triplet states of aromatic ketones.

Since the lowest $n\pi^*$ and $\pi\pi^*$ triplet states of chromone locate close to each other, we have also studied its reaction with Bu_3SnH in 2-propanol with the aid of a CIDEP technique [6]. Fig. 2 shows observed CIDEP spectra. In the absence of Bu_3SnH , the signals due to the 2-propanol (Diagram a of Fig. 2(A)) and ketyl (Diagram b of Fig. 2(A)) radicals were observed. The reaction scheme is represented by Eq.1 of Fig. 3.

In the presence of Bu_3SnH , we have found a new radical (Diagram c of Fig. 2(C)). This radical can be assigned to the α -keto alkyl radical, which is also produced through the $\pi\pi^*$ triplet state of chromone as shown by Eq.4 of Fig. 3. Weak signals due to the cyclohexadienyl-type radical were also observed in Fig. 2(C). This reaction occurs through Eq.6 of Fig. 3.

It is noteworthy that the signals of this α -keto alkyl radical can also be seen in the spectrum measured without Bu_3SnH as shown in Fig. 2(B). This reaction occurs through Eq.2 of Fig. 3. This series of CIDEP studies has revealed that the hydro-

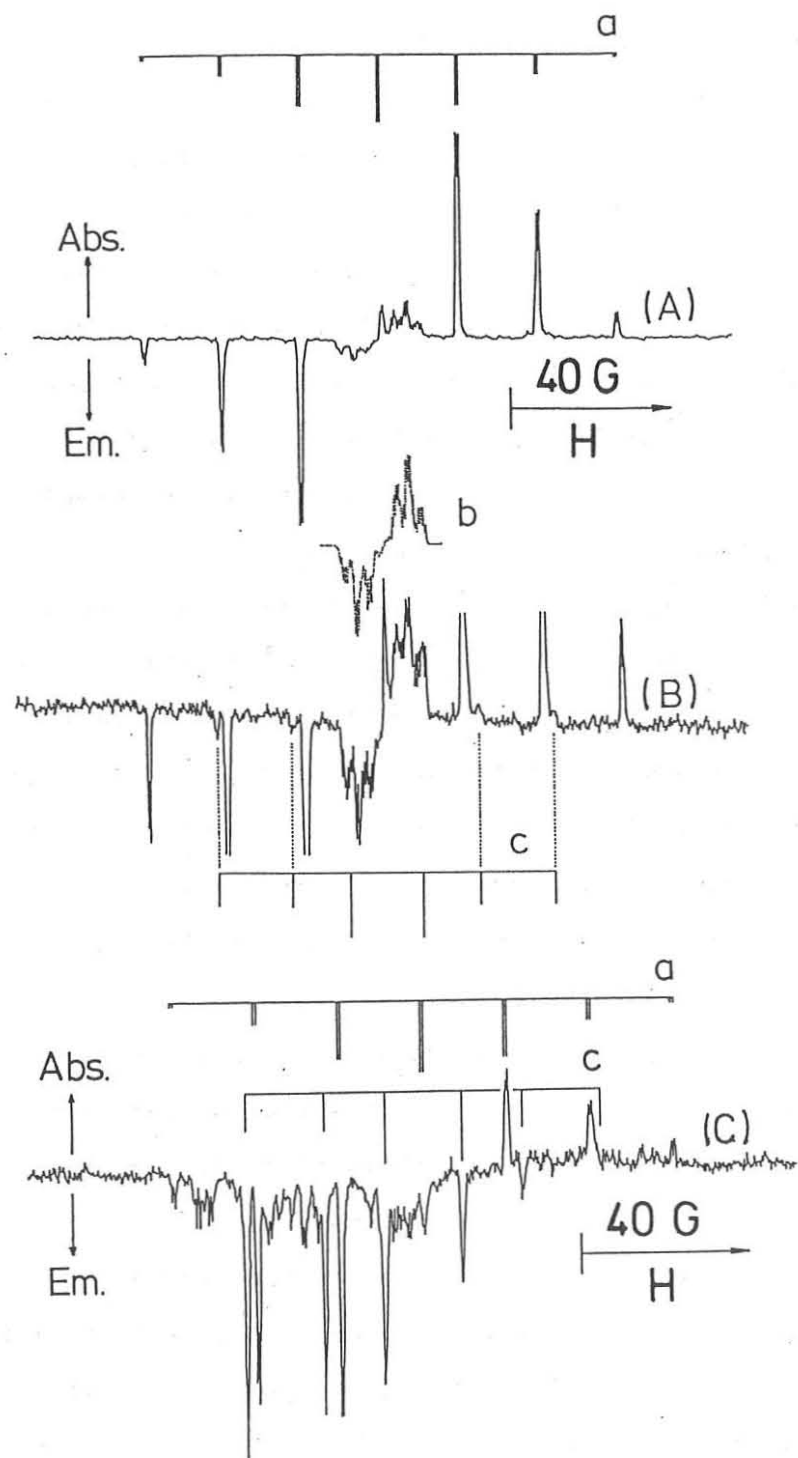
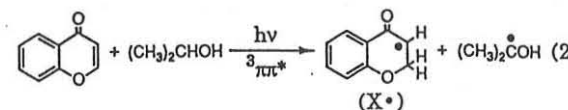
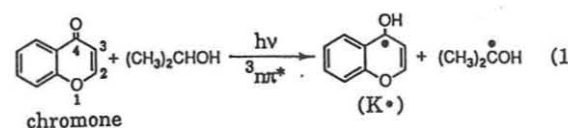


Fig. 2. CIDEP spectra observed for the reactions of triplet chromone in 2-propanol (A and B) without and (C) with Bu_3SnH .

gen abstraction of triplet ketones can occur at C-atoms other than the carbonyl-oxygen with the reactions of not only hydride-type hydrogen donors but also usual ones such as 2-propanol.

In 2-propanol without Bu_3SnH



In 2-propanol with Bu_3SnH

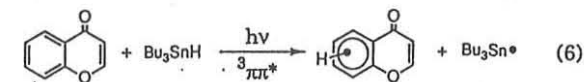
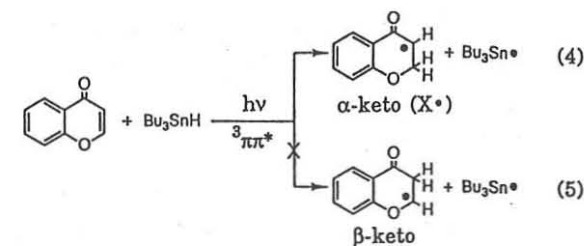
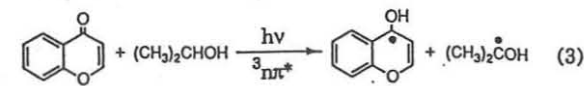


Fig. 3. Reaction scheme of triplet chromone with and without Bu_3SnH in 2-propanol

References

- [1] H. Hayashi in J. F. Rabek (ed.) *Photochemistry and Photophysics*, CRC Press, Boca Raton, Florida, 1990, Vol.1, p.59.
- [2] H. Hayashi and Y. Sakaguchi in J.-P. Fouassier and J. F. Rabek (eds.) *Applications of Lasers in Polymer Science and Technology*, CRC Press, Boca Raton, Florida, 1990, Vol. 2, p.1.
- [3] Y. Sakaguchi et al., *Chem. Phys. Lett.*, 120 (1985) 401.
- [4] H. Hayashi et al., *J. Phys. Chem.*, 90 (1986) 4403.
- [5] Y. Sakaguchi et al., *J. Phys. Chem.*, 90 (1986) 6416.
- [6] M. Igarashi et al., *Chem. Phys. Lett.*, in press.

A-7 CIDNP and CIDEP Studies of Intramolecular
20:00 Hydrogen Abstraction Reaction of
~22:00 Polymethylene linked System.

Kiminori Maeda, Naotoshi Suzuki, Qing-Xiang Meng,
Kouei Suzuki, Masahide Terazima⁺), Tohru Azumi.
Department of Chemistry, Faculty of Science,
Tohoku University, Sendai 980, Japan.
Yoshifumi Tanimoto
Department of Chemistry, Faculty of Science,
Hiroshima University, Hiroshima 730, Japan.

Intramolecular hydrogen abstraction reaction of a polymethylene linked xanthone and xanthene (XO-(n)-XH₂ n=3,6,12) was investigated by using chemically induced dynamic nuclear and electron polarization (CIDNP and CIDEP) methods. In this system, the biradical lifetime has been obtained from the transient absorption, and the effect of the exchange interaction was suggested mainly from the magnetic field effects of the biradical lifetime.¹⁾ But it is difficult to measure the exact value of the exchange integral with using the optical methods. In this study, the exchange integral J between the two terminal radicals of the polymethylene linked system is obtained from both of the simulation of the radical pair CIDEP spectrum and the magnetic field effect of the low field CIDNP respectively.

The CIDEP spectrum of XO-(12)-XH₂ at -60°C is shown in Figure 1. This CIDEP spectrum cannot be interpreted either by the conventional radical pair mechanism or by the triplet mechanism and can be simulated based on the spin correlated radical pair CIDEP mechanism. In the simulation process of this CIDEP, we used the spin correlated CIDEP theory shown in Figure 2 modified with (a) the fast population relaxation between the central S-T₀ mixed state,²⁾ (b) the contribution from the triplet mechanism, and (c) hyperfine line dependent line width.³⁾ We changed J value as the fitting parameter and simulate the observed spectrum. The observed spectrum can be reproduced well with $-0.0 > J > -0.18\text{mT}$. Figure 1 b is an example of the simulation spectrum with

⁺) Present address: Department of Chemistry Faculty of Science, Kyoto University, Kyoto, Japan.

1) Tanimoto, Y.; Takashima, M.; Hasegawa, K.; Itoh, M. *Chem. Phys. Lett.* 1987, 137, 330.

2) Terazima, M.; Maeda, K.; Azumi, T.; Tanimoto, Y.; Okada, N.; Itoh, M. *Chem. Phys. Lett.* 1989, 164, 562.

3) Maeda, K.; Terazima, M.; Azumi, T.; Tanimoto, Y. *J. Phys. Chem.* 1991, 95, 197.

$J=-0.1\text{mT}$, $\alpha=6.5\times 10^{-3}$. The finite value of α means that the triplet mechanism exists in the spin correlated radical pair CIDEP spectrum. The agreement between the calculated and observed CIDEP is very good. From the simulation the effective J value of the intermediate biradical is determined for the three different polymethylene chains.

The low field CIDNP spectrum of XO-(3)-XH₂ below 25mT shows total emission pattern. In Figure 3, the spectrum measured at 5mT is depicted for example. The pattern is totally different from that measured in high magnetic field (2.5T) reported previously. The spectrum in high field is satisfactorily explained by the S-T₀ mixing mechanism and the Kaptein's rule is used for the assignment of the observed peaks. The total emission feature in low field, on the contrary, can be explained well by the S-T-mixing mechanism. In the biradical system, the exchange integral J value is significant because of restriction of interradical diffusion and the S-T-mixing is effective. In ref.3 we have assigned the peak at 4.5 ppm to the methine proton of intramolecular geminate recombination product from the high field CIDNP spectrum.

The magnetic field dependence of the CIDNP signal intensity of this peak is shown in Figure 4. We simulated the magnetic field effect curve with the stochastic Liouville method. For the simulation spectrum, the reported hyperfine coupling constants of the individual radicals are used. The difference of the g values between XOH and XH is too small to be determined from the CIDEP spectrum in the hydrogen abstraction reaction of free xanthone from the xanthene. The same g value (2.00331) for the two radicals was used. The hyperfine coupling constant $A=1.264\text{ mT}$ and the parameter $J_0=-9.48 \times 10^8\text{ mT}^4$ from the literature and $\alpha = 1.80\text{ \AA}^{-1}$ as the fitting parameter. The effective diffusion constant calculated from the solvent viscosity 5×10^{-5} is used for the effective diffusion constant D'. We used the kinetic parameter $k_T=1.0 \times 10^8\text{ s}^{-1}$ and $k_S=1.0 \times 10^6\text{ s}^{-1}$. They are almost the same with the other work and the curve of the magnetic field effect is not sensitive to such kinetic parameters.

The magnetic field effect of the CIDNP polarization in XO-(n)-XH₂ n=3,6,12 is shown in Figure 4. The curve of the magnetic field effect is normalized by the peak intensity. The peak positions of the magnetic field effects shift to high field with decreasing the chain length n. This shift indicates that the |J| value increases with the decrease of the chain length. The probability function P₀(r) of the interradical distance in the

4) Kanter, F.J.J.; Sagdeev, R. Z.; Kaptein, R. *Chem. Phys. Lett.* 1978, 58, 334.

equilibrium shows that the mean distance between the radicals (XOH and XH) increases with the increase of chain length.

The $|J_{\text{eff}}|$ value of the XO-(n)-XH₂ determined from the magnetic field dependence of the low CIDNP intensity and spin correlated CIDEP methods are shown in Table 1. Both of the methods shows increasing of the absolute $|J|$ value with decreasing of the polymethylene chain length n. But the absolute $|J|$ value observed from low field CIDNP is larger than that of spin correlated CIDEP spectrum. This difference suggests that the two methods observe different components of biradicals; CIDEP method can observe the conformers which have longer interradsical distance, and CIDNP is sensitive to those of relative shorter distance.

From Table 1 $|J_{\text{eff}}|$ is shifted to larger value in shorter interradsical chain length. Recently Tanimoto et. al. reported the magnetic field effects on the biradical lifetime in this system. They suggested that the chainlength dependence of the biradical lifetime is the effect of the change of the $|J|$ value. Mainly the decay of the biradical is caused by the geminate recombination between the terminal radicals. The geminate recombination products, which shows CIDNP, is formed through the geminate recombination process concerned with the decay of the biradicals. Therefore the $|J_{\text{eff}}|$ from CIDNP seems to be better to explain the chainlength dependence of the magnetic field effect of biradical lifetimes. Indeed, the shift of the J value obtained from CIDEP is so small that it is difficult to explain the result of the transient absorption, but the shift of the $|J_{\text{eff}}|$ obtained from CIDNP is larger than that of CIDEP and more explainable to the chainlength dependence of the magnetic field effect.

Table 1

The effective J values obtained from the CIDEP spectrum and the magnetic field effect of CIDNP.

	$ J_{\text{eff}} (\text{CIDEP})/\text{mT}$	$ J_{\text{eff}} (\text{CIDNP})/\text{mT}$
n=3	~ 7.0	2.5
n=6	0.28 ~ 0.38	1.5 ~ 2.5
n=12	~ 0.18	1.3 ~ 1.7

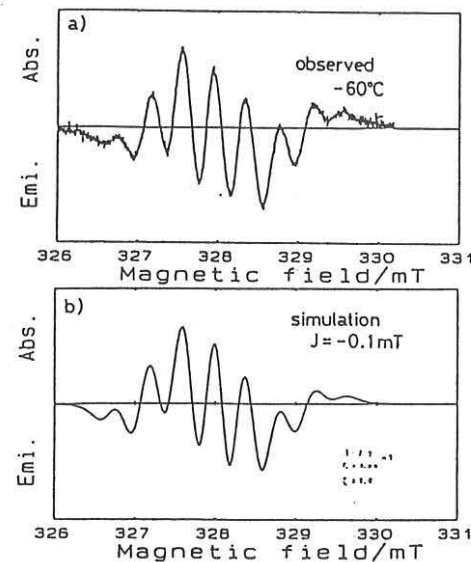


Figure 1
a) The CIDEP spectrum of XO-(12)-XH₂ at -60°C. Delay time is 1 μs. b) Simulation spectrum.

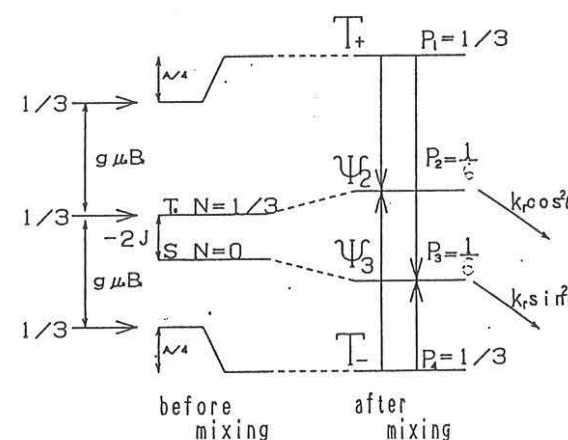


Figure 2
Spin correlated radical pair CIDEP theory.

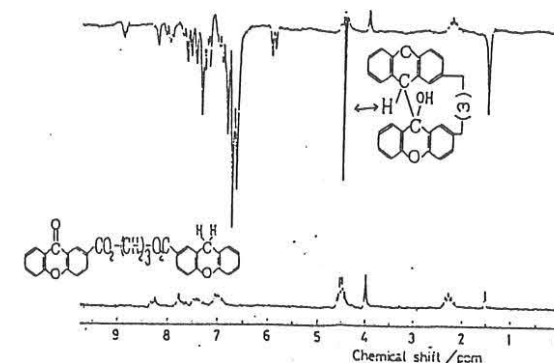


Figure 3
The CIDNP spectrum of XO-(3)-XH₂ in the magnetic field 5mT.

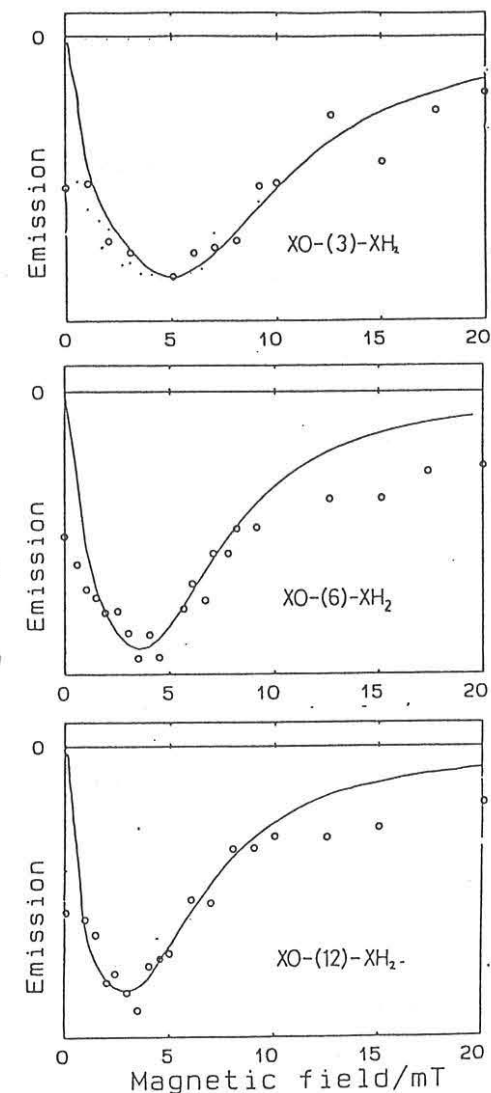


Figure 4
Magnetic field effect of CIDNP intensity.
(a) XO-(3)-XH₂, (b) XO-(6)-XH₂, (c) XO-(12)-XH₂.

DMPO [1]. Also it was found that oxidative conversion of DMPO to HDMPN was accelerated by the addition of ferric ion to sonicated aqueous DMPO solution which contains both DMPO and DMPO-OH. The reaction intermediate, from which HDMPO and HDMPN formed, was, therefore, found to be DMPO-OH (Fig.2). Unidentified background ESR signals in biological systems were consistent with nitroxide radicals (HDMPO-OH and DMPOX) that were oxidized HDMPO and HDMPN by hydroxyl radical (Fig.2). Conclusively it has been elucidated that in the system, DMPO-Fe(III) complex is immediately formed and through the reactions due to this complex, DMPO-OH is produced by nucleophilic addition of water molecules, which is further deprotonated to produce oxidation products. These products have been found here to give rise to such background ESR signals.

Also, we investigated fundamental reactions of various analogous spin traps such as 2,5,5-trimethyl-1-pyrroline-N-oxide (M₃PO) and 3,3,5,5-tetramethyl-1-pyrroline-N-oxide (M₄PO). (Fig.3) M₃PO was not subjected to the reactions described above, because of CH₃ group at C2. M₄PO was degraded at the lower rate due to the CH₃ groups at C3. These results are consistent with the above conclusion.

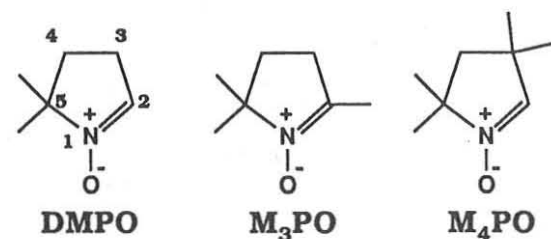


Fig. 3 Spin traps studied in the present study.

In summary, we would stress that in the presence of Fe(III), DMPO-OH is produced through the formation of DMPO-Fe(III) complex followed by the nucleophilic addition of water molecule to the DMPO and the elimination of

hydrogen atom. This will result in the misleading ESR signals. Also, it has been found that DMPO-OH is an intermediate for the production of HDMPO and HDMPN which will give rise to ESR signals in the presence of oxidative species. This also makes it difficult to analyze ESR signals obtained. Since these series of reactions are accelerated when H₂O₂ coexists in the systems, assignment of each ESR signal obtained in systems such as some biological samples should be carried out extremely carefully. Such undesirable reactions could be prevented by using spin traps which have CH₃ at C2.

Reference

- [1] K. Makino, T. Hagiwara, A. Hagi, M. Nishi, and A. Murakami, BBRC, 172 (1990) 1073.

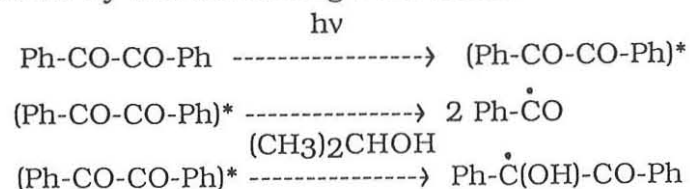
A9

20:00
~22:00

CIDEP of Benzil

Masahiro Mukai, Seigo Yamauchi⁺ and Noboru Hirota
Department of Chemistry, Faculty of Science
Kyoto University, Kyoto 606, Japan

CIDEP studies of benzil in 2-propanol have shown anomalous polarizations of the radicals involved.¹⁾ Transient radicals detected by TREPR(time-resolved EPR) are benzoyl and benzil ketyl radicals produced by the following reactions,



The TREPR spectra of both radicals show emissive signals (Fig.1).

This polarization is considered to be due to TM (triplet

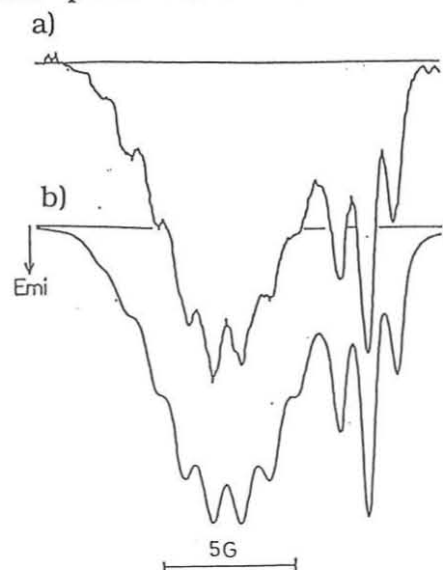


Fig.1, CIDEP spectrum of benzil in 2-propanol
a) observed, b) simulated

mechanism), but cannot be explained on the basis of the reactions from the T₁ state of benzil, because absorptive signals are expected for the reactions from T₁ benzil. It was found that the signal intensities are proportional to the square of the intensity of the excitation laser. These observations led us to propose that the reactions take place from higher excited triplet

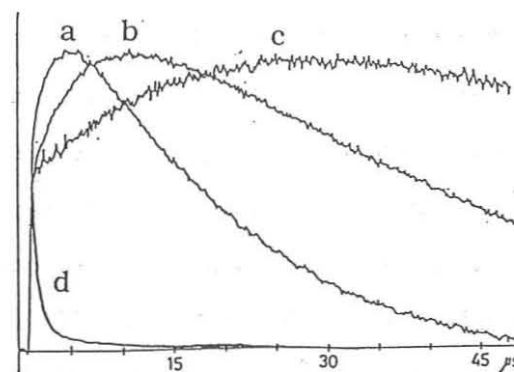


Fig.2, Time profiles of the CIDEP signals. Benzil ketyl, a) -10°C, b) -40°C, c) -70°C, benzoyl radical d), under nitrogen bubbling

to the emissive signals observed immediately after the photolysis there is a slow rising component in the ketyl signal. This slow component becomes quite evident at lower temperatures as shown in Fig.2. Here we try to clarify the mechanism to produce this slow component.

It was recently suggested by Blättler et al.²⁾ that such a slow rising polarization might be produced by the encounter between the radical and triplet molecule (Radical Triplet Pair Mechanism, RTPM). We first consider this possibility. Since this mechanism requires the presence of relatively

long-lived triplet state, we have compared the CIDEP signals under nitrogen and oxygen bubbling conditions. The triplet state of benzil is quenched effectively by oxygen and the triplet lifetimes under oxygen bubbling conditions becomes 0.2 and 0.3 μs at -10

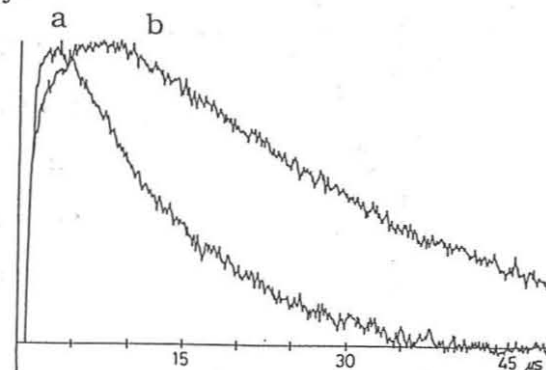


Fig.3, Time profiles of the CIDEP signals of ketyl radical under oxygen bubbling, a) -10°C, b) -40°C

states via two-photon processes.¹⁾ Fig.2 shows the time profiles of the CIDEP signals of the benzil ketyl and benzoyl radicals. The benzoyl radical signal decays very rapidly presumably because of a very fast spin-lattice relaxation time, but the decay of the ketyl signal is very slow. In addition

and $-40\text{ }^{\circ}\text{C}$, respectively. They are about fifty times shorter than those under nitrogen bubbling conditions. As shown in Fig.3 the time profiles of the ketyl signals under oxygen bubbling conditions also show slow rising components as under nitrogen bubbling conditions, though the rise times as well as the signal intensities somewhat decreased. This result clearly indicates that the RTPM cannot account for the slow rising polarization entirely, though it may contribute partly.

Next we consider the free pair RPM (Radical Pair Mechanism).³⁾ Both benzoyl and benzil ketyl radicals are stable and long-lived. Since the g value difference between the benzoyl and the ketyl radicals is significantly large, it is possible to obtain a relatively large emissive signal of the benzil ketyl. In this case the benzoyl radical is expected to give an absorptive signal. The absorptive signal was not detected experimentally, but this observation may be rationalized on the basis of a very short spin

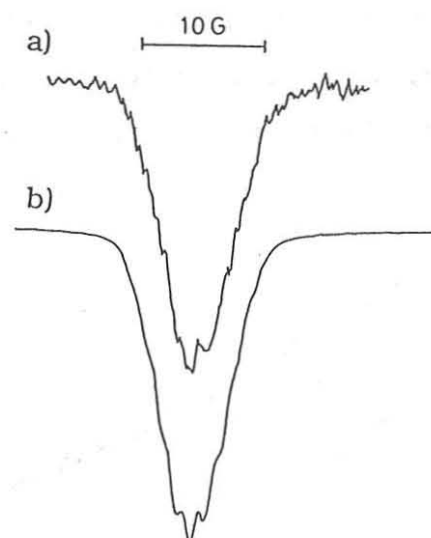


Fig.4, Spectrum of the benzil ketyl at a longer time
a) observed at $t=20\mu\text{s}$
b) simulated by the RPM

lattice relaxation time of the benzoyl radical. The spectrum simulated for the benzil ketyl radical by the RPM is shown in Fig.4 together with the spectrum observed at $20\mu\text{s}$ after photolysis. The agreement between the observed and the simulated spectra are considered to be satisfactory. The rise and decay of the ketyl signal become very slow at low temperatures as shown in Fig.2, indicating that the polarization is dependent on the diffusion process

in solution. The time profile of the slow rise and decay are also affected by the laser intensity as shown in Fig.5. These observations are considered to be consistent with the free pair RPM.

In conclusion we think that the free pair RPM is most likely to be the main mechanism to produce the slow rising emissive polarization observed in the photolysis of benzil.

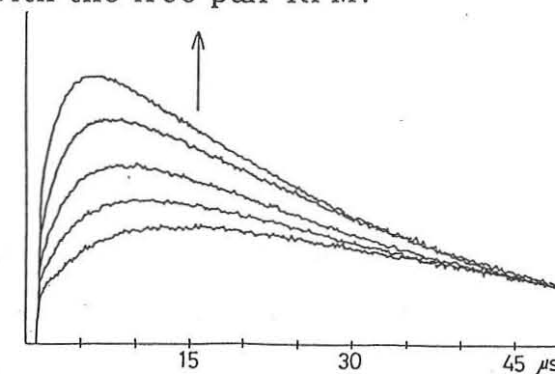


Fig.5, The dependence of the time profile of the benzil ketyl signal on the laser intensity

References

- (1) M.Mukai, S.Yamauchi and N.Hirota, *J.Phys.Chem.* 93(1989)4411
- (2) C.Blattler, F.Jent and H.Paul, *Chem.Phys.Lett.* 166(1990)375
- (3) J.B.Pedersen, *J.Chem.Phys.* 59(1973)2656

+ present address

Institute for Chemical reaction Science,
Tohoku University, Sendai 920, Japan

A10

20:00

~22:00

Investigation of Novel Radical Pair Interaction:
Ionic System and Micellar System.

Hisao Murai, Hidekazu Honma, Natsuo Ishiwata and
Keiji Kuwata

Department of Chemistry, Faculty of Science,
Osaka University, Toyonaka, Osaka 560, Japan

Recent development of CIDEP studies is clarifying the details of the radical pair interactions as the important initial steps of chemical reaction. These interactions are also known to be the cause of the external magnetic field effects on chemical reaction. The investigation of radical pair interactions, however, has not been completed yet. In this presentation, quite novel phenomena of radical pair interactions observed by the aid of a time-resolved ESR technique will be given concerning two independent systems. First system is the photooxidation of *N,N,N',N'*-tetramethyl-*p*-phenylenediamine (TMPD) with maleic anhydride (MA), and an ionic interaction between two geminate radicals is postulated. In the second system, a new information of radical pair formed in the photoreaction of xanthone (Xn) with phenol derivatives in well known SDS micelles is presented. In both systems, the exchange interaction may play an important role.

A DC detected X-band time-resolved ESR spectrometer and a boxcar integrator (or a transient memory combined with a computer) were used for the CIDEP measurements. In the first system, an excimer laser ($\lambda = 351$ nm) was mainly used for the light source. The concentration of TMPD was 1.2×10^{-2} M. The concentration of MA was varied from 5×10^{-4} to 3×10^{-2} M. 2-Propanol was mainly used as the solvent. In the second system,

an excimer laser ($\lambda = 308$ nm) was used for the excitation. The concentrations of Xn and SDS in distilled water were 1×10^{-3} M and 5×10^{-2} M, respectively. As the phenol derivatives (1×10^{-3} M), 2,6-di-*t*-butylphenol (DTBP), 2,4,6-tri-*t*-butylphenol (TTBP) and 2,6-di-*t*-butyl-*p*-cresol (DTBC) were employed.

1) Enhanced S-T₁ Mixing of Radical Ion Pair¹⁾

Fig. 1a shows the CIDEP spectrum observed in the photolysis of TMPD in the presence of the high concentration of MA (3×10^{-2} M) in 2-propanol. This spectrum is assigned to the anion radical of MA, and the polarization pattern is explained by the superposition of an E/A pattern of the RPM (S-T₀ mixing) on the emissive TM. It is concluded that this reaction takes place via the excited triplet state of TMPD.



Fig. 1b shows the CIDEP spectrum observed under the condition of the low concentration of MA (5×10^{-4} M). As shown in this figure, the low and middle resonant field lines show almost the same intensity, while the highest one almost disappears or shows a weak E/A shape. Under the low concentration region of MA (2×10^{-3} - 5×10^{-4} M), the polarization pattern did not alter, and the rise of the signal depended on the concentration of MA, probably because it reflected the reaction rate. Under these conditions, the contribution of

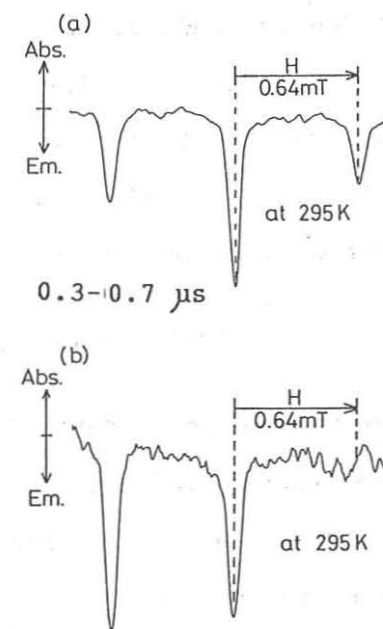
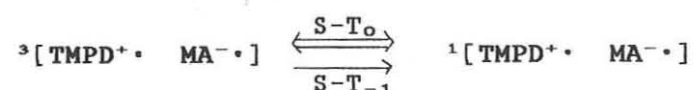


Fig. 1. trESR spectra of MA^{•-}.

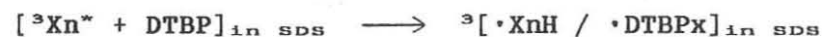
TM to the emissive component is unlikely. In fact, the plots of the ratio of the emissive TM-like component and the E/A pattern component versus MA concentration indicate that the TM contributes to the emissive component under only the high concentration region of MA. At this stage it is tentatively proposed that the emissive component under the condition of the low concentration of MA is due to the S-T₋₁ mixing of the radical ion pair.



The S-T₋₁ mixing may be enhanced by the coulombic interaction of the geminately formed ion radicals. It should be noted that the S-T₋₁ mixing occurs even under the conditions of small hfc of radicals, the ordinary non-viscous solvent such as 2-propanol, and also at room temperature in this particular system.

2) Special Radical Pair in an SDS Micelle

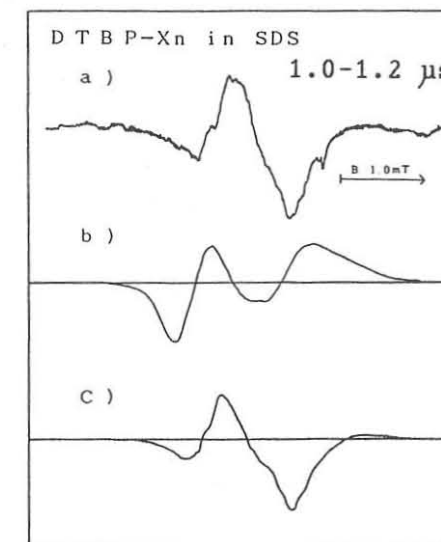
Fig. 2a shows the trESR spectrum of radical pair observed in the photolysis of xanthone and DTBP in an SDS micelle in aqueous solution. In this system, Xn exclusively reacts with DTBP to form metastable radical pair in the micelle.



where $\cdot\text{XnH}$ and $\cdot\text{DTBPx}$ denote xanthone ketyl radical and di-*t*-butylphenoxy radical, respectively.

There are two distinct points which are newly discovered in this system. (1) the signal decayed for a few μs with keeping the same spectrum pattern. (2) The calculation trial of this spectrum by the ordinary assumption of radical pair failed as

shown in Fig. 2b. The same phenomena were observed when TTBP and DTBC were used. The unusual spectrum shape (2) was finally reproduced by introducing quick relaxation between middle two mixed states to the calculation (Fig. 2c where a slight emissive component is added). The phenomenon (2) in an SDS micelle



is very similar to that reported in the system of methylene linked biradicals²⁾. This fast relaxation must have something to do with the exchange interaction between two spins.

It is noteworthy that the radical pairs in micelles reported so far show the conversion of the spectrum to the normal S-T₀ mixing (an E/A pattern)³⁾, while no S-T₀ mixing appears in this system. The preservation of the spectral pattern (1) implies that the diffusional motion of these particular radical pair systems is anomalously slow in the restraint environment.

References

- [1] Preliminary report appeared in 29th ESR symposium at Tokyo (1990).
- [2] M. Terazima, K. Maeda, T. Azumi, Y. Tanimoto, N. Okada and M. Itoh, *Chem. Phys. Letters*, (1989) **164**, 562.
- [3] Y. Sakaguchi, H. Hayashi, H. Murai and Y. J. I'Haya, *Chem. Phys. Letters*, (1984) **110**, 275; Y. Sakaguchi, H. Hayashi, H. Murai, Y. J. I'Haya and K. Mochida, *Chem. Phys. Letters*, (1985) **120**, 401.

A-11 Temperature Dependence of the Magnetic Field Effect of the
CIDNP in the Photocleavage of Cycloalkanone

20:00
~22:00

Naotoshi Suzuki, Kiminori Maeda, Qing-Xiang Meng,
Kouei Suzuki, Masahide Terazima[†], Tohru Azumi.

Department of Chemistry, Faculty of Science, Tohoku
University, Sendai 980, Japan

[†] Present address: Department of Chemistry, Faculty of
Science, Kyoto University, Kyoto, Japan

Biradicals generated from the Norrish type I reaction of
cycloalkanone have been well investigated. In this system the
biradical chain dynamics is connected with the spin dynamics
through the exchange integral J . So the interradsical distance
is very important for the reaction of biradicals.

Wang et al. reported the temperature dependence of the
biradical lifetimes in the substituted cycloalkanone, and
discuss the mechanism of intersystem crossing from Arrhenius
plots¹. This temperature dependence is caused by the
temperature dependence of the mean end to end distance of the
biradical. Recently we found an evidence of the shrinking of
the intermediate biradicals in the polymethylene linked systems
through the simulation of the radical pair CIDEP spectrum².
Staerk et al. recently reported the temperature dependence of
the magnetic field effect on reaction yield of radical ion pair
linked with polymethylene chain³. The peak position of
magnetic field effect curve shifts to the higher field at the

higher temperature. They explained the temperature dependence
of this magnetic field effect as due to motional shift rather
than the shrinking of the end-to-end distance.

In this work, we measured the magnetic field effect
(MFE) of CIDNP on the photocleavage of cyclodecanone in various
temperatures, and determined the effective J value of the
biradicals in each temperature from the peak position of the
MFE of CIDNP. We simulated this curve with a stochastic
Liouville equation⁴, and discuss the cause of the temperature
effect.

We used sample flow system in order to measure the
magnetic field effect of CIDNP. The measurement is performed
at -9, 4, 23, 40 °C. The NMR spectrum before and during light
irradiation of cyclodecanone are shown in Fig.1. All peaks of
spectrum are emissive. This fact indicate that S-T₁ mixing
mainly contributes to the intersystem crossing.

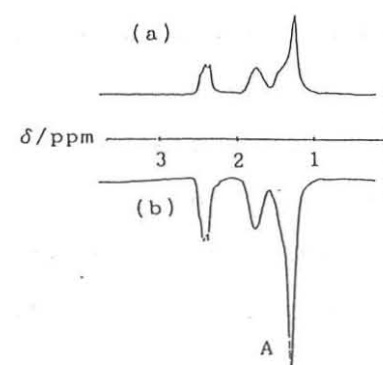


Fig 1 NMR spectrum of cyclodecanone (0.03 M) in chloroform-d at
room temperature: (a) before the light irradiation, (b)
during the light irradiation in the magnetic field $B=80\text{mT}$.

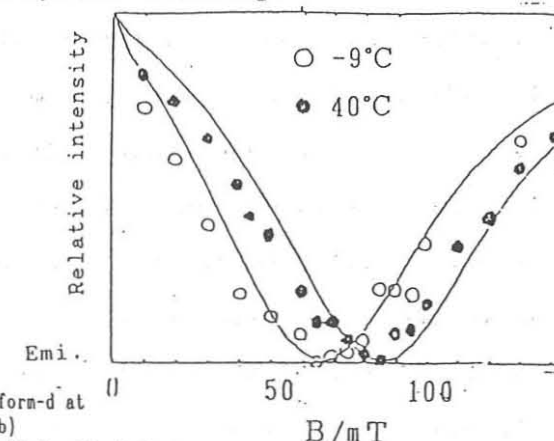


Fig 2 The temperature dependence of HFE on CIDNP of
cyclodecanone at -9°C and 40°C, solid curve is simulation
spectrum with parameters shown in Table.2.

We observed the temperature dependence of magnetic field effect
on CIDNP signal of peak A marked in Fig.1. The temperature

dependence of MFE of CIDNP of cyclodecanone is shown in Fig.2. The peak position of the MFE curve shifts to higher field at higher temperature. When the exchange interaction is negative and relatively large compared with the hyperfine interaction, T₋S mixing plays the most important role. The maximum T₋S mixing and the maximum nuclear polarization must arise in the field when the T₋S mixing appear in resonance. So the effective exchange integral J_{eff} is related with the magnetic field B_{max} which cause resonance in T₋S mixing, as

$$g\mu_B B_{\text{max}} = 2J_{\text{eff}}$$

Therefore we can obtain the effective $|J_{\text{eff}}|$ value from the peak position of MFE of CIDNP. The effective exchange integral J thus determined at various temperatures are shown in Table.1. The effective J value increases as temperature increases.

In order to clarify the cause of the shift of the MFE curve, we simulated this curve with the stochastic Liouville equation proposed by Kanter et al. We examine the temperature dependence of the diffusional motion and that of the distribution of interradsical distance. The diffusional motion of biradical is discussed by the restricted diffusion model. With the neglected the activation energy of C-C bond rotation neglected, the effective diffusion constant D' is related with the viscosity of solvent by Einstein-Stocks equation. The effective diffusion constant D' is varied from 7.6×10^{-5} (-9°C) to 15.1×10^{-5} (40°C). If the temperature dependence of the distribution function is neglected, the peak in the calculated the MFE curve is independent of the effective diffusion constant D' . This means that the temperature dependence of the

distribution function plays an important role. The distribution function is calculated by the following method. The only three conformations around the C-C bond is taken into account in the polymethylene chain. The all conformations of the polymethylene chain are counted up. The distribution function at an interradsical distance r can be obtained at any temperature from the Boltzmann factor of individual conformations. The results show that temperature dependence of the mean interradsical distance r_{av} is small, but none the less meaningful.; $r_{\text{av}}(40^\circ\text{C}) \approx 9.15\text{\AA}$, $r_{\text{av}}(-9^\circ\text{C}) \approx 9.29\text{\AA}$. We simulate the MFE of CIDNP with this distribution function. Parameters shown Table.2 can fit the experimental MFE curve. Therefore we conclude that the shift of J_{eff} with temperature is caused by temperature dependence of distribution function.

Table 1 The temperature dependence of the exchange integral J determined from MFE of CIDNP of cyclodecanone.

	$J_{\text{eff}} / \text{mT}$
-9°C	33
4°C	36
22°C	39
40°C	42

Table 2 The parameter used for simulation of MFE of CIDNP.

$J_0 / \text{rad} \cdot \text{s}^{-1}$	0.65×10^{15}
$\alpha / \text{\AA}^{-1}$	1.43
	7.6×10^{-5}
	(-9°C)
	9.4×10^{-5}
	(4°C)
$D / \text{cm}^2 \cdot \text{s}^{-1}$	12.0×10^{-5}
	(22°C)
	15.1×10^{-5}
	(40°C)

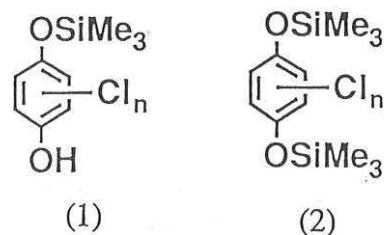
1. Wang, J.; Doubleday, C.; Turro, N.J. J. Am. Chem. Soc. 1989, 111, 3962
2. Maeda, K.; Terazima, M.; Azumi, T.; Tanimoto, Y. J. Chem. Phys. 1991, 95, 197
3. Staerk, H.; Busmann, H.G.; Kühnle, W.; Treichel, R. J. phys. Chem. 1991, 95, 1906
4. Kanter, F.J.J.; Hollander, J.A.; Huizer, A.H.; Kaptein, R. Mol. phys. 1977, 34, 857

Photo-Induced Electron Transfer Reaction Between Hexamethyl-
disilane and Quinones as Studied by CIDNP Technique

Masanobu Wakasa, Masatoshi Igarashi, Yoshio Sakaguchi,
and Hisaharu Hayashi
The Institute of Physical and Chemical Research, Wako,
Saitama 351-01 (Japan)

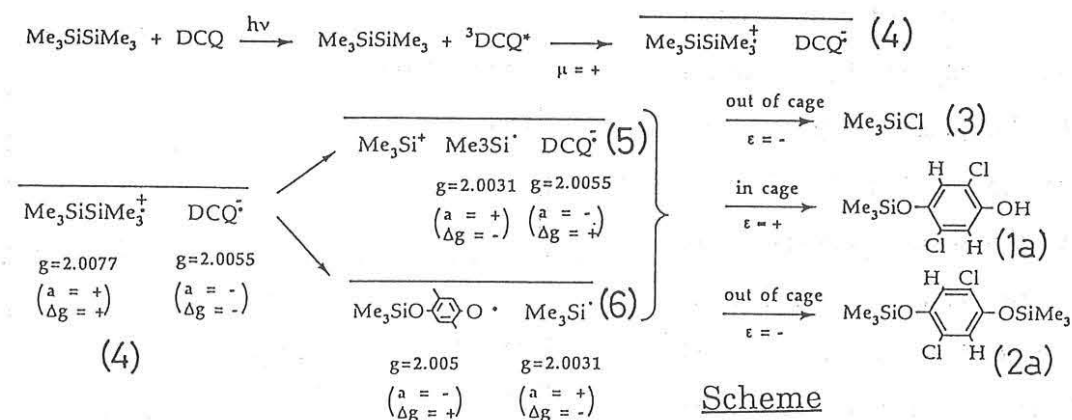
The σ -bonds between group 14 elements (Si-Si, Ge-Ge, Sn-Sn etc.) have rather low ionization potentials [1], and the photo-induced electron transfer between group 14 element compounds and electron acceptors have been studied for interests in the reaction mechanism and the synthetic chemistry during last decade [2]. However, there has been no report elucidating clearly the reaction intermediates and mechanism. In addition, almost all reports use nitriles like cyanobenzenes and cyanoethylenes as electron acceptors. Then, we used quinones instead of nitriles as electron acceptors, and carried out the photo-induced electron transfer reactions of hexamethyldisilane ($\text{Me}_3\text{Si-SiMe}_3$) with high potential quinones (Q's); 1,4-benzoquinone (BQ), chloro-1,4-benzoquinone (MCQ), 2,5-dichloro-1,4-benzoquinone (2,5-DCQ), 2,6-dichloro-1,4-benzoquinone (2,6-DCQ), and tetrachloro-1,4-benzoquinone (TCQ). Based on the CIDNP spectra and product analysis, we describe their reaction intermediates and mechanism [3].

Chloroform solution of $\text{Me}_3\text{Si-SiMe}_3$ (273 mM) and quinones (2,5-DCQ and 2,6-DCQ; 252 mM) were irradiated with a 1-kW high pressure mercury lamp under a nitrogen atmosphere. The products were analyzed by GC and GC-MS. The main products were dichloro-4-trimethylsiloxyphenols (1), dichloro-1,4-bis-(trimethylsiloxy)benzenes (2) and trimethylsilyl chloride (3).



The mass spectrum of 1a (2,5-dichloro-) formed in CDCl_3 showed the same parent m/e peak ($M^+ 250$) observed in CHCl_3 . By means of the NMR spectrum measurement, the hydroxyl-H of 1a is not deuterium. In addition, the strong CIDNP signal of hydroxyl-H, as described later, stands against the formation of deuterated 1a and following D-H exchange by the trace H_2O in CDCl_3 . Consequently, the hydrogen of the solvent is not introduced to 1a.

Here, we would like to construct the reaction scheme. The irradiation generates $^3\text{Q}^*$, and the triplet radical pair of $\text{Me}_3\text{Si-SiMe}_3^{+\cdot}$ and $\text{Q}^{\cdot-}$ is formed by electron transfer from $\text{Me}_3\text{Si-SiMe}_3$ to $^3\text{Q}^*$. The initial radical pair 4 of $\text{Me}_3\text{Si-SiMe}_3^{+\cdot}$ and $\text{Q}^{\cdot-}$ can be transformed to radical pair 5 of $\text{Me}_3\text{Si}^{\cdot}$ and $\text{Q}^{\cdot-}$ by spontaneous Si-Si bond fission. The radical pair 6 of the trimethylsiloxyphenoxy radical ($\text{Me}_3\text{SiO}^{\cdot}$) and $\text{Me}_3\text{Si}^{\cdot}$ can be formed by the reactive fission of $\text{Me}_3\text{Si-SiMe}_3^{+\cdot}$ with $\text{Q}^{\cdot-}$.



CIDNP (Chemically Induced Dynamic Nuclear Polarization)

$\Gamma = \epsilon \cdot \mu \cdot \Delta g \cdot a$ $\Gamma = +$: Enhanced Absorption
 $\Gamma = -$: Emission

ϵ : + = in cage, - = out of cage
 μ : spin multiplicity (+ = triplet, - = singlet)
 Δg : difference between the g values
 a : hyperfine coupling constant

At the initial stage, radical pairs are all in the cages. To elucidate the reaction scheme, we should classify the products into "in-cage" and "out-of-cage" reaction products. For this purpose, we scavenged escaping radicals by oxygen. The formation rate of 2 was much suppressed by oxygen compared with that of 1. Thus, 2 is attributable to an "out-of-cage" reaction product. On the other hand, 1 is considered to be an "in-cage" reaction product.

In the next place, we tried to measure the CIDNP spectra to decide the importance of radical pair 4, 5, and 6. The CIDNP technique is suitable to determine this reaction path, since this reaction includes a radical pair at its initial stage. The NMR spectra of $\text{Me}_3\text{Si-SiMe}_3$ (12.5 mM) and 2,5-DCQ (50 mM) in CDCl_3 were measured on irradiation with the high pressure mercury lamp. Those obtained before, during, and after irradiation are shown in Fig. 1. The signals at 4.38 and 7.40 ppm are assigned to be the hydroxyl-H and ring-H of 1a. These signals are ascribed to the enhanced absorption (A) signals due to CIDNP. The CIDNP measurements were also carried out with other quinones. 2,6-DCQ gave the same A polarization of ring-H and hydroxyl-H like 2,5-DCQ. MCQ gave also A phase of hydroxyl-H of 1, but its polarization was too weak to observe that of ring-H. When BQ was used, we could not observe any CIDNP signal. This may be due to the low reactivity of BQ.

The reaction mechanism was analyzed by Kaptein's CIDNP phase rule [4]. In the reaction of $\text{Me}_3\text{Si-SiMe}_3$ and Q, we found the A polarization on ring-H and hydroxyl-H of 1. As mentioned above, the initial reaction proceeds *via* the triplet radical pair ($\mu = +$), and 1 is an "in-cage" reaction product ($\epsilon = +$). On the other hand, the signs of Δg and a are dependent on the radical pair, which enables us to discriminate the reaction mechanism. The g values and the signs of the hfc for the component

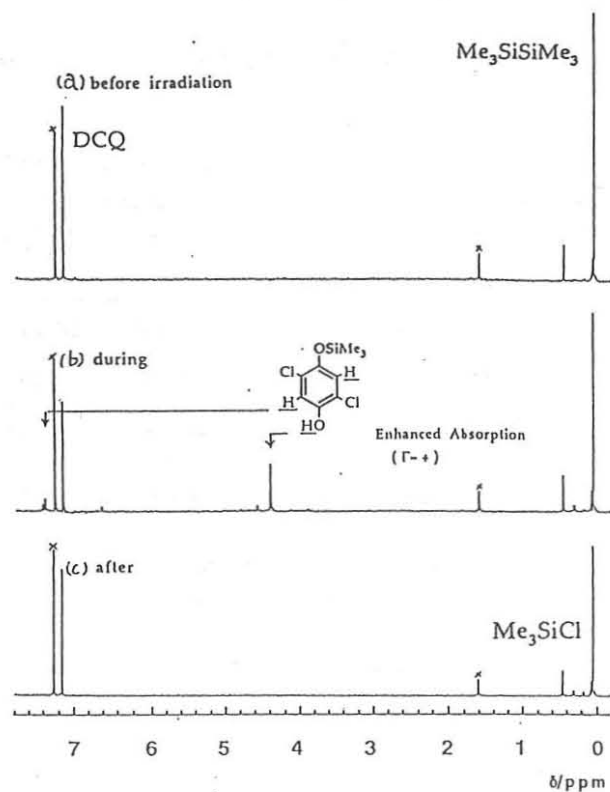
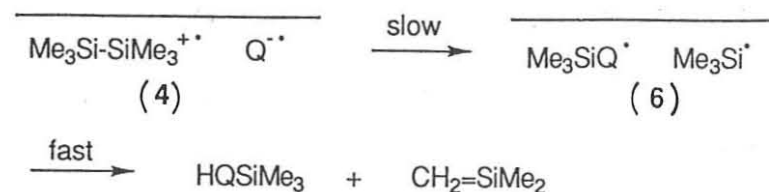


Fig. 1 ^1H NMR spectra of $\text{Me}_3\text{Si-SiMe}_3$ (12.5 mM) and 2,5-DCQ (50 mM) in CDCl_3 (a) before, (b) during, and (c) after irradiation. All of them are obtained by 32 times accumulation. Spectra (b) and (c) are obtained by 4sec \times 32 irradiation. The arrows denote the CIDNP signals of 1a.

radicals in each radical pair, 4, 5, and 6, are summarized in Scheme. From these parameters, we concluded that the reaction precursor is the radical pair 4 of hexamethyldisilane cation radical and quinone anion radical rather than the radical pair 5 and 6.

The polarization phase of 1a derived from radical pair 4 indicates that radical pair 4 has long lifetime, namely Si-Si bond fission of $\text{Me}_3\text{Si-SiMe}_3^{+\cdot}$ is not so fast. To get the polarization for hydroxyl-H, the hydrogen must come from the initial radical pair. To generate 1, the reaction must proceed *via* radical pair 6, but the polarization due to radical pair 6 was not observed. The appearance of the polarization due to radical pair 4 instead of radical pair 6 is explained by "memory effect" [5]. Consequently, the lifetime of radical pair 6 is considered to be short owing to the disproportionation.



Details of the mechanism on this photo-induced electron transfer reaction will be discussed.

References

- [1] H. Bock, B. Solouki, "The Chemistry of Functional Groups, The Chemistry of Organic Silicon Compounds", S. Patai and Z. Rappoport, Eds., J. Wiley, New York (1989) part 1, p. 555; K. Mochida, A. Itani, M. Yokoyama, T. Tsuchiya, S. D. Worley, and J. K. Kochi, Bull. Chem. Soc. Jpn., 58 (1985) 2149.
- [2] H. Watanabe, M. Kato, E. Tabei, H. Kuwabara, N. Hirai, T. Sato, and Y. Nagai, J. Chem. Soc., Chem. Commun., (1986) 1662; J. K. Kochi, Angew. Chem. Int. Ed. Engl., 27 (1988) 1227; S. Kyshin, Y. Ehara, Y. Nakadaira, and M. Ohashi, J. Chem. Soc., Chem. Commun., (1989) 279.
- [3] M. Igarashi, T. Ueda, M. Wakasa, and Y. Sakaguchi, submitted for publication.
- [4] R. Kaptein, J. Am. Chem. Soc., 94 (1972) 6251.
- [5] R. Kaptein, *ibid.*, 94 (1972) 6262.

Tu-3
10:45
~11:15

Determination of the Enhancement Factor of CIDNP in the
Photochemical α -Cleavage of Ketones

Tomomi Sakata, Masahide Terazima, and Tohru Azumi

Department of Chemistry, Faculty of Science, Tohoku
University, Sendai 980, Japan

The determination of the enhancement factor of CIDNP is very important in understanding the mechanism of photochemical reactions. In this paper, we wish to point out that qualitative analysis of the sign of the CIDNP polarization alone may sometimes lead to erroneous conclusion. Let us illustrate how it is important to determine the enhancement factor by taking the photochemical α -cleavage of dibenzyl ketone (DBK),



as an example.

Figure 1 shows the NMR spectra measured (a) before the light irradiation and (b) after the light irradiation.

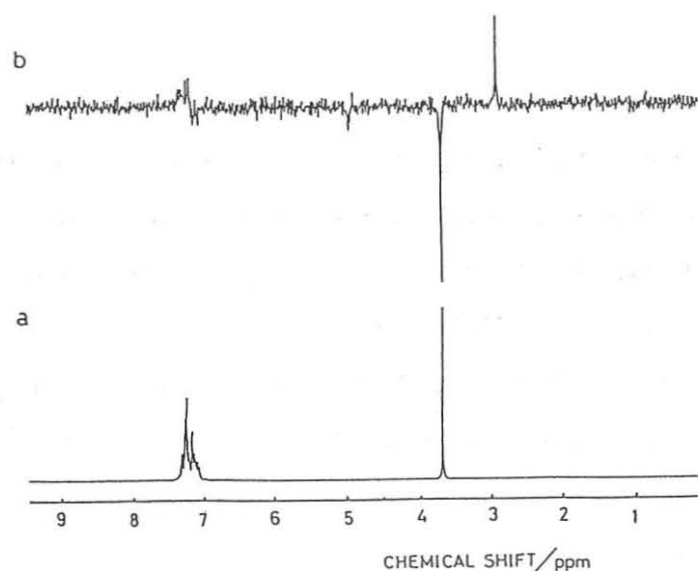


Figure 1. NMR spectra of DBK at room temperature (a) before light irradiation and (b) during the irradiation under the conditions of $P_{\text{sat}} = P_{\text{obs}} = 12.0 \mu\text{s}$, $\tau = 0.50 \text{ s}$, and $\tau_{\text{obs}} = 1.50 \text{ s}$.

The CIDNP signal for the benzyl protons of DBK (the recombination product) at 3.7 ppm is emissive, and the CIDNP signal for the methylene proton of dibenzyl (escaped product) at 2.9 ppm is absorptive. By application of the Kaptein rule, the precursor is predicted to be the triplet state, and this prediction agrees with the results of numerous studies reported so far. Complication arises, however, if reaction occurs from both triplet and singlet states. We should note that the enhancement factor of CIDNP greatly differs between the singlet precursor and the triplet precursor. Sometimes the absolute magnitude of the enhancement factor for the triplet precursor can be several orders of magnitude larger than that for singlet precursor. In order to avoid such misdetermination of the reaction precursor, not only the sign but also the magnitude of the enhancement factor of CIDNP should be analyzed with the aid of theoretical values.

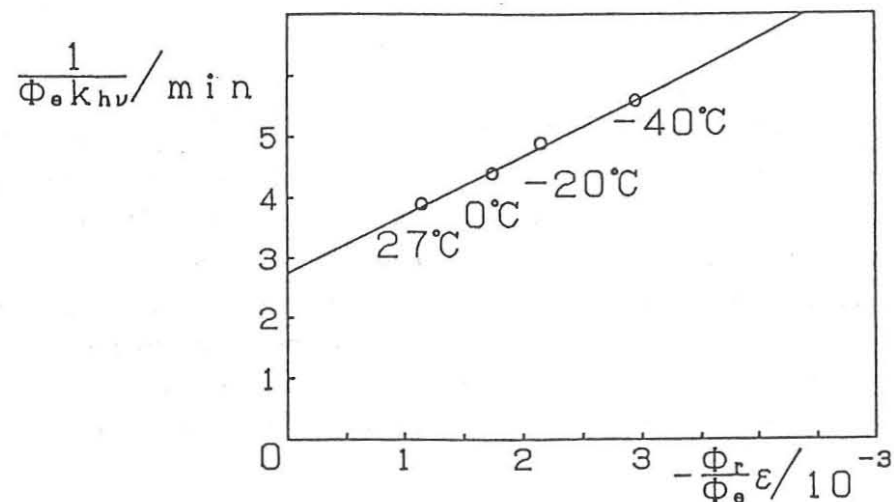
Experimental determination of the enhancement factor is, however, very difficult. First of all, the observed CIDNP intensity is affected by relaxation and thus this effect should be properly taken into account. Second, in the present DBK photophysics case, the recombination product is chemically identical species with the reactant, and thus the amount of DBK produced by the reaction is hard to determine.

In this paper, the first difficulty was overcome by utilizing the saturation recovery pulse sequence, $(P_{\text{sat}} - \tau - P_{\text{obs}} - t_{\text{obs}})N$, proposed by Lawler and Barbara. The second difficulty was overcome by the temperature dependence method to be outlined below. The observable physical quantities are a) CIDNP intensity I of DBK, (b) decrease of the NMR intensity $-\delta I_e$ of DBK by the light irradiation, and (c) the consumption rate constant K of DBK. From kinetic consideration we obtain the following expression

$$\frac{1}{K} = \left(\frac{I}{-\delta I_e} \right) \frac{1}{k_{h\nu} E} + \frac{1}{k_{h\nu}}$$

where $k_{h\nu}$ is the rate constant which represents the efficiency of the creation of the radical pair by the light irradiation. Thus we expect that the plot of $1/K$ versus the $I/(-\delta I_e)$ ratio obtained at various temperatures should become a straight line and the

slope/intercept ratio of this straight line can yield the enhancement factor E or the Boltzmann population corrected enhancement factor $\epsilon = (g_N \mu_N B / 2kT)E$. The experimentally obtained plots are shown in Figure 2.



We indeed obtained a rather good straight line, and this observation supports several underlining assumptions made in developing the above kinetics.

The ϵ value determined from Figure 2 is -2.88×10^{-3} . This value does not depend on the concentration of DBK in the 0.01 - 0.06 M range.

We are also able to obtain the quantum yield of the recombination (Φ_c) of DBK after the photocleavage reaction by the formula $E[\Phi_c / (1 - \Phi_c)] = 1 / (-\delta I_e)$. The results are shown in Table 1.

Table 1. Temperature dependence of the quantum yield of the recombination (Φ_c) of DBK after the photocleavage reaction.

Temp.	Φ_c
- 40 °C.	0.505
- 20 °C.	0.422
0 °C.	0.381
27 °C.	0.283

In order to analyze the experimentally obtained enhancement factor, ϵ values were calculated theoretically based on the theory of Pedersen and Freed. The theoretical value for the triplet precursor ϵ_T is -0.2237 . On the other hand, the theoretical value for the singlet precursor ϵ_S is a very small positive value. ($\epsilon_S = 5.5 \times 10^{-4}$ at 27°C , $\epsilon_S = 3.75 \times 10^{-4}$ at -40°C .)

Although the qualitative features (the emissive polarization and temperature independence of ϵ) suggests that the precursor of the photocleavage of DBK is the triplet state, the quantitative analyses of the experimental results encounters difficulties in two points. First difficulty is a great discrepancy between the observed and the calculated enhancement factor. The calculated ϵ value for the triplet precursor is two orders magnitude as large as the experimental value (-2.88×10^{-3}). The second difficulty is that the yield of cage product (Φ_c) exceeds $1/3$ below 0°C . (Table 1). Since the photoreaction occurs in the high magnetic field (2.349T), only the T_0 state of the radical pair can mix with the S state. In such a case, Φ_c for the triplet precursor should be less than $1/3$. We might be able to conceive of the following five possibilities for the origin of the discrepancies between the experimental results and theoretical expectation in ϵ and Φ_c . a) Participation of the spin-lattice relaxation of individual radical which composes the radical pair, b) participation of the spin-orbit coupling (SOC) in the radical pair state, c) regeneration of DBK from free radicals, d) Overhauser effect, and e) participation of the singlet precursor.

Having examined these five possibilities very carefully, we have finally reached the conclusion that the possibility e) is most likely. From the examination of the data, we conclude that nearly 80 % of the reaction takes place from singlet excited state. This conclusion was also supported by the triplet sensitizer experiments.

Tu-5
14:30
~14:50

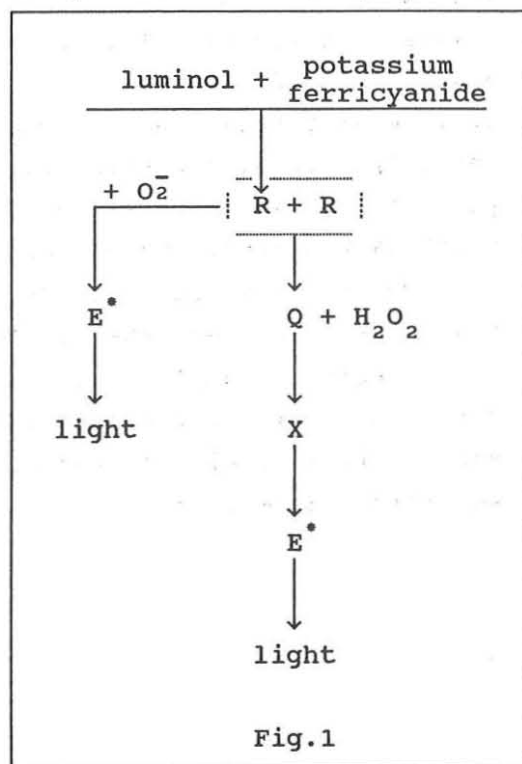
Phase Shift of the Magnetic Field Effects
in Luminol Chemiluminescence in Water
Solution as the New Method of Intermediate
Species Lifetime Determination

Michael Triebel, Andrew Morozov,
Maxim Totrov, Eugene Frankevich

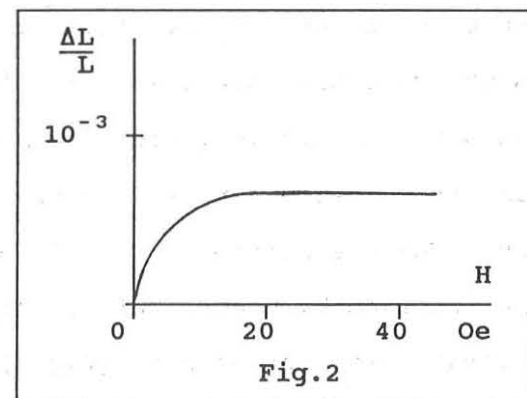
The Institute of Energetic Problems
of Chemical Physics USSR Academy
of Sciences, Moscow, 334, USSR

The magnetic field effect (MFE) on the intensity of the light from chemiluminescent luminol reaction was studied using technique arranged to provide rapid continuous mixing of luminol and potassium ferricyanide water solutions at predetermined ratios. Blue-luminescent solution was passed through the optical cell situated between two pairs of Helmholtz coils one of which designed for linear sweeping of magnetic field and the other for sine-shaped modulation. Photomultiplier and lock-in amplifier were used for detection. Sensitivity of setup was about $10^{-3}\%$.

We propose here some simplified reaction mechanism of luminol oxidation by potassium ferricyanide (Fig.1) which make clear



the role of the luminol radical (R) in the light generation. A light emitter (E*) which is an excited dianion of aminophtalic acid was formed through the interaction of the luminol radical (R) with superoxide-ion (O₂⁻). Recombination of the radicals (R) was the other channel of their loss. A direct product of the recombination was quinone (Q). The light couldn't appear in this channel in the absence of hydrogen peroxide. So the luminol radicals took part in two competitive processes: one led to the light generation and the other didn't. The external magnetic field decreased the recombination rate constant and consequently increased the concentration [R] and therefore increased the light generation rate through the R - O₂⁻ interaction. The characteristic dependence of the chemiluminescence intensity versus magnetic field strength (Fig.2) and the value of the half-saturation field



strength (10 Oe) were typical for hyperfine interaction mechanism of MFE. The magnitude of the MFE was about $10^{-1}\%$.

We have revealed the phase shift between the modulation of the magnetic field and the modulation of the chemiluminescence intensity. The value of the phase shift ϕ depended upon cyclic frequency of the magnetic field ω according to the equation $\text{tg } \phi = \omega\tau$, where τ was the characteristic time of reaction. The phase shift was due to an inertia of changing of radical concentration [R] with time τ , while the changes of radical's recombination rate constant was inertialess. For this reason variations of chemiluminescence intensity in magnetic field had the same time delay as [R]. The time τ is a function of rate constants and concentrations of particles taking part in the reaction. We have

measured dependencies of τ and the value of MFE ($\Delta L/L$) upon concentrations of luminol, potassium ferricyanide, oxygen and pH. Values of τ obtained are of the millisecond range. An addition of hydrogen peroxide to above reaction resulted in enhancing of chemiluminescence intensity but the phase shift became more than

90° . The reaction of H_2O_2 with quinone Q is known to lead to the same light emitter E^* as in the case of $R - O_2^-$ reaction. Therefore magnetic field increased light generation in the $R-O_2^-$ reaction and in the same time decreased it in the $H_2O_2 - Q$ reaction. Negative MFE was inertialess up to several kcps. The description of MFE on the reaction by means of vector diagram was convenient (Fig.3).

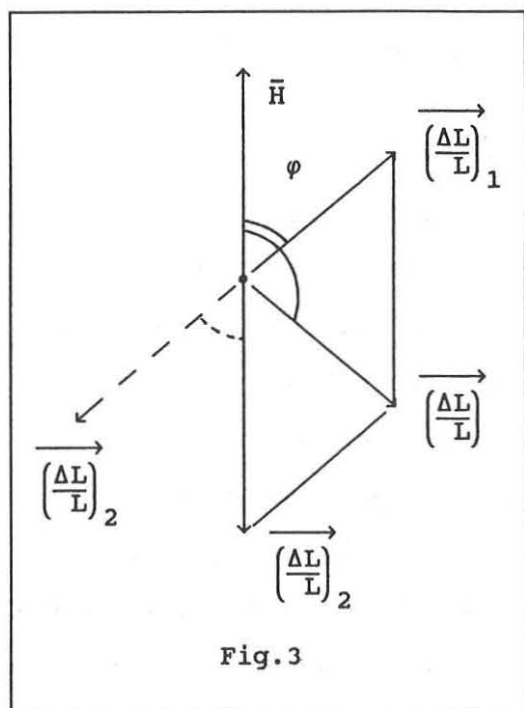


Fig.3

Vector $(\Delta L/L)_1$ represents positive magnetic field effect lagged by phase behind the vector of the magnetic field modulation H . Vector $(\Delta L/L)_2$ represents the negative effect lagged 180° by phase behind the vector \bar{H} . Vector $(\Delta L/L)$ represents overall magnetic field effect.

Increasing of modulation frequency led to decreasing of positive MFE value (vector $(\Delta L/L)_1$), so at frequencies more than 1 kcps vector $(\Delta L/L)_2$ remained alone. It gave the opportunity to study concentration dependencies of negative MFE.

Increasing of modulation frequency up to range 10 - 100 kcps demonstrated delay of negative MFE due to the presence of two successive transient particles Q and X between the radical pair and light emitter E^* . The particles Q and X had lifetimes of micro-

second range. The lifetime of quinone Q was function of concentration $[H_2O_2]$. Rate constant of the interaction of quinone with hydrogen peroxide ($10^8 M^{-1}s^{-1}$ approximately) was measured at pH 13.

This modulation technique obviously can be applied for any magnetic field sensitive reaction which gives the possibility of a rapid detection of the product yield variations induced by magnetic field and if transient active particles exist with a lifetime comparable with the period of magnetic field modulation.

References:

1. K.-D.Gundermann, F.MacCapra. Chemiluminescence in Organic Chemistry. Berlin, Springer-Verlag. 1988.
2. H.O.Albrecht. Z.Physik.Chem. B-1, 136 (1928), 321.
3. J.H.Baxendale. J.Chem.Soc., Faraday Trans.I, 69 (1973), 1665.
4. G.Merenyi, J.Lind, T.E.Eriksen. J.Phys.Chem. 88 (1984), 2320.
5. G.Merenyi, J.Lind, T.E.Eriksen. Photochem.Photobiol. 41 (1985), 203.

Tu-6
15:00
~15:20

Temperature Dependence of Lifetime of Chain-Linked Biradicals in the Absence and Presence of a Magnetic Field

Yoshifumi Tanimoto

Department of Chemistry, Faculty of Science,
Hiroshima University, Naka-ku, Hiroshima 730,
Japan

Dynamics of chain-linked biradicals are of great interest in order to clarify the role of chain motion and spin motion in their reaction. In the present paper, we have studied temperature dependence of lifetime of triplet biradicals generated from the xanthone-xanthene linked system in the absence and presence of a magnetic field by laser flash photolysis.

1. In the Absence of a Magnetic Field

Upon laser excitation of XO-16-XH in ethyl acetate, the excited triplet XO chromophore undergoes hydrogen abstraction from XH at the other end of the chain, generating the triplet biradical ($\cdot\text{XOH-16-X}\cdot$) composed of a xanthone ketyl radical ($\text{XOH}\cdot$) and a xanthenyl radical ($\text{X}\cdot$) (Scheme 1)[1]. "Apparent" lifetime of the biradical were defined as those calculated under the single exponential approximation.

85

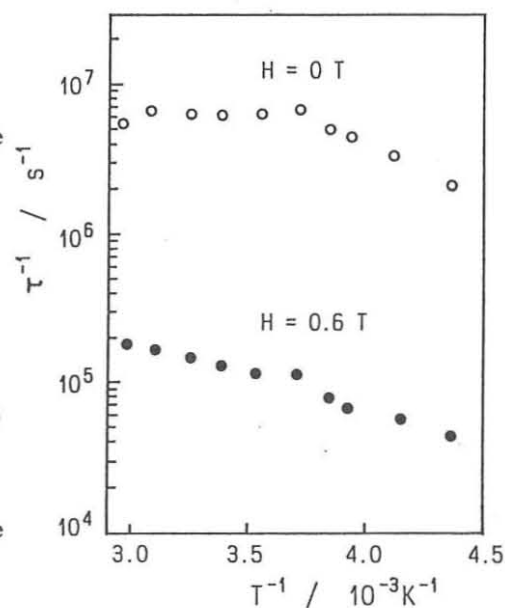
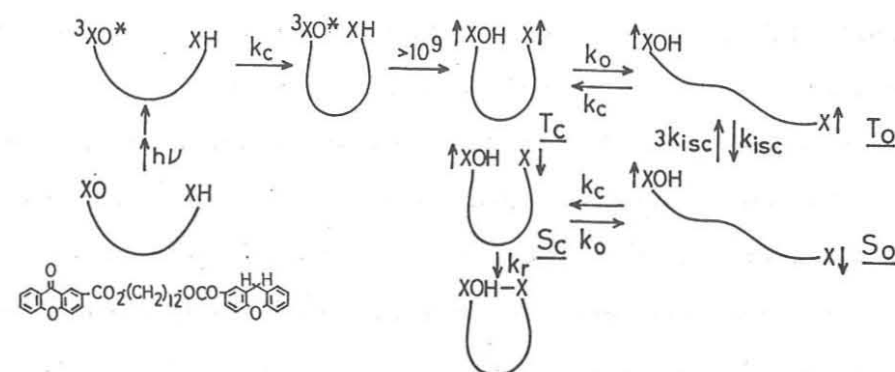


Fig. 1. Temperature dependence of the lifetime τ of $\cdot\text{XOH-16-X}\cdot$.

Tu-6-i



Scheme 1. Reaction pathways of XO-16-XH.

Figure 1 shows temperature dependence of the lifetime of $\cdot\text{XOH-16-X}\cdot$. At zero field, the dependence may be divided into two regions at about 0 °C. In the high temperature region, the lifetime becomes slightly longer with increasing temperature, in marked contrast to the lifetime in the low temperature region. Interestingly, analogous temperature dependence of the lifetimes were observed in the biradicals with different chain lengths.

In the chain-linked systems, decay rate of a biradical is considered as the functions of chain motion, spin motion and recombination reaction rate, when intermolecular process is negligibly slow. Thus an attempt was made to analyze the decay curves of transient signal of $\cdot\text{XOH-16-X}\cdot$ within a framework shown in Scheme 1. Here, T_c is a triplet biradical with closed form, T_o a triplet one with open form, S_o a singlet one with closed form, and S_c a singlet one with closed form. k 's are the rate constants of the respective process. Observed time dependence of the biradical concentration $I(t)$ can be given;

$$I(t) \propto [T_c] + [T_o] + [S_o] + [S_c] \quad (1)$$

In the present calculation, k_c was estimated from the rate of the biradical formation which was calculated from the growth curves of the transient signal at low temperatures. The

86

Tu-6-ii

rate constant, k_{isc} , was used a theoretical value ($k_{isc} = 5 \times 10^8 \text{ s}^{-1}$) evaluated from the hyperfine coupling constants of component radicals and was assumed to be temperature-independent. In this way, simulation of decay curves was carried out for the two unknown parameters, k_o and k_r , by numerically solving the differential equations derived from Scheme 1. Temperature dependence of k_o and k_r calculated, with that of observed k_c , are shown in Fig. 2. Analogous dependence of rate constants were obtained for other chain molecules.

The unusual temperature dependence of "apparent" biradical lifetime (Fig. 1) is clearly explained by the rate constants shown in Fig. 2. The observed lifetime are chiefly determined by the rate constants associated with S_C . In the low temperature region ($< 0^\circ \text{C}$), the order of rate constants is $k_c < k_o < k_r$. The lifetime change is attributable mainly to k_c , since recombination rate (k_r) is faster than the dissociation rate (k_o) in

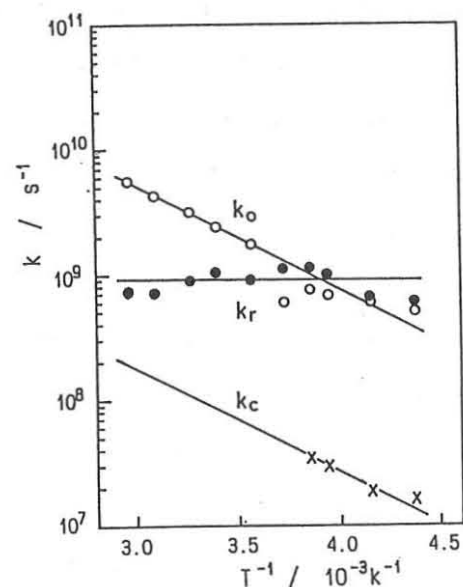


Fig. 2. Temperature dependence of k_o , k_r , and k_c .

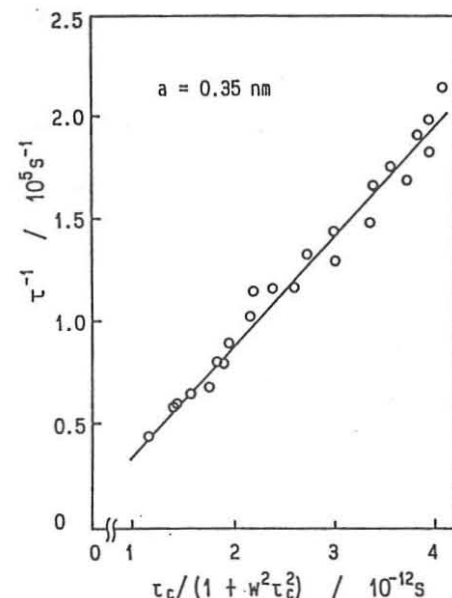


Fig. 3. Plots of τ vs. $\tau_c / (1 + \omega^2 \tau_c^2)$.

S_C . On the other hand, in the high temperature region, the order of the rate constants becomes $k_c < k_r < k_o$. Thus, fraction of recombination $k_r / (k_r + k_o)$ in S_C decreases with increasing temperature, though the overall rate is still mainly controlled by the slowest process, k_c . This may result in the slight decrease in the apparent biradical lifetime in the high temperature region.

2. In the Presence of a Magnetic Field

In the presence of a magnetic field (0.6 T), the lifetime of $\cdot\text{XOH-16-X}\cdot$ is about 8 μs at room temperature, which is about 50 times longer than that at zero field (160 ns). The lifetime change caused by the magnetic field is so drastic that the biradical lifetime at 0.6 T is most probably controlled by spin-conversion process. In order to clarify whether the spin relaxation is the rate-controlling process in the field, the temperature dependence of the lifetime at 0.6 T was analyzed with the theoretical equation (2) for the temperature dependence of the relaxation time [2]:

$$1/\tau = \gamma^2 |H_{loc}|^2 \tau_c / (1 + \omega^2 \tau_c^2) \quad (2)$$

Here, τ_c is correlation time and ω the Larmor frequency. As shown in Fig. 3, the observed data exhibit the linear relationship as expected from eq. 2. It is concluded that a locally fluctuating field $|H_{loc}|$ of about 13 gauss, induced by rotational motion of $\text{X}\cdot$ and/or $\cdot\text{XOH}$ group, is the origin of the spin relaxation in $\cdot\text{XOH-16-X}\cdot$ at 0.6 T.

References

- [1] Y. Tanimoto et al., Bull. Chem. Soc. Jpn., **62**, 3923 (1989).
- [2] A. Carrington and A. D. McLachlan, "Introduction to Magnetic Resonance", Harper & Row, New York, 1967.

Tu-7

16:00

~16:30

MECHANISMS OF SPIN-ORBIT COUPLING DEPENDENT
MAGNETIC FIELD EFFECTS IN CHEMICAL KINETICS

U.E. Steiner, D. Baumann, W. Haas, , H.-J. Wolff and

D. Bürßner

Fakultät für Chemie, Universität Konstanz,

D-7750 Konstanz, Germany

The mechanisms by which magnetic field effects (MFEs) on chemical kinetics ensue, almost exclusively conform to the following general pattern [1]: A manifold of close lying spin(-orbit) states of a reaction intermediate - usually a pair of reacting species with unpaired spins- is coupled to some reaction channel in a spin-substate selective way, while other non-spin-selective channels may also exist. The magnetokinetic effect is based on a recoupling of the spin substates by a magnetic field and may be detected either directly as a magnetic field dependent decay kinetics of the reaction intermediate or, indirectly, as a magnetic field dependent yield into one of the available reaction channels, that need not be a spin-selective one.

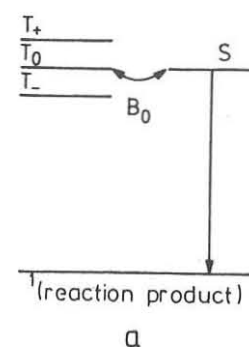
Spin-orbit coupling (SOC) may be involved in such a mechanism in two ways. (i) It may modify the interaction of the reactive components of the intermediate with the external magnetic field and thereby increase the magnetic coupling between the eigenstates of the zero-field Hamiltonian, or (ii) it may be responsible for the reactive coupling of the reaction intermediate to a product channel and thereby cause a sublevel selectivity of this channel.

In our paper three mechanistic cases of such SOC-assisted MFEs (cf. Scheme I) will be specified and experimental examples employing photoinduced electron transfer reactions will be provided for them.

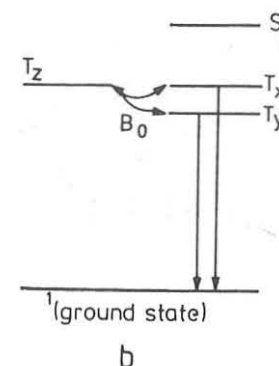
Case (a) of Scheme I is encountered as a feature of the well known radical pair mechanism (RPM). Different SOC in the radicals

SCHEME I

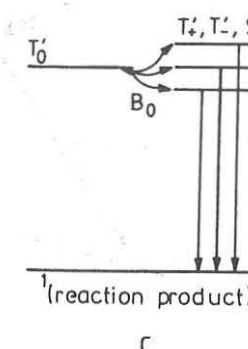
Δg -type
Radical Pair Mechanism



Triplet Mechanism



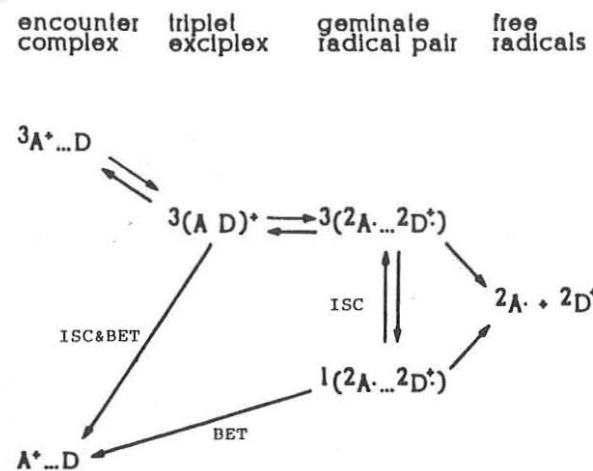
RPM with strongly
spin-orbit mixed
Kramers doublet



of the pair will cause their g -factors to be different, so that a magnetic field dependent coupling of T_0 and S ensues. This effect, belongs to type (i) of the cases specified above.

Case (b) is a variant of the so-called triplet mechanism (TM). Here we consider an electronically excited reactant with a distinct T_1/S_1 splitting. Spin-substate selective decay of the triplet occurs by intersystem crossing to the singlet ground state. This process is driven by SOC, an interaction which is triplet substate selective. An external magnetic field recouples the zero-field triplet substates and thereby changes the overall decay kinetics and the yield into chemical reaction channels that may be present. In this mechanism the effect of SOC is of case (ii) type.

Regarding case (c) we will show that it is encountered as a hybrid of cases (a) and (b) for redox pairs involving as one component a strongly spin-orbit coupled Kramers doublet species. Here the true singlet spin character cannot be concentrated in one single spin-orbit substate of the pair as in the RPM (a). Therefore, even in zero field, several of the eigenstates of the spin Hamiltonian have a finite reaction probability. The effect of an external magnetic field includes both Δg -type T_0'/S' mixing and a TM type T' substate mixing.



Application of these mechanistic cases (a)- (c) will be demonstrated with experiments utilizing photoelectron transfer reactions with excited triplet species. Transients exhibiting the magnetic field effects are triplet exciplexes and spin-correlated radical pairs (cf. Scheme II). A spin selective reaction channel is provided by fast BET regenerating the singlet ground state reactants. A spin-independent chemical channel is the formation of free radicals.

Cases (a) and (b) apply to the reaction of excited dye triplets, like methylene blue, with heavy atom substituted electron donors like p-I-aniline, where the heavy atom substituent provides the strong SOC required to maximize magnetokinetic effects of this type. Figure 1 shows examples of results with this system. The initial field dependence of the free radical yield is due to the TM in triplet exciplexes formed as primary reaction products, whereas the high-field part is due to the Δg -type RPM. The observed magnetic field dependence can be quantitatively reproduced by the two mechanisms and the characteristic kinetic parameters of the triplet exciplexes with lifetimes in the 20-50 ps region can be obtained (cf. ref [2]).

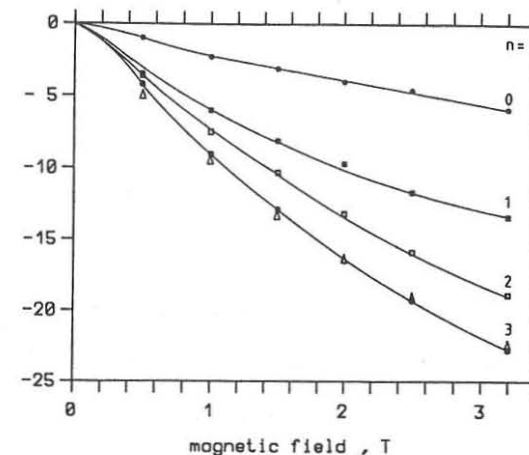
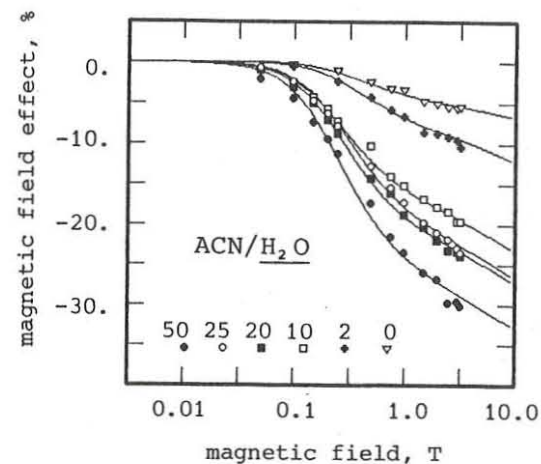


Figure 1. (left) Magnetic field dependence of free radical yield from electron transfer between p-I-aniline and methylene blue triplet in acetonitril/water solvent mixtures.

Figure 2 (right) Magnetic field dependence of methylviologen radical yield in the quenching of photoexcited complexes $[\text{Ru}(\text{bpy})_n(\text{dce})_{3-n}]^{++}$.

Case (c) applies to the reaction of photoexcited Ru(II)-tris-chelate complexes with the electron acceptor methylviologen [3-5]. As an example the MFES with the series of $\text{Ru}(\text{bpy})_n(\text{dce})_{3-n}^{++}$ (bpy = bipyridyl, dce = 4,4'-dicarboethoxy-bpy) is shown in Fig.2. One of the main results in the theoretical modelling of the case (c) effects is the extremely short spin-relaxation time of the Ru(III) complexes in the primary redox pair, to which our magnetokinetic investigations provide quantitative access.

References

- [1] U.E. Steiner and T. Ulrich, Chem. Rev. **89** (1989) 51; U.E. Steiner and H.-J. Wolff, in J.J. Rabek and G.W. Scott, Eds., CRC Series, Photochemistry and Photophysics Vol. IV, in press
- [2] U.E. Steiner and W. Haas, J. Phys. Chem. **95** (1991) 1880
- [3] U.E. Steiner, H.-J. Wolff, T. Ulrich and T. Ohno, J. Phys. Chem. **93** (1989), 5147
- [4] U.E. Steiner and D. Bürbner, Z. Physik. Chem. N.F. **169** (1990) 159
- [5] H.-J. Wolff and U.E. Steiner, Z. Physik. Chem. N.F. **169** (1990) 147

Tu-9
17:30
~17:50

Paramagnetic Ion Quenching of the Magnetic Field Effect in the
Photochemical Reaction of Naphthoquinone in Micelles

Yoshio Sakaguchi and Hisaharu Hayashi

The Institute of Physical and Chemical Research, Wako,
Saitama 351-01, Japan

The photochemical reactions of naphthoquinone (NQ) in micelles (RH) were observed to occur as follows [1,2];

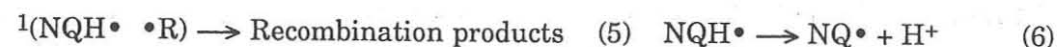
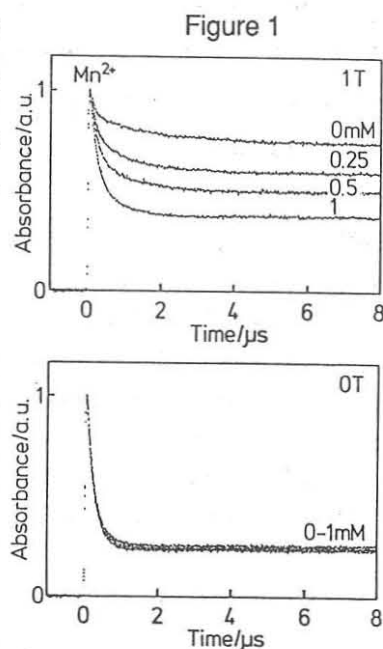


Figure 1 shows the decay of time-resolved optical absorption, TROA, of naphtho-semiquinone radical, NQH•, for SDS (sodium dodecyl sulfate, 80mM) micellar solutions of NQ (0.4mM) containing a metal ion, Mn²⁺ (0~1mM) [3]. At first, let us consider the results without Mn²⁺. In the absence of a magnetic field, the decay (reactions 3+5) was terminated within 1μs and the escape of radical pair, (NQH••R), (reaction 4), was suppressed. In the presence of a magnetic field of 1T, the decay became slow and the escape increased, which is attributable to the decrease of the rate of the reaction 3 by the external magnetic field. We found that the magnetically induced change continued beyond the magnitude of their hfc interactions (~0.01T) and it could not be explained by the conventional mechanisms.

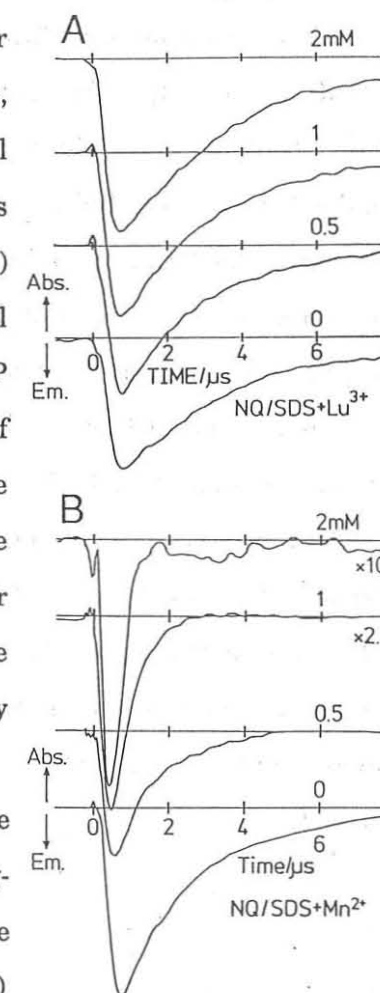
We proposed the "relaxation mechanism", RM, [1,4] that the magnetic field dependence of the electron spin relaxation of the odd electrons in a radical pair (RP) is important for the reaction of the long-lived RP's, such as a RP in a micelle and a chained RP. The time-resolved ESR measurement of the above reaction gave strongly polarized, CIDEP, signals of



NQH• and alkyl radical, R•. Figure 2 shows the decay of NQH• signal containing a metal ion, Lu³⁺ or Mn²⁺ (0~2mM) [3]. In the absence of the metal ions, the decay of the CIDEP signal is slow and the signal almost disappears in 6~8μs. The comparison of this decay and that of the TROA at 0.34T (=ESR field) revealed that the decay of the CIDEP signal corresponded with the recombination of the RP (reactions 3+5) and not with the total disappearance of NQH•, indicating that the intersystem crossing of the RP is governed by the electron spin relaxation of the component radicals. This result is an evidence for RM. We further investigated the contribution of the electron spin relaxation with enhancing it by paramagnetic metal ions.

The effect of a paramagnetic ion, Mn²⁺, on the TROA is shown in Fig. 1. In the presence of a magnetic field of 1T, the recombination (reactions 3+5) rate increased and the yield of escaping NQH• (reaction 4) decreased with increasing the concentration of Mn²⁺. The same effects were also observed at 0.1T. On the other hand, they were not observed in the absence of a magnetic field. In these cases, Mn²⁺ does not affect the decay of escaping NQH•, indicating no chemical activity toward NQH•. Other paramagnetic lanthanoid (Ln³⁺) and transition metal (Trⁿ⁺) ions, such as Gd³⁺, Fe²⁺, Ni²⁺, etc., showed the same behavior. Cu²⁺ oxidized NQH• a little along with the same effect by these paramagnetic ions. On the contrary, the diamagnetic metal ions, such as La³⁺, Lu³⁺, Sc³⁺, and Zn²⁺, showed no effect irrespective of the magnetic field. The acceleration of the reaction 3 by paramagnetic metal ions and its absence by diamagnetic ions strongly indicate that this effect is due to the enhancement of the

Figure 2



electron spin relaxation.

This conclusion is confirmed by the effects of paramagnetic ions on the decay of CIDEP signals [3]. As shown in Fig. 2B, with increasing the concentration of Mn^{2+} , the decay of the signal becomes faster. Paramagnetic Gd^{3+} and Cu^{2+} showed similar behavior to Mn^{2+} . As shown in Fig. 2A, diamagnetic Lu^{3+} did not change the decay, indicating no induction of the electron spin relaxation. The correspondence between the results of the TROA and CIDEP measurements, we can conclude that the relaxation of the electron spins of a RP are retarded by the external magnetic field and that they can be re-accelerated by paramagnetic metal ions. This is a clear-cut support for RM.

The relative quenching rates of Ln^{3+} and Tr^{n+} are shown in Figs. 3 and 4, respectively. In the case of Ln^{3+} , the rate is largest in the middle of the series, Gd^{3+} , and decreases to each side. In the case of Tr^{n+} , the quenching rates are similar to each other, and the values are larger than that of Gd^{3+} , the largest one among Ln^{3+} .

Figure 3

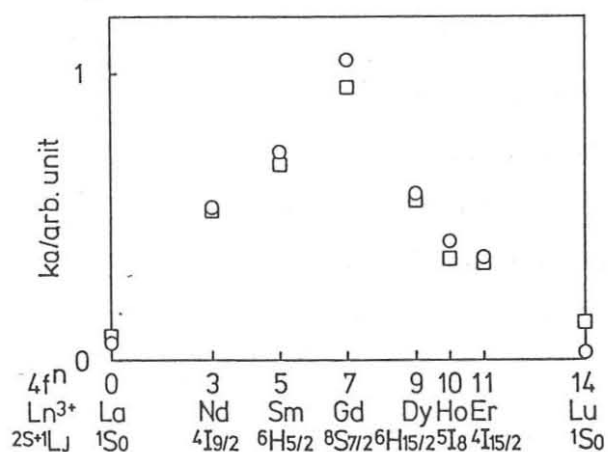
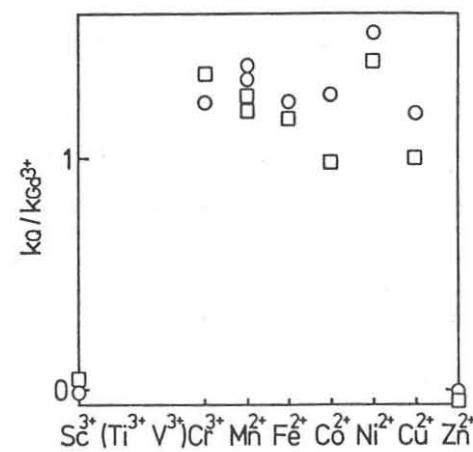


Figure 4



The quenching effects by paramagnetic Ln^{3+} have been applied for several reaction systems, such as the reaction within a micelle [6], that in a homogeneous solution [7], and a biradical [8]. As a mechanism to induce the relaxation, the exchange [7] and dipole-dipole [8] mechanisms are proposed for Ln^{3+} . In the case of Tr^{n+} , their larger quenching rates than Ln^{3+} stand against the dipole-dipole mechanism for Tr^{n+} because the dipole of Gd^{3+} is larger than that of Mn^{2+} , the

largest among Tr^{n+} . The absence of the characters of each Tr^{n+} implies the strong exchange interaction between the radicals and the metal ion and that the interaction time between them is longer than the electron spin relaxation time of the metal ion. This is very plausible owing to the attraction between the metal cation and the anionic surface of the SDS micelle. In the hexadecyl trimethylammonium chloride (cationic) micelle, we could not detect the effect of metal cations, but the effect of $Fe(CN)_6^{3-}$ was observed in this solution.

The paramagnetic ion quenching is not only a strong support for the "relaxation mechanism" of the magnetic field effect but also a convenient method to induce the intersystem crossing of the radical pair irrespective of the presence of a magnetic field. The effects of transition metal ions will not be equal in homogeneous solutions since the interaction time is not long enough compared to the relaxation times of each metal ions. These studies are of importance.

Acknowledgement We are indebted to Professor Yasumasa J. T'Haya and Dr. Hisao Murai of the University of Electro-Communications for their kindness in allowing us to have their time-resolved ESR apparatus at our disposal.

References

- [1] Y. Sakaguchi and H. Hayashi, *J. Phys. Chem.*, 88 (1984) 1437.
- [2] Y. Sakaguchi, H. Hayashi, H. Murai, and Y. J. I'Haya, *Chem. Phys. Lett.*, 110 (1984) 275.
- [3] Y. Sakaguchi and H. Hayashi, *Chem. Phys.*, submitted for publication.
- [4] H. Hayashi and S. Nagakura, *Bull. Chem. Soc. Jpn.*, 97 (1984) 322.
- [5] Y. Sakaguchi and H. Hayashi, *Chem. Phys. Lett.*, 106 (1984) 420.
- [6] N. J. Turro, X. Lei, I. R. Gould and M. B. Zimmt, *Chem. Phys. Lett.*, 120 (1985) 397.
- [7] S. Basu, L. Kundu, and M. Chowdhury, *Chem. Phys. Lett.*, 141 (1987) 115. S. Basu, D. Nath, and M. Chowdhury, *J. Lumin.*, 40/41 (1988) 252.
- [8] Y. Tanimoto, A. Kita, M. Itoh, M. Okazaki, R. Nakagaki and S. Nagakura, *Chem. Phys. Lett.*, 165 (1990) 184.

B1

20:00
~22:00

Heavy Atom Effect on Magnetic Field Effect
on Isomerization of Stilbene

Yasunao Kuriyama, Tastuo Arai, Hirochika Sakuragi
and Katsumi Tokumaru

Department of Chemistry, University of Tsukuba,
Tsukuba, Ibaraki 305, Japan

We have studied the mechanism for electron transfer induced isomerization of stilbene.^{1,2)} The isomerization proceeds through free radical cations or through radical ion pairs in the solvent cage.¹⁾ We have shown that cis radical cations of 4,4'-disubstituted stilbenes with methyl, methoxy and bromo groups isomerize unimolecularly to the corresponding trans radical cations at ambient temperature in acetonitrile.²⁾ However, the radical cation of cis stilbene does not isomerize within 100 μ s.

On laser irradiation of 9,10-dicyanoanthracence (DCA) in the presence of cis-stilbene we observed the cis and trans radical cations of stilbene 3 μ s after laser pulse. These intermediates were assigned to free ions because of their second order kinetic decay. They should be produced from triplet radical ion pairs, in which cis-to-trans conversion occurs. If the triplet pairs play an important role in isomerization, the external magnetic fields might affect the isomerization efficiency. Actually we observed magnetic field effects on isomerization of unsubstituted stilbene. The efficiency of isomerization was reduced in applied magnetic fields.¹⁾ The intersystem crossing between singlet S_0 and triplet T_+ , T_- states induced by the hyperfine interaction is appreciably diminished in the presence of the high magnetic fields thereby attenuating the quantum yields of the triplet radical ion pairs. In this paper we will report heavy atom effects on magnetic field effects on

isomerization of bromine substituted stilbene sensitized by DCA in acetonitrile.

Deaerated solutions of DCA (4.0×10^{-4} M) and cis-4,4'-dibromostilbene (cis-DBrSt) (1×10^{-3} M) were irradiated at ambient temperature with filtered light ($\lambda > 400$ nm) in the earthy and applied magnetic fields at 0.5 and 1 kG. Irradiated solutions were analyzed by means of high-performance liquid chromatography to determine the yields of trans-DBrSt. The efficiency of isomerization was reduced at the applied magnetic fields compared with that at the earthy magnetic field. The relative quantum yields for isomerization [$\Phi_{c \rightarrow t}(H)/\Phi_{c \rightarrow t}(0)$] were ca. 0.88 at H= 0.5 and 1 kG, where $\Phi_{c \rightarrow t}(H)$ and $\Phi_{c \rightarrow t}(0)$ show the quantum yields in the presence and absence of magnetic fields, respectively. The magnetic field effects on isomerization of DBrSt is smaller than that of stilbene. In the case of unsubstituted stilbene [$\Phi_{c \rightarrow t}(H)/\Phi_{c \rightarrow t}(0)$] value was 0.65 at H > 500 G.

The bromine substitution (heavy atoms) apparently reduced the magnetic fields effect due to the hyperfine interaction. There may be some possibilities such as the so-called heavy atom effect in intersystem crossing and involvement of other isomerization mechanisms. Detailed isomerization mechanism of cis-DBrSt will be discussed.

Reference

- 1) Y. Kuriyama, T. Arai, H. Sakuragi and K. Tokumaru, *Chem. Letters* (1989) 251.
- 2) Y. Kuriyama, T. Arai, H. Sakuragi and K. Tokumaru, *Chem. Phys. Letters* 173 (1990) 253.

B2

20:00
~22:00

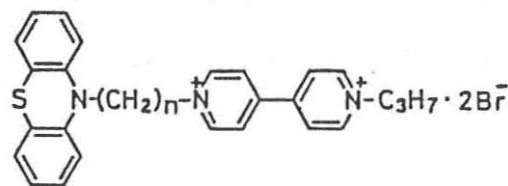
Magnetic Field Effects in Photoinduced Electron-Transfer in
Phenothiazine-Viologen Systems

Taku Matsuo, Hiroshi Nakamura, Hiroaki Yonemura

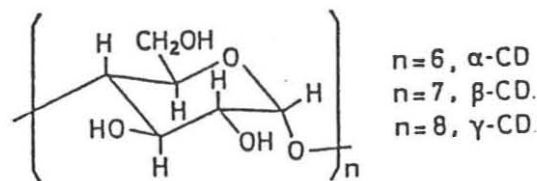
Department of Chemical Science and Technology,
Faculty of Engineering, Kyushu University, Hakozaki,
Fukuoka 812, Japan

Donor-acceptor linked compounds, as represented by porphyrin-viologen pair, are useful model systems for the study of photoreaction center in artificial photosynthesis. The studies have always been plagued with the flexibility of the spacer chain. A novel method to solve the problem was developed by complexing the donor-acceptor linked compounds with cyclodextrins (abbreviated to CD).

The following phenothiazine-viologen linked compounds were examined to elucidate the effect of spacer chain length. Three CDs were used to examine the effect of pore size on the complexing behavior of the phenothiazine-viologen linked compounds.



PHnV



n=6, α -CD
n=7, β -CD.
n=8, γ -CD.

Photogenerated radical pairs could be observed when either α - or β -CD was combined with phenothiazine-viologen pair separated by a relatively long spacer ($n=8$ or above). Examples of external magnetic field effects (EMFES) for PH₁₂V are shown in Figure 1. In the presence of α -CD, the yield of photogenerated radical pairs considerably increased in comparison with the case of β -CD. No radical was generated with the solution containing PH₁₂V and γ -CD. Laser excitation of PH₄V did not afford radical pair either, in spite of elaborate examination under various conditions (external magnetic field strength and choice of CD).

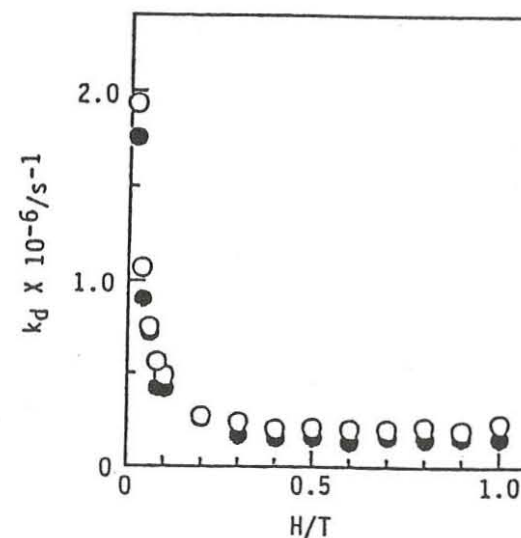


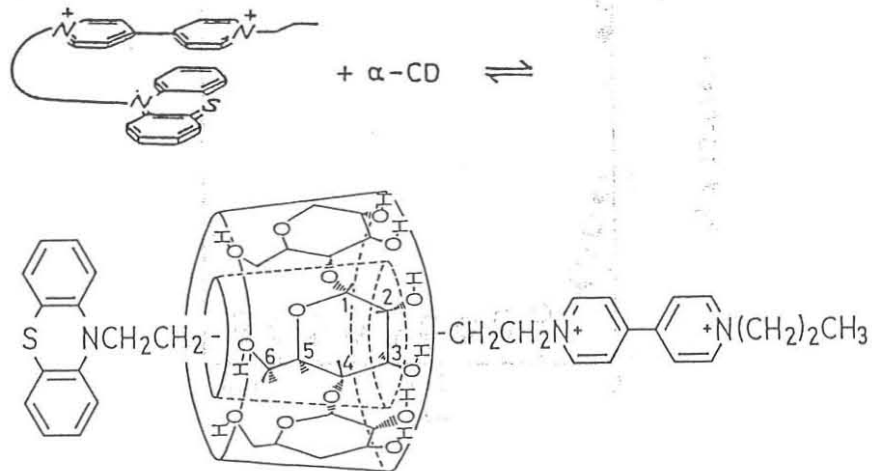
Figure 1. External magnetic field effects on the k_d -values for the radical pairs as evaluated from the absorbance of the photoreduced viologen units (603 nm) on laser excitation of PH₁₂V: α -CD system (●) and β -CD system (○).

Intensity of fluorescence emission from phenothiazine moiety also was strongly affected by the choice of the combination between the linked compound and CD. Emission from either PH₄V or PH₁₂V was hardly observed in the absence of CD. On the addition of CD, the fluorescence from PH₁₂V was intensified in the following order: α -CD > β -CD > γ -CD = without CD. In the case of PH₄V, the

fluorescence intensity did not increase even on the addition of CD. These data clearly indicate that deactivation of singlet, photoexcited PH₁₂V is suppressed by complexation of the linked compound with either α - or β -CD.

The difference in the complexation behavior was also revealed by the inspection of ¹H NMR spectra. When D₂O solution contained PH₁₂V and either α - or β -CD, distinct signals due to phenothiazine and viologen moieties in the complexed species were observed apart from the free species (Case A). The observed spectra are reasonably explained if one assumes that the viologen moieties are located on the top of the central part of the phenothiazine moieties in the free species and also that the complex formation enforces open, flat structure with extended spacer chain in the cavity of CD as in the following scheme.

Scheme 1



In the case of a solution containing PH₁₂V and γ -CD, the aromatic proton signals simply shifted, which indicates rapid exchange between the complex and the free species (Case B). Rapid exchange was also indicated in the NMR spectroscopic studies of PH₄V-CD systems. These observations are in fair agreement with those of fluorescence studies. The case A complexes are stable enough in NMR time scale, and energy dissipating, direct interaction between phenothiazine and viologen moieties appears to be suppressed in these complexes. As a consequence, the fluorescence intensity increases, and the branching ratio to

the triplet manifold leading to the radical pair will also increase. In the rapid exchange limit (Case B), which is usual for ordinary CD complexes, the photoexcited PH₄V and PH₁₂V may be easily deactivated by intramolecular interactions between phenothiazine and viologen moieties of the linked compound in the flexible, free species. Relevant intramolecular processes involved in photoinduced electron-transfer and the reverse reactions in the phenothiazine-viologen linked compounds are summarized in Scheme 2.

Scheme 2

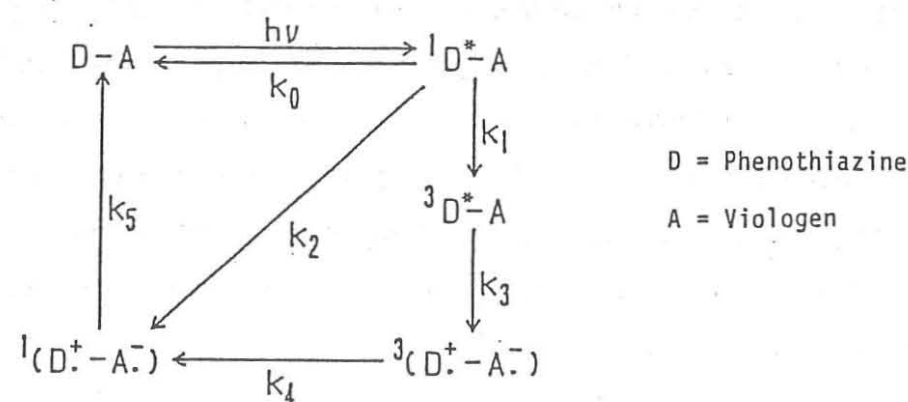


Table 1. External magnetic field effects on the decay rate constants of α -CD complex systems.

H/T	k_d / s		
	n=8	n=10	n=12
0	8.1×10^5	5.0×10^6	6.0×10^6
1	1.3×10^5	1.3×10^5	1.5×10^5

The k_d -value is practically identical with the intersystem-crossing rate (k_4). Effects of spacer chain length on the k_d -value, as summarized in Table 1, are then ascribed to variation of triplet-singlet energy separation with the spacer length. Essentially the same EMFES were obtained with the linked compounds in reversed micelles, which also afforded time-resolved ESR spectra. The reaction mechanism will be discussed further in details on the basis of the CIDEP spectra.

B3
20:00
~22:00

Magnetic Field Effects in Photoinduced Electron-Transfer in Porphyrin-Viologen Systems

Taku Matsuo, Hiroshi Nakamura, and Hiroaki Yonemura

Department of Chemical Science and Technology,
Faculty of Engineering, Kyushu University,
Hakozaki, Fukuoka 812, Japan

A series of porphyrin-viologen linked compounds with polymethylene groups as a spacer were prepared, and the decay process of the laser-generated radical pair was investigated. The linked compounds (ZP_nV) were incorporated into molecular bilayers of dihexadecylammonium chloride (DHAC) and the decay rate constant of the radical pair was evaluated. The initial rapid decay followed the first order kinetics, which could be ascribed to intramolecular reverse electron-transfer reaction in the donor-acceptor system. The first order decay rate constant (k_d) was strongly reduced in the presence of external magnetic fields (EMF) as shown in Figure 1. The k_d -value rapidly decreased with the increase of EMF, and reached an asymptotic value at EMF above ca. 0.2 T. The k_d -value at zero magnetic field increased with the spacer chain length, while the asymptotic value at high EMF was independent of the spacer length.

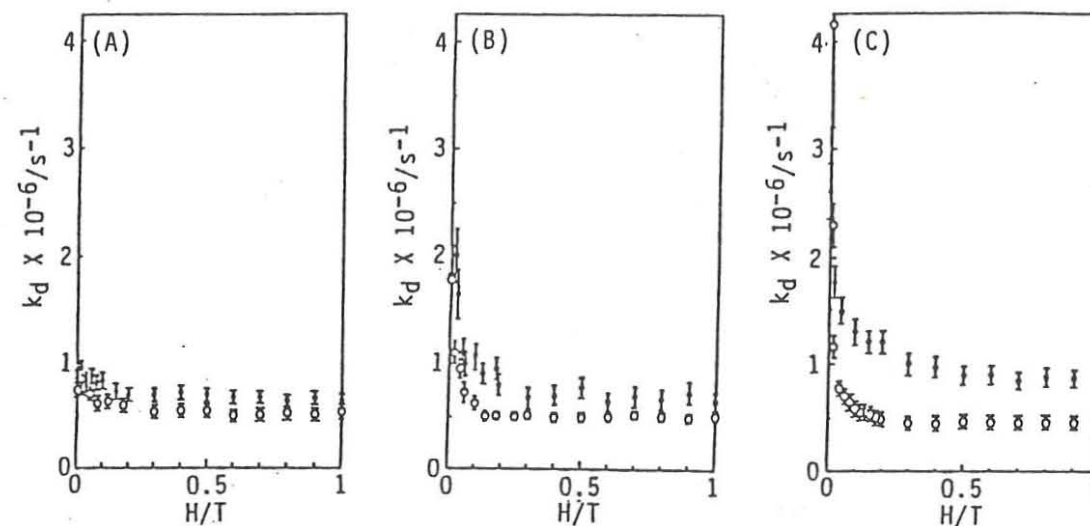
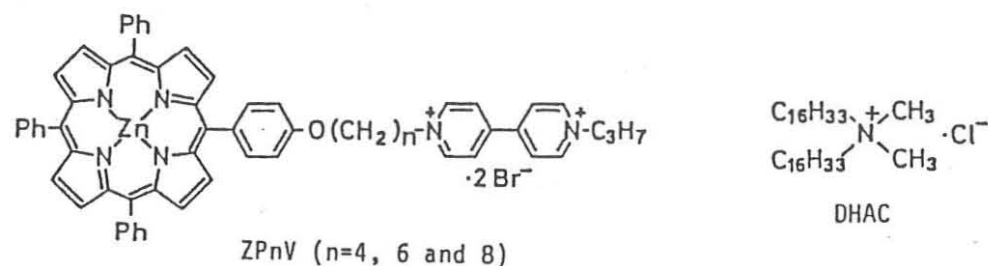


FIGURE 1
The effect of magnetic fields on the rate of k_d -values in the photogenerated radical pairs of porphyrin-viologen linked compound in aqueous acetonitrile (\ominus) and DHAC molecular bilayers (\boxplus): (A) ZP4V, (B) ZP6V and (C) ZP8V.

The above described remarkable, external magnetic field effects (EMFES) on the radical-pair decay rates was further investigated by the use of reversed micelles to elucidate the cause of EMFES. Decay rates of radical pairs obtained with two porphyrin-viologen linked compounds (ZP_4V and ZP_6V) were examined. The porphyrin moiety of the linked compounds was fixed to the wall of the reversed micelles, while water-soluble viologen moiety was confined to the water pool. General features of EMFES observed with the reversed micellar systems were identical to those in the DHAC molecular bilayers.

Effects of lanthanide ions on the decay rate of the radical pairs provided extremely useful information to elucidate the origin of EMFES. Laser-generated radical pairs were examined in the presence of three different lanthanide ions (La^{3+} , Dy^{3+} , and Gd^{3+}) in the water pool of the reversed micelles. The results are summarized in Figure 2 for ZP_4V . In the presence of high EMF (0.5 T), the decay rates considerably increased on the addition of either Dy^{3+} ($S=5/2$, and $J=15/2$) or Gd^{3+} ($S=J=7/2$), while no effect was observed with La^{3+} ($S=J=0$). These data clearly indicate that the radical pairs decay faster in the presence of

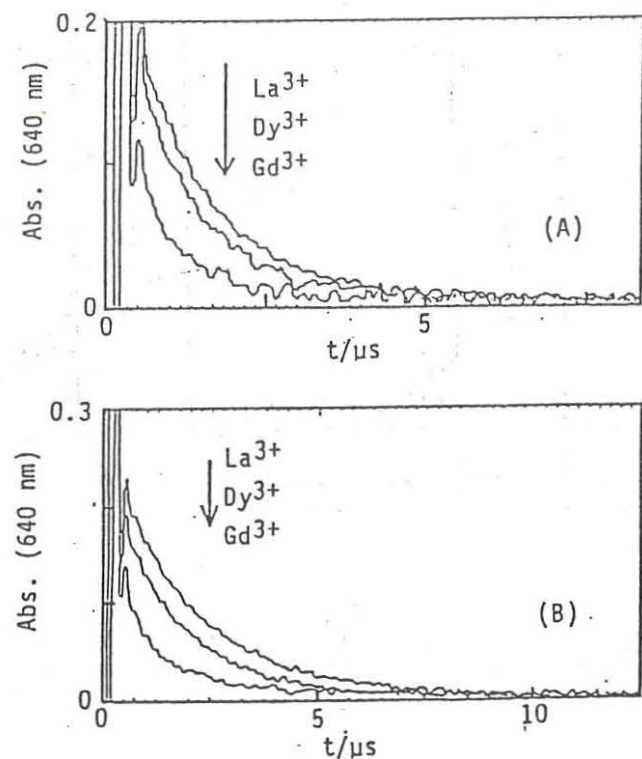


FIGURE 2
Effects of lanthanide ions (0.5 mM) on the decay rates of radical pairs in the porphyrin-viologen linked compound (ZP4V): (A) zero magnetic field, and (B) 0.5 T.

lanthanide ions with higher spin multiplicities. Exactly the same lanthanide effects were observed with the radical pairs for ZP₆V at 0.5 T.

The above observations strongly indicate that the EMFES are originated from Zeeman splitting of triplet sublevels of the radical pairs. The spin flipping relaxation from the triplet sublevels to the singlet state of the radical pairs appears to be the rate determining step, which has been well known as Relaxation Mechanism of EMFES.

In the absence of EMF, the lanthanide ions affected the radical decay process for ZP₄V and ZP₆V in entirely different manner. As to ZP₄V, the decay rate of the radical pair was affected by the three lanthanide ions to almost the same extent as observed at high EMF. In the case of the radical pairs generated from ZP₆V, however, the decay rate was hardly affected at 0 T. The most important difference

between ZP₄V and ZP₆V is the fact that the radical pair generated from ZP₆V decayed much faster than those from ZP₄V at 0 T. This may be related to the difference in the spacer chain length between the porphyrin and viologen moieties. On going from ZP₄V to ZP₆V, the spacer chain length increases by two methylene units, and the electron spin exchange interaction (ΔE) in the radical pair is expected to decrease accordingly. As ΔE -value approaches zero, the singlet and the triplet energy levels of the radical pair become degenerated to each other. In this extreme case, the intersystem crossing from the triplet to the singlet is expected to proceed easily via hyperfine coupling- and/or Δg -mechanisms, and the rate will not be appreciably affected by paramagnetic additives such as lanthanide ions. The relevant factors for EMFES are shown in Figure 3.

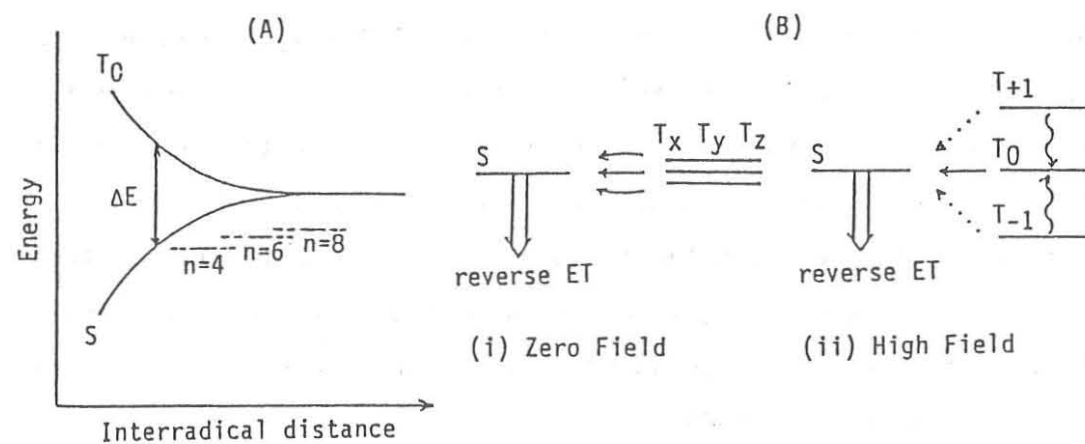


FIGURE 3
Schematic presentation of phenomena relevant to EMFES on the decay rate of photogenerated geminate radical pairs: (A) variation of the triplet-singlet energy separation with the interradical distance, and (B) two extreme modes of radical decay via intersystem crossing at degenerated S-T levels.

Time resolved ESR spectra were obtained with all of the three ZP_nV. CIDEP spectra, as expected of typical radical-pair mechanisms, were observed with ZP₆V and ZP₈V, while significant S-T. mixing was suggested to contribute in the spectra of ZP₄V.

B4
20:00
~22:00

External magnetic field effects
on bichromophoric photochemistry

Ryoichi Nakagaki

Faculty of Pharmaceutical Sciences,
Kanazawa University, Kanazawa,
Ishikawa 920 (Japan)

We have studied photochemistry of bichromophoric chain species containing electron donor (D) and acceptor (A) moieties, $D-(CH_2)_n-A$ and found that photochemistry of some bifunctional chain molecules depends upon the chain length linking the two aromatic chromophores as well as magnetic field strengths. A typical donor moiety is anilino group, while a nitro-aromatic chromophore is chosen as an acceptor. The photochemistry of $O_2N-4-C_{10}H_6-1-O(CH_2)_n-NHC_6H_5$ will be described here in some detail. When the chain length is short an intramolecular nucleophilic photo-substitution (photo-Smiles rearrangement) takes place, whereas a photo-redox process becomes dominant in the case of longer chain compounds.

Figure 1 summarizes the reaction mechanism for photo-redox reaction of the naphthoxyl species with a long chain ($n=12$). The primary event of photo-redox process is either electron transfer in polar media or hydrogen abstraction in non-polar solvents, which results in formation of a triplet biradical since the nitro-aromatic moiety in the lowest triplet manifold is involved in the photochemical reaction [1-4]. The triplet biradical undergoes intersystem crossing to the singlet biradical or an escape

process. It is to be noted that the cage process is an intramolecular photo-redox reaction whereas the escape process is a bimolecular reaction in which the triplet biradical reacts with a starting species in the ground state. Although the numbers of the species involved in these two processes are completely different, the both processes can be characterized as a photo-oxidative bond cleavage at the methylene group adjacent to the anilino nitrogen.

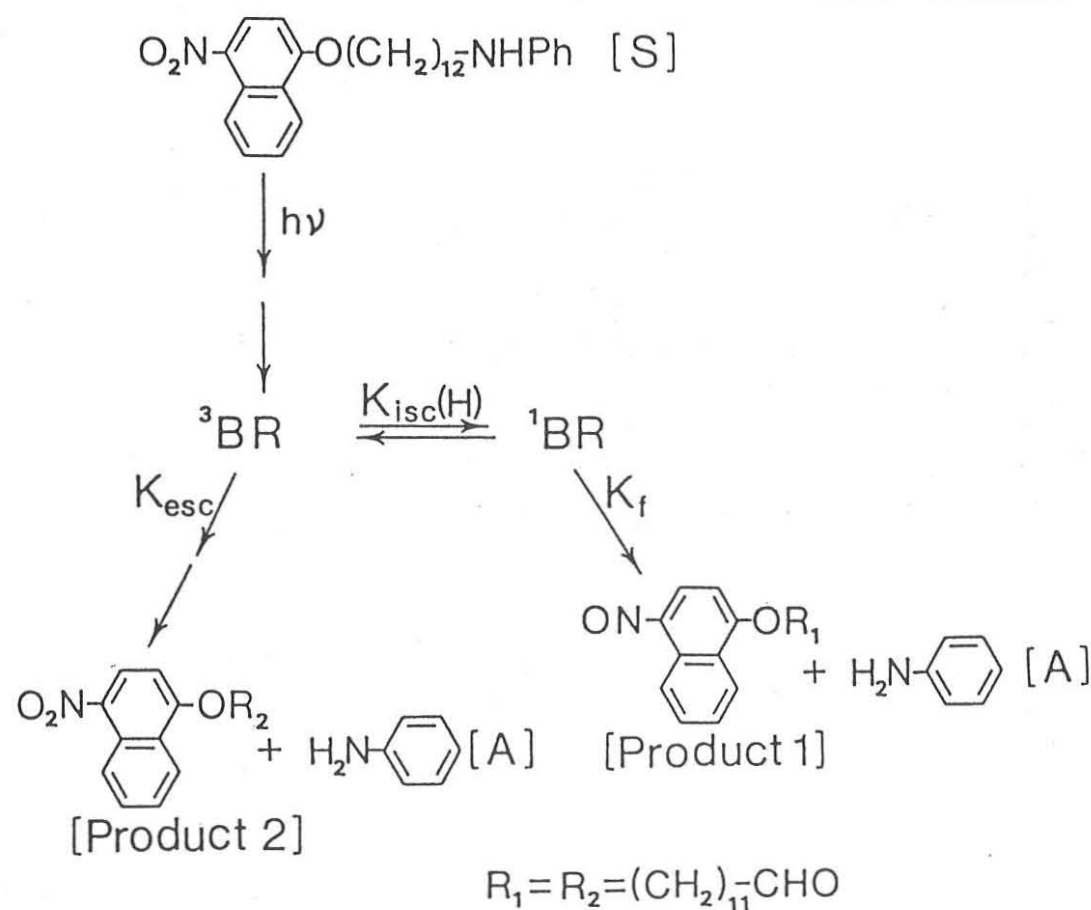


Fig. 1. Scheme for the photo-redox reaction of species $n=12$.
BR = biradical intermediate.
Superscripts 1 and 3 refer to the spin multiplicity.

A remarkable influence on the product yields for photo-redox reactions has been observed on application of an external magnetic field (0.64 T). Figure 2 illustrates the magnetic field effects upon the product distribution for the two distinct reaction pathways in terms of percentages. At the particular chain length of 8, the cage product is dominant in the zero-field, while the escape process predominates under the magnetic field. As far as we know, this is one of very few examples of a reaction switching due to external magnetic field effects.

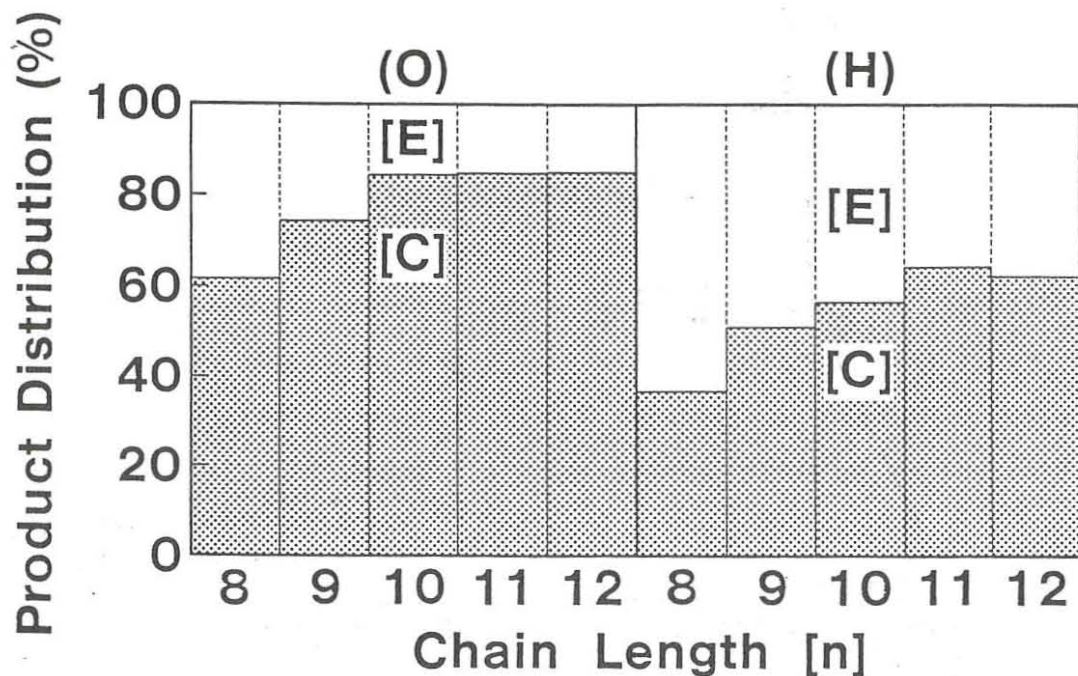


Fig. 2. Product distribution for photo-redox reactions of $O_2N-4-C_{10}H_6-1-O(CH_2)_n-NHC_6H_5$ in benzene recorded as a function of chain length n . O (left) and H (right) refer to the zero-field and the presence of an external magnetic field (0.64T). [C]: cage product, [E]: escape product.

Although magnetic fields ($\ll 1T$) generated by an ordinary electromagnet can cause rather small Zeeman splittings in a biradical intermediate with triplet spin multiplicity, intersystem crossing rate may be reduced to ca. 1/3 of the zero-field value when the magnetic field effects are mainly due to hyperfine coupling mechanism. Thus, the external magnetic field effects on radical pair reactions provide us with useful tools for elucidating the reaction mechanism, for controlling reaction rates and product yields, or for selecting a favourable reaction pathway from others.

References

- [1] R. Nakagaki, M. Hiramatsu, K. Mutai, Y. Tanimoto, and S. Nagakura, *Chem. Phys. Lett.*, 134 (1987) 171.
- [2] R. Nakagaki, K. Mutai, M. Hiramatsu, H. Tukada, and S. Nagakura, *Can. J. Chem.*, 66 (1988) 1989.
- [3] R. Nakagaki, K. Mutai, and S. Nagakura, *Chem. Phys. Lett.*, 154 (1989) 581.
- [4] R. Nakagaki, K. Mutai, and S. Nagakura, *Chem. Phys. Lett.*, 167 (1990) 439.

External Magnetic Field Effect on the H_2-O_2 Reaction on SnO_2 Surface

Hisao Ohnishi, Hirokazu Sasaki and Masamichi Ippommatsu
Fundamental Research Laboratories, Osaka Gas Co., Ltd.,
6-19-9, Torishima, Konohana-ku, Osaka 554, JAPAN

The authors report on the first findings regarding external magnetic field effects on the H_2-O_2 reaction on a SnO_2 surface by the measurements of the electric conductivity of SnO_2 thin films. Further, we have succeeded in directly measuring external magnetic field effects on H_2-O_2 reaction on an SnO_2 surface and found that the rate of increase in the reaction rate reached approximately 14% under the condition of 623 K and 5 T.

1. Introduction

Extensive studies of external magnetic field effects on catalytic reactions have been made by Misono [1], Selwood [2], and other researchers. However, the reaction systems were limited to the ortho-para conversion of hydrogen molecule on magnetic catalysts. It is recognized that the conductivity of sintered SnO_2 semiconductor changes when in contact with flammable gases. Making use of this property, SnO_2 semiconductor gas sensors are widely used for domestic gas leak alarm systems and are produced more than ten millions annually. This presentation reports on the external magnetic field effects on the H_2-O_2 reaction on the SnO_2 surface. This is the first finding of the magnetic field effect on an industrially important catalytic reaction.

2. Experimental Section

Sample Preparation. i) SnO_2 thin film. A SnO_2 thin film of the Greek cross form was deposited on a sapphire substrate by the reactive RF magnetron sputtering technique. The SnO_2 thin film (2.2 μm thick) had a columnar structure

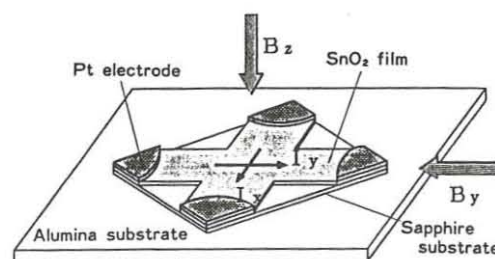


Fig. 1 SnO_2 thin film specimen.

that consisted of primary particles size of approximately 10 to 20 nm. Pt electrodes (1 μm thick) were deposited on the SnO_2 thin film by RF magnetron sputtering technique (Fig. 1).

ii) SnO_2 powder. A 99.999% pure Sn metal was dissolved in nitric acid, and the solution was neutralized by an ammonia solution, then obtained gel was washed by water, dried, and calcined

for 24 hr. at 1073 K in air atmosphere. The produced SnO_2 powder had primary particle size of approximately 20 to 30 nm and a B.E.T. surface area of 20 to 40 m^2/g and was used for directly measurement of the H_2-O_2 reaction rate.

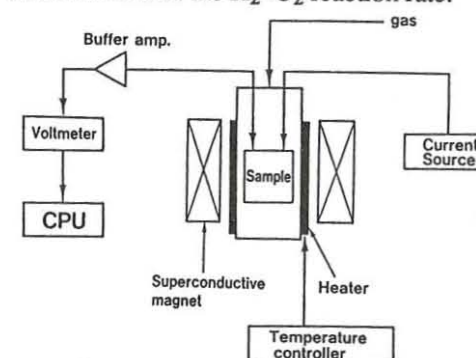


Fig. 2 Conductivity measurement system.

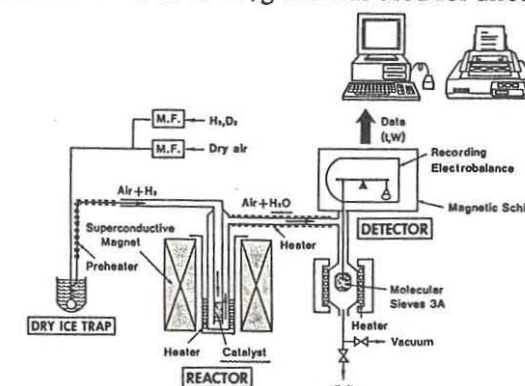


Fig. 3 The reaction rate measurement system for H_2-O_2 surface reaction

Measuring the conductivity. A diagram of the measurement system is shown in Fig. 2. The flow rate of the surrounding gases was made constant with mass flow controllers. The magnetic field was applied to the sample vertically using a superconductive magnet and was varied in the range from -5.0 to 5.0 T. Sweeping velocity of the magnetic field was 20 T/min.

Measuring the reaction rate. The measuring apparatus using flow method is shown in Fig. 3. Dry air containing 0.1% H_2 was supplied into the reaction cell, and the H_2O molecules in the produced gas was adsorbed by molecular sieves 3A. By measuring the increases in weight of H_2O adsorbed using a microbalance CAHN-2000, the reaction rate was successfully evaluated with an accuracy of $\pm 0.1\%$.

3. Results and Discussion

3-1. Backgrounds

The electric conductivity of SnO_2 is proportional to carrier electron density [3]. The carrier electron density is determined by the balance between the rate of the reaction producing electrons (reaction A, B in Fig. 4) and the rate of the reaction consuming electrons (reaction C) [4],[5]. Finally, the reaction rate between flammable gases and surface-adsorbed oxygen is proportional to the conductivity of SnO_2 in air containing H_2 [6].

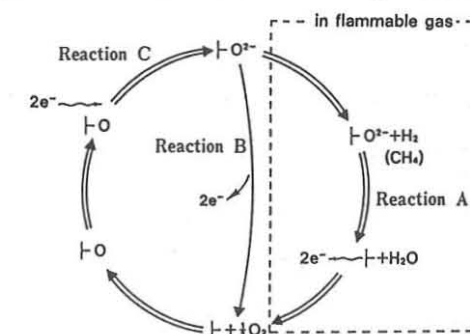


Fig. 4 Reaction mechanisms model on the SnO_2 surface.

3-2. Observation of magnetic field effect by the conductivity measurements

An increase in the conductivity of SnO₂ thin film by applying magnetic field was observed when a H₂-O₂ reaction was proceeding on the SnO₂ surface in an oxygen atmosphere at 773 K. The rate of increase in the conductivity was proportional to the square of the magnetic field intensity and was independent of H₂ concentration, as shown in Fig. 5. This phenomenon was distinguished from changes in electron mobility, such as magnetic resistance or hall effect, by measurement of the dependence of increase in the conductivity on magnetic field direction (Table I) and surrounding gases (Table II). Because this phenomenon was a characteristic feature when H₂-O₂ reactions on SnO₂ surfaces occurred, it can be concluded that this phenomenon was caused by the external magnetic field effect characteristics of the H₂-O₂ reaction on the SnO₂ surface. The increase rate of conductivity indicates the increase in reaction rate.

Moreover, we measured the transient response of the conductivity of SnO₂ thin film to fluctuations in the magnetic field intensity, as indicated by ° marks in Fig. 6.

The response had a lag for several seconds, therefore these results supposed that this phenomenon is based on the reaction. we were able to describe the transient response properties of external magnetic field effects, as indicated by solid

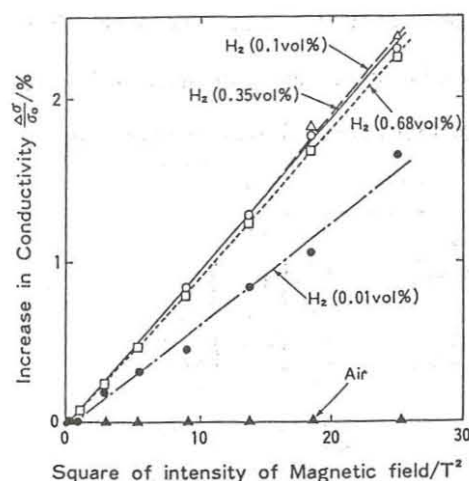


Fig. 5 Rate of increase in Conductivity of SnO₂ by applying magnetic field. (773 K)

Table I Dependence on magnetic field direction.

I vs. B vs. S	σ_0	σ_1	$\Delta\sigma/\sigma_0$ (%)
I ⊥ B // S (By, I x)	1.2877	1.3222	2.679
I // B // S (By, I y)	1.3134	1.3486	2.682
I ⊥ B ⊥ S (Bz, I y)	1.3283	1.3630	2.612

Table II Dependence on surrounding gases.

Surrounding Gases	$\Delta\sigma/\sigma_0$ (%)
1) Air (O ₂ + N ₂)	0.00
2) H ₂ (0.35vol.%) in Air	2.32
3) CH ₄ (0.35vol.%) in Air	0.00
4) H ₂ (0.10vol.%) in N ₂	0.00
5) H ₂ O (1.50vol.%) in Air	0.00
6) H ₂ (0.35vol.%) in Air (+1.5vol. %H ₂ O)	1.43

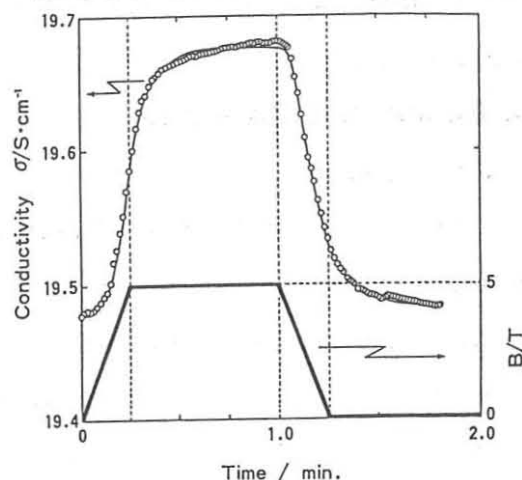


Fig. 6 Transient response of conductivity for varying magnetic field intensity. (0.36 % H₂, 773 K)

line in Fig. 6, by applying a simple magnetic field term $(1 + 2kB^2)$ to the H₂-O₂ reaction term in a equation, derived from analyzing the relation between conductivity changes and reaction rate of surface reactions in Fig. 4.

$$d\sigma/dt = \{ (1 + 2kB^2) a P_G + b \} / \sigma - c \sigma \quad (1)$$

Here, k is the constant, B is the magnetic field intensity, P_G is the concentration of H₂ in air, σ the conductivity of the SnO₂ thin film, t the time, a , b and c the constant proportional to the kinetic for reactions A, B and C in Fig. 4.

3-3. Direct measurement of magnetic field effects

Table III shows the results of the experiment to obtain H₂-O₂ reaction rates with and without the application of 5 T magnetic field in dried air containing 0.1% H₂ at 623 K. The results shows that its reaction rate increased by approximately 12% (approximately 14% after the blank value was deducted) by the application of the magnetic field.

Further, an isotope effect on magnetic field effects exists between H₂ and D₂ and the effect is reduced to 2/3 when

D₂ is used instead of H₂.

These results have strongly suggested that an activated complex of this reaction has a structure in which there is only a weak interaction between hydrogen molecules that do not dissolve nor separate and surface-adsorbed O²⁻, and the magnetic field affects the nuclear spin of H-H in activated complexes.(Fig. 7)

References

- [1] M. Misono and P. W. Selwood, *J. Am. Chem. Soc.* **90** (1968) 2977.
- [2] P. W. Selwood, *Adv. Catal.* **27** (1978) 23.
- [3] M. Ippommatsu, H. Ohnishi, H. Sasaki and T. Matsumoto, *J. Appl. Phys.* **69**(12) (1991), in press.
- [4] M. Ippommatsu and H. Sasaki, *J. Electrochem. Soc.* **136** (1989) 2123.
- [5] M. Ippommatsu and H. Sasaki, *J. Materials Sci.* **25** (1990) 259.
- [6] H. Sasaki, H. Ohnishi and M. Ippommatsu, *J. Phys. Chem.* **94** (1990) 4281.

	Increase rate of molecular sieves weight (μg / sec.)		Increase percentage of reaction rate (%)
	B=0T	B=5T	
Blank test	1.921 x 10 ⁻²	1.921 x 10 ⁻²	0.0
SnO ₂ pow.	1.680 x 10 ⁻¹	1.886 x 10 ⁻¹	12.3 (13.8*)

The changing percentage of increase rate of molecular sieves weight is equal to the changing percentage of H₂-O₂ reaction rate. * after the blank value was deducted.

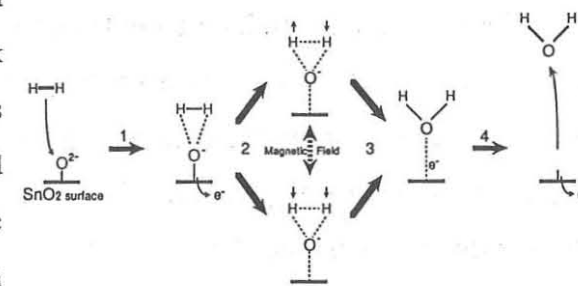


Fig. 7 Reaction process of H₂-O₂ reaction on SnO₂ surface.

Solvent Dependence of Magnetic Field Effects on Photoisomerization of a Butenylnaphthalene in the Presence of Electron Acceptor

Hirochika Sakuragi, Kazuhiko Naitoh, Takahisa Oguchi, Tatsuo Arai, and Katsumi Tokumaru,

Department of Chemistry, University of Tsukuba, Tsukuba, Ibaraki 305, Japan

Ryoichi Nakagaki, and Saburo Nagakura

Institute for Molecular Science, Myodaiji, Okazaki 444, Japan

Quenching of olefins in excited states by electron acceptors in polar solvents may generate radical pairs which are precursors of geometrical isomerization of the olefins. The excited singlet state of *trans*-2-(3,3-dimethyl-1-butenyl)naphthalene (2-NpCH=CHBu^t, *t*-BN) is efficiently quenched by electron acceptors to afford the *cis* isomer (*c*-BN) in various solvents ranging from nonpolar benzene to polar acetonitrile.^{1,2)} Previously, we demonstrated that the precursor of *t*-BN isomerization in acetonitrile is the olefin triplet arising from intersystem crossing of a singlet radical pair.¹⁾ In benzene, however, the quenching was accompanied by emissions ascribable to exciplexes, suggesting that the isomerization in nonpolar solvents proceeds through the olefin triplet generated from the exciplexes.²⁾ In order to clarify the reaction intermediates and their contribution to the isomerization, we employed laser flash photolyses (LFP) and external magnetic field effects (MFE) upon the isomerization quantum yield on steady irradiation in various solvents.¹⁾

Irradiation of *t*-BN (0.01 M) at 313 nm in various solvents afforded *c*-BN with varying quantum yields ($\phi_{t \rightarrow c}^0$), as shown in Table 1. The isomerization was assumed to proceed mainly on the singlet manifold since the quantum yield was not

Table 1. Isomerization quantum yields of *t*-BN in the absence ($\phi_{t \rightarrow c}^0$) and presence of *p*-DCB ($\phi_{t \rightarrow c}^\infty$) and the asymptotic $\eta(H)/\eta(0)$ values at the high magnetic field in isomerization of *t*-BN in the presence of *p*-DCB in various solvents

Solvent	ϵ	K_{SV}	$\phi_{t \rightarrow c}^0$	$\phi_{t \rightarrow c}^\infty$	$\eta(H)/\eta(0)$
Benzene	2.28	540	0.13	0.23	≈ 1
Chloroform	4.81	200	0.14	0.29	≈ 0.98
Tetrahydrofuran	7.58	560	0.13	0.20	≈ 0.90
Dichloromethane	8.93	400	0.19	0.18	≈ 0.87
1,2-Dichloroethane	10.4	230	0.19	0.14	≈ 0.84
Propionitrile	27.2	690	0.15	0.05	≈ 0.79
Acetonitrile	37.5	870	0.14	0.04	≈ 0.67

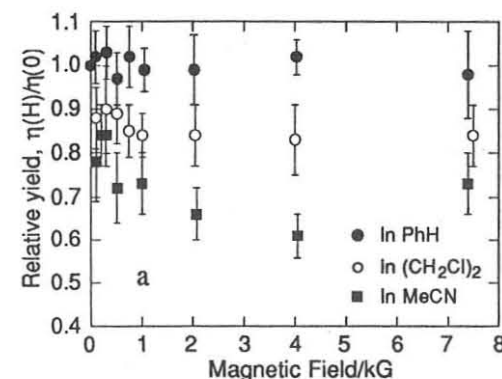


Fig. 1. Plots of relative yields of *c*-BN at magnetic fields of varying intensity.

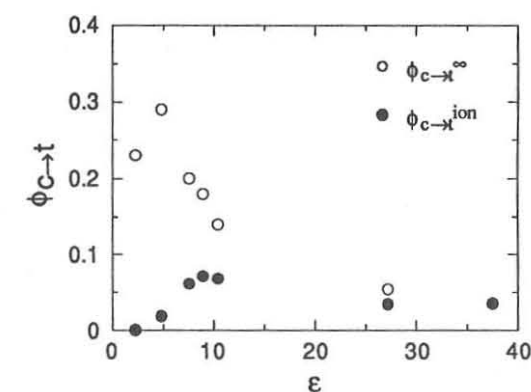


Fig. 2. Contribution of ionic intermediates (●) to the isomerization of *t*-BN in the presence of *p*-DCB (○) in various solvents.

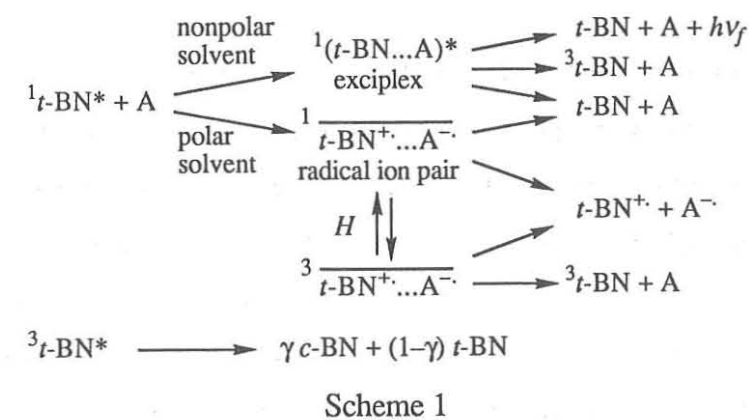
affected by triplet quenchers.^{1,2)} In the presence of *p*-dicyanobenzene (*p*-DCB), the quantum yield ($\phi_{t \rightarrow c}$) decreased remarkably in propionitrile and acetonitrile, but increased noticeably in benzene, chloroform, and THF, with increasing acceptor concentration to approach the limiting quantum yields ($\phi_{t \rightarrow c}^\infty$), as summarized in Table 1, where K_{SV} ($=k_q\tau^0$) represents the Stern-Volmer constant for the quenching of the excited singlet *t*-BN by a quencher.

The transient absorption spectrum of the *t*-BN/*p*-DCB system in various solvents show unambiguously that photoinduced electron transfer takes place between the excited singlet *t*-BN and the ground-state electron acceptor in polar solvents such as acetonitrile and dichloromethane; however, in nonpolar solvents such as benzene and chloroform no ionic species were generated.

Deaerated solutions (3 ml) of *t*-BN (2×10^{-4} M) and *p*-DCB (5×10^{-2} M) in various solvents were irradiated for 10–20 min with filtered light ($\lambda \geq 330$ nm) from a 300-W xenon lamp at ambient temperature. The sample solutions were examined after irradiation using an HPLC apparatus to determine the concentrations of *c*-BN produced. Under these irradiation conditions the light was absorbed only by *t*-BN; *p*-DCB and *c*-BN formed were not practically excited, and the conversion was controlled at 6–8%. The yield of *c*-BN [$\eta(H)/\eta(0)$] at various applied magnetic fields relative to that at the zero magnetic field strength are plotted in Fig. 1. This figure shows that the relative yields of *c*-BN are reduced, except for the case of benzene as solvent, at the field strengths lower than 1 kG and reached nearly constant values at the higher strength region. The effect of magnetic field on isomerization quantum yield arises from the hyperfine interaction in radical pairs.²⁾ The asymptotic $\eta(H)/\eta(0)$ values estimated from Fig. 1 are also summarized in Table 1.

The isomerization mechanism in nonpolar and polar solvents can be described by Scheme 1, where the olefin triplet is the key intermediate.¹⁾ In the *t*-BN/*p*-DCB system the largest magnetic field effect was observed in acetonitrile, and the effect was reduced in the order of acetonitrile, propionitrile, 1,2-dichloroethane, dichloromethane, THF, chloroform, and benzene. It can be reasonably assumed that the isomerization proceeds exclusively through radical ions in acetonitrile. Accordingly, the asymptotic $\eta(H)/\eta(0)$ values at the high magnetic field in various solvents relative to that in acetonitrile correspond to contributions of the ionic intermediates to the isomerization in the respective solvents. Figure 2 plots the total quantum yields for isomerization ($\phi_{t \rightarrow c}^{\infty}$) and quantum yields due to ionic intermediates ($\phi_{t \rightarrow c}^{\text{ion}}$) estimated using the asymptotic values, and shows that the isomeriza-

tion or triplet formation from the interaction of the olefin and acceptor is more efficient through exciplexes than through ion radicals and the maximum efficiency appears at $\epsilon=4.8$ (chloroform). The contribution of radical ions to the total quantum yield decreases with decreasing polarity of solvents but the isomerization due to radical ions reaches a maximum value at a medium ϵ value of 8.9 (dichloroethane). It can be concluded that the isomerization proceeds through *t*-BN triplets generated from the interactions of *t*-BN singlets with the acceptors, and that the efficiency of triplet formation decreases with increasing polarity of the solvent by switching of the precursors of *t*-BN triplets from exciplexes to radical ion pairs.



References

- 1) H. Sakuragi, R. Nakagaki, T. Oguchi, T. Arai, K. Tokumaru, and S. Nagakura, *Chem. Phys. Lett.*, **135**, 325 (1987).
- 2) T. Oguchi, T. Arai, H. Sakuragi, and K. Tokumaru, *Bull. Chem. Soc. Jpn.*, **60**, 2395 (1987).

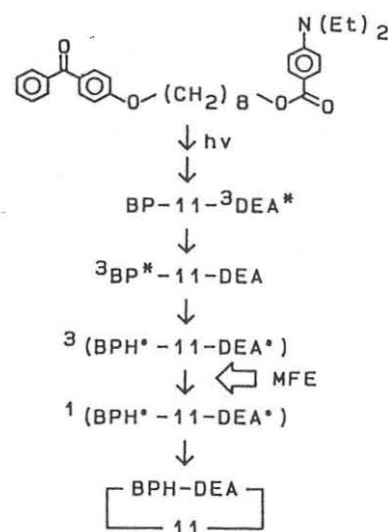
B7
20:00
~22:00

Laser Flash Photolysis Studies of the Magnetic
Field Effects on the Bifunctional Chain Molecules
Containing Benzophenone and N,N-Diethylaniline

Yoshifumi Tanimoto, Yoshihisa Fujiwara, Akinori
Saegusa, and Michiro Hayashi

Department of Chemistry, Faculty of Science,
Hiroshima University, Naka-ku, Hiroshima 730,
Japan

The magnetic field effect (MFE) of intramolecular photoreac-
tion of α -(4-benzoyl)phenoxy- ω -(4-N,N-diethylamino)benzoylox-
yalkane (BP-n-DEA, n=6~11) in dimethylformamide (DMF) solvent
was investigated by laser flash photolysis as a function of the
total number (n) of the chain unit linking the two chromophores.
MFE on the lifetime of the biradical intermediate increased
together with the number of n and the maximum MFE was obtained in



REACTION SCHEME

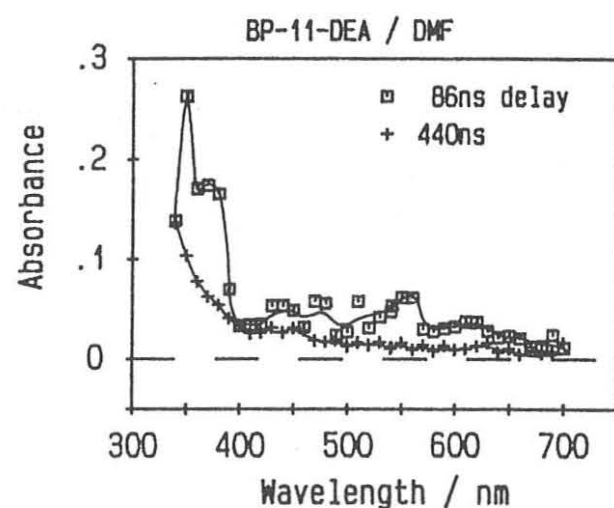


Fig.1 Transient Absorption Spectra.

BP-11-DEA compound. An effective singlet-triplet level degen-
eracy may occur when $n > 9$.

Fig. 1 displays a typical transient absorption spectra of
BP-11-DEA obtained by the 337 nm laser excitation. The absorp-
tion band (λ_{max} 350 and 560 nm) ascribed to a BP ketyl radical
appeared immediately after photoexcitation and decayed with a
relatively short lifetime ($< 1 \mu s$) at zero magnetic field. No
transient absorption attributable to the ion radicals was detect-
ed in the nanosecond photolysis. Analogous transient spectra
were observed in BP-n-DEA (n=6-13).

A tentative reaction mechanism is shown in Scheme. The
337 nm excitation produces the excited triplet state of DEA
selectively, causing the fast triplet energy transfer into BP.
The triplet BP gives rise to the hydrogen abstraction reaction
from DEA leading to the formation of a triplet biradical which

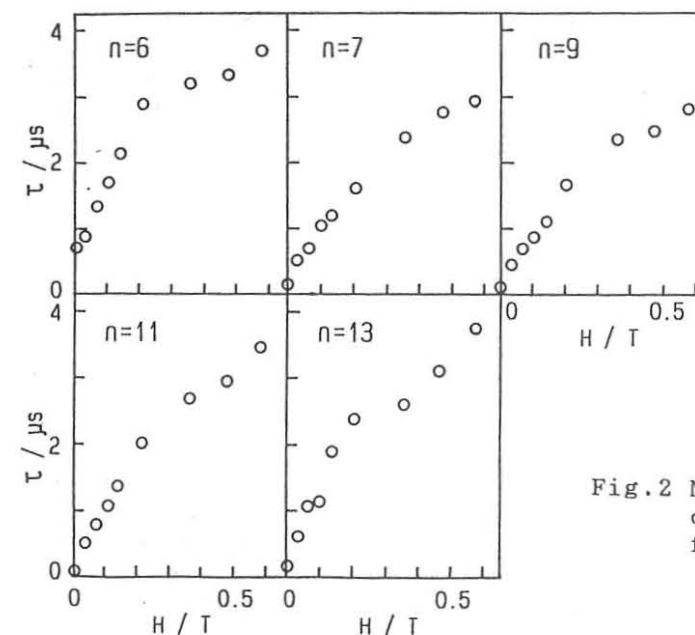


Fig.2 MFE on the lifetime
of biradicals generated
from BP-n-DEA in DMF.

consists of BP ketyl and DEA radicals.

Anomalous increase in the biradical lifetime occurs along with increasing the strength of a magnetic field. Fig. 2 shows conspicuous MFE in the lifetime of all compounds in the magnetic field range of 0~0.6 T. The magnitude of maximum MFE surprisingly reached up to more than 40 times in $n=11$ at 0.6 T. Magnetic fields may restrain the triplet-singlet intersystem crossing process of the biradical because of the Zeeman splitting of the triplet sublevels (T_- and T_+) and the lifetime in higher fields may be determined by the spin relaxation process in triplet sublevels as observed in the previous chain molecules [1, 2].

The chain length dependence (n) of the biradical lifetime ratio in the presence and absence of a magnetic field is given in Fig. 3. It makes clear the dependence of MFE on the chain number (n). It is noteworthy that the magnitude of MFE is increasing together with n and saturating at around $n=11$. This may imply that the singlet-triplet degeneracy of the biradical takes place when $n > 9$. The result is in good agreement with those of xanthone-xanthene ($n > 10$) [1], benzophenone-

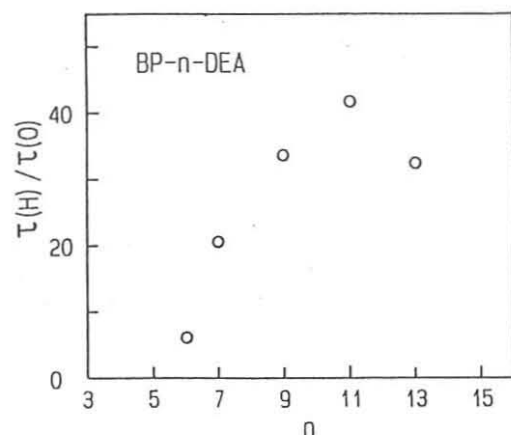


Fig.3
Chain length dependence of the lifetime ratio $\tau(H)/\tau(0)$ of the biradicals generated from BP- n -DEA in the presence and absence of a magnetic field ($H=0.57T$).

diphenylamine ($n > 8$) [2] and phenanthrene-dimethylaniline linked systems [3].

In the present model system, no magnetic field dependence attributable to the T_- -S level crossing was observed (Fig. 2), in contrast to a benzophenone-diphenylamine linked system. This discrepancy might be responsible for the difference in the structure of the respective terminal groups (-O- or -COO-) of the chain.

References

- [1] Y. Tanimoto et al., Bull. Chem. Soc. Jpn., 62, 3923 (1989).
- [2] Y. Tanimoto et al., Bull. Chem. Soc. Jpn., 63, 1342 (1990).
- [3] Y. Tanimoto et al., J. Phys. Chem., 93, 3586 (1989).

B8

20:00

~22:00

Application of Pulsed EPR Spectroscopy to the
Study of Radical Reactions

Tsuneki Ichikawa and Hiroshi Yoshida

Faculty of Engineering, Hokkaido University

Sapporo, 060 Japan

CW and pulsed EPR measurements of alkyl radicals generated from alkanes and alcohols by γ -irradiation have been carried out for studying the mechanism of radical reactions in solids. A pulsed EPR spectrum, obtained by measuring the intensity of electron spin echo (ESE) signals while sweeping the magnetic field very slowly (field-swept ESE spectrum), is so sensitive to the rate of paramagnetic relaxation that overlapping EPR spectra are possible to be differentiated if the relaxation rates of the paramagnetic species are different with each other. The field-swept EPR spectrum is also sensitive to the fluctuation of hyperfine fields so that the analysis of the spectrum gives the information about the molecular motion of the radicals.

The results obtained by the application of the pulsed EPR spectroscopy are summarized as follows;

1) Comparison of the CW and the field-swept EPR spectra of alkyl radicals. Two types of secondary alkyl radicals are known to be generated and stabilized in γ -irradiated alkane crystals at 77 K. They are the penultimate alkyl radical with the unpaired electron on a carbon second to the end of the carbon chain and the inner alkyl radical with the unpaired electron on a carbon farther than the second one. The irradiated crystals show the overlapping CW EPR spectra of these radicals. On the other hand, the field-swept

ESE spectra show the EPR spectrum of the penultimate radical. This difference arises from the fast paramagnetic relaxation of the penultimate radical induced by time fluctuation of the EPR spectrum, or spectral diffusion. The spectral diffusion of the penultimate radical are much faster than the inner one, because the bending motion of the C- \dot{C} H-C bond, the source of the fluctuation of α and β proton hyperfine couplings, is faster for the penultimate radical. The resolution of the field-swept ESE spectrum increases with the time of longitudinal relaxation, which implies that the relaxation is slower for the spins near the peak of the spectrum. The resolution enhancement is caused by the spectral diffusion. When an EPR spectrum is broadened due to the dynamic change of the spectrum, the relative intensity of the spectrum is proportional to the lifetime of the spins staying at the observed spectral position. The longitudinal relaxation due to the spectral diffusion is therefore slower for the spins near the peak of the spectrum.

The shape of a field-swept ESE spectrum is usually similar to the corresponding CW EPR spectrum. However the field-swept ESE spectrum of 2-hydroxyethyl radical at 77 K shows four lines instead of five CW EPR lines. This discrepancy arises from the hindered rotation of the methyl group. The methyl group of the 2-hydroxyethyl radical is not freely rotated and the hyperfine couplings with the three methyl protons are not averaged out. The rotation of the methyl group thereby causes the fast spectral diffusion, if the nuclear spin states of the methyl protons are not all the same. The spectrum of the radical with the methyl protons of the spin state $\pm(1/2, 1/2, 1/2)$ is not changed by the rotation of the methyl group, so that this radical is selectively

detected on the field-swept ESE spectrum.

2) Selectivity of alkyl radical formation by tunneling C-H hydrogen abstraction. Several types of alkyl radicals are expected to be formed and stabilized in γ -irradiated solid alkanes. These are primary radicals, penultimate and inner secondary radicals, and tertiary radicals for branched alkanes. The CW EPR spectra of these radicals are similar, since the proton hyperfine coupling constants are not much different. The identification of the radicals from the CW EPR spectrum of the irradiated solid is therefore not an easy task, especially when there are more than one radical species. Overlapping ESR spectra are differentiated into each component by measuring the field-swept ESE spectrum. The field-swept spectra indicate that the radicals in γ -irradiated branched alkane glasses at 77 K are the primary and the penultimate secondary radicals. The formation of the inner secondary radical and the tertiary radical is prohibited at 77 K. The primary radical gradually converts to the penultimate secondary radical by the abstraction of a penultimate C-H hydrogen on an adjacent molecule. The hydrogen abstraction proceeds by quantum-mechanical hydrogen tunnelling process. The penultimate radical is also formed through the tunneling C-H hydrogen abstraction by a hydrogen atom.

Although a considerable amount of inner radicals are generated in n-alkane crystals γ -irradiated at 77 K, only the penultimate secondary radical is observed in glassy solids. The selective formation of the penultimate radical from n-alkanes is induced by the tunneling C-H hydrogen abstraction. The difference of the selectivity between the crystal and the glass arises from the effect of solid phases on a specific molecular motion assisting

the tunneling of the C-H hydrogen.

The selectivity of alkyl radical formation in alkane liquids simply depends on the strength of the C-H bonds. The tertiary C-H bond is the weakest, so that a considerable amount of the tertiary radicals are generated from branched alkanes even the number of the tertiary C-H bonds is the smallest.

It is concluded from these results that the selectivity of alkyl radical formation in solids is determined by the rate of tunneling C-H hydrogen abstraction. The tunneling rate is determined not only by the activation energy for the abstraction but also by the easiness of molecular motion assisting the hydrogen abstraction. In the glassy matrix, a $sp^3 \leftrightarrow (sp^2 + p)$ umbrella motion assisting the abstraction of the C-H hydrogen is slower for the tertiary and the inner carbons than the penultimate secondary carbons, because three carbon chains for the tertiary carbon and two carbon chains for the inner carbon prevent the umbrella motion. The rates of the tertiary and the inner secondary radical formation are therefore slower than that of the penultimate radical formation even the activation energies are lower than and the same as that for the penultimate secondary carbon, respectively.

In a crystalline solid all the carbon atoms in a molecule are on the molecular plane. The crystal has a structure close to a layered one. The accordion motion of the C-C chain is therefore easy to take place in the crystal. Since the accordion motion causes the change of $sp^3 \leftrightarrow (sp^2 + p)$ for all the carbons, the tunneling C-H hydrogen abstraction also takes place on the inner carbons.

Effect of Electron Spin Diffusion on Electron
Spin Echo Decay

Vadim V. Kurshev and Tsuneki Ichikawa

Faculty of Engineering, Hokkaido University,
Sapporo, 060 Japan

Dipole-dipole (d-d) interactions between paramagnetic centers in solids induce the phase relaxation of electron spins which can be detected as the decay of an electron spin echo (ESE) envelope. The investigation of the ESE decay allows one to evaluate physical parameters in various spin relaxation processes and to obtain information concerning the motion and the spatial arrangement of paramagnetic centers (1-2). One of the most powerful methods for this purpose is to analyze the ESE decay due to instantaneous diffusion (ID) mechanism, since ID is created by perturbation of spin coupling by microwave pulses and therefore artificially controllable relaxation process. A novel pulse sequence suitable for extracting ID has recently been invented (3). In this method, called 2+1 pulse ESE, additional ID is induced by strong microwave pulse inserted between the first labelling pulse and a refocusing pulse, and the decay of a two pulse ESE envelope due to the additional ID is measured as a function of the time interval between the first and the additional pulses.

The analytical expression for the 2+1 ESE decay is easily obtained by neglecting a flip-flop term, S_+S_- , in the Hamiltonian of d-d interaction. Although the flip-flop is expected to give a significant effect on ID, most of theoretical and experimental works did not take it into consideration. For clarifying the applicability of the two and 2+1 pulse ESE method to the study of

d-d interaction, it is therefore necessary to know the effect of the flip-flop on the ESE decay due to the ID mechanism.

Experiments with a hydrogen atoms stabilized at 77K in γ -irradiated quartz glass shows the effect of electron flip-flops on the manifestation of d-d interactions in ESE decay, Fig.1. The

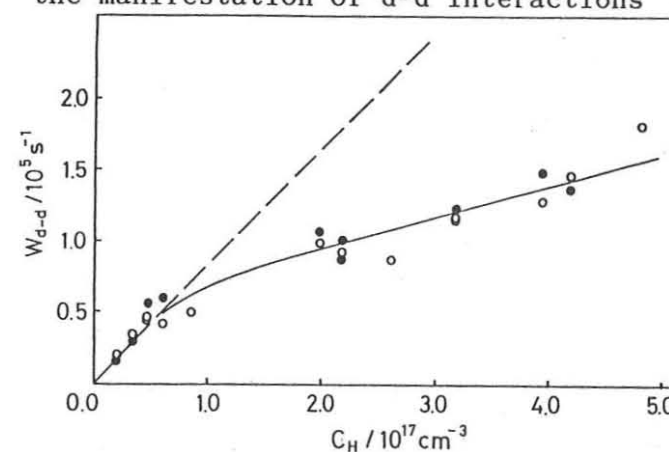


Fig.1. Strength of d-d interaction estimated from (\circ) two and (\bullet) 2+1 pulse ESE decay under the assumption of no flip-flops. The real strength is shown with a broken line.

dependence of the dipole broadening of ESR line on the concentration of hydrogen atoms estimated from two and 2+1 pulse ESE decays deviates from linear, predicted by stochastic theory (4).

The effect of the flip-flop can be divided into two categories: direct and indirect effects. The direct effect is due to the flip-flop between an observed spin and its partner one. The indirect effect is due to the flip-flop between a pair of spins near an observed spin. The flip-flop of the pair of spins causes the spectral diffusion of the observed spin through the change of the local magnetic field. Since the spectral diffusion is faster for spin groups with stronger d-d interactions, the average d-d interaction for the ESE-detected spin group decreases with increasing time τ between the labelling and the refocusing pulses. Therefore, if the observed ID is analyzed by using a theory including no flip-flop term, it gives a weaker d-d interaction and a longer spin-spin distance than real ones.

Exact calculations of density matrix evolution revealed

unimportance of direct effect on the ESE decay both in two and 2+1 pulse methods. The influence of flip-flop interaction of observed spins linearly increase with a concentration of paramagnetic centers as well as effect of ID mechanism. Therefore the relative effect of direct interaction does not increase, and it is important only for a very short initial time interval of ESE decays.

The indirect effect is induced by interaction between many particles. Instead of solving a density matrix for spin groups under multiple d-d interactions, we treat a pair case in which an observed spin interacts with a partner spin without flip-flop but the partner spin flip-flops with another spins with the rate of $2W$. Provided the flip-flop rate is the same for all the spins, the decay kinetics of identical spins under the random spatial distribution is given by

$$E(2\tau) = E_{ID}(2\tau)E_{SD}(2\tau)E_0(2\tau) \quad (1)$$

where $E_{ID}(2\tau)$ and $E_{SD}(2\tau)$ denote the ESE decay due to ID and spectral diffusion by the d-d interaction, respectively; $E_0(2\tau)$ is the decay due to another reasons. E_{ID} and E_{SD} can be represented as

$$\begin{aligned} E_{ID}(2\tau) &= \exp[-\sin^2(\theta/2)\gamma^2\hbar CD_A(2W\tau)\tau]; \\ E_{SD}(2\tau) &= \exp[-\gamma^2\hbar CD_B(2W\tau)\tau] \end{aligned} \quad (2)$$

where θ is the angle of spins turn by refocussing pulse, γ is hyromagnetic ratio, C is the concentration of hydrogen atoms,

$$\begin{aligned} D_A(x) &\approx 5.07/(1 + 1.08x^{1/2} - 2.04x + 2.51x^{3/2}); \\ D_B(x) &\approx 2.53x/(1 + 0.25x^{1/2} + 0.63x^{3/2}) \end{aligned} \quad (3)$$

The decay kinetics in 2+1 pulse ESE is given by

$$E(2\tau, \tau') \approx \exp[-\sin^2(\phi/2)\cos\theta\gamma^2\hbar CD_A(2W\tau')\tau'] \quad (4)$$

where ϕ is the angle of spins turn by additional pulse.

It can be seen from Eqs.(3,4) that the increase of x ($= 2W\tau$) causes the deviation of the ID decay kinetics from the exponential function and the decrease of the decay rate. Assuming 10 % accuracy for the observed decay rate, the flip-flop term is negligible only if $x < 0.02$. The ESE decay due to ID is very sensitive to the flip-flop. The flip of only one of 50 spins gives the observable effect. The flip-flop also accelerates the ESE decay due to spectral diffusion. In experiments with a hydrogen atoms in γ -irradiated at 77K quartz testify the increasing of decay rate of $E_{SD}(2\tau)$ with a concentration of hydrogen in accordance with Eq.(3). The increase of the decay rate indicates that the indirect effect is the main source of diminishing the effect of ID on the ESE decay.

The result of this work can be resumed as follow. Flip-flops between electron spins diminish the effect of instantaneous diffusion on two and 2+1 pulse ESE envelope decays even if the longitudinal relaxation is much slower than the phase relaxation. The main mechanism diminishing the effect of instantaneous diffusion is not the direct flip-flop of observed spins but the flip-flop of spin pairs adjacent to them. A theory including no flip-flop term is not applicable to the analysis of observed ESE decay kinetics if the microwave power-independent phase relaxation rate depends on the spin concentration.

References

- [1]K. M. Salikhov et al., J. Magn. Reson. 42, 255 (1981).
- [2]M. Romanelli and L. Kevan, J. Magn. Reson. 91, 549 (1991).
- [3]V. V. Kurshev, et al., J. Magn. Reson. 81, 441 (1989).
- [4]A. Abragam, "The Principles of Nuclear Magnetism", Clarendon, Oxford, 1961.

B10

20:00

~22:00

ESEEM OF COPPER(II) COMPLEXES COORDINATED BY IMIDAZOLE
CONTAINING LIGANDS

Yasunori Ohba, Yukihiro Yoshida, and Masamoto Iwaizumi

Institute for Chemical Reaction Science,

Tohoku University, Katahira 2 Chome, Aobaku Sendai 980,

Japan

Electron Spin Echo Envelope Modulation (ESEEM) has been widely used for studies of copper(II) complexes coordinated by imidazoles. The noncoordinating nitrogen of the imidazole ligand (far nitrogen) shows strong ESEEM effects and the ESEEM frequencies correspond to the ^{14}N ENDOR frequencies. The imidazole coordination to a copper(II) ion was found by this strong ESEEM effects for many biological systems.¹⁾ However the coordination structures of the systems have not been made clear in their ESEEM studies. In this paper we attempted to use ESEEM for determination of structures of copper (II) complexes coordinated by imidazole containing ligands. We focussed attention to the orientation dependence of the ESEEM effects which are caused by the quadrupole interaction of the far nitrogen of imidazole ring for the purpose. The complexes used are bis(2-(2'-pyridyl)imidazole)copper(II), $[\text{Cu}(\text{pim})_2]^{2+}$, bis(2-(2'-pyridyl)benzimidazole)copper(II)

$[\text{Cu}(\text{pbi})_2]^{2+}$, and the six coordination species of these complexes formed by addition of N bases, $[\text{Cu}(\text{pim})_2\text{B}_2]^{2+}$ and

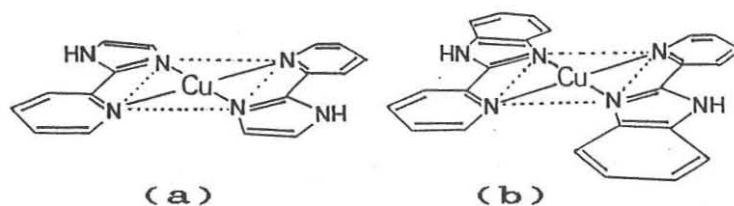


Figure 1. Structure of (a) $[\text{Cu}(\text{pim})_2]^{2+}$ and (b) $[\text{Cu}(\text{pbi})_2]^{2+}$.

$[\text{Cu}(\text{pbi})_2\text{B}_2]^{2+}$, where B is a N base such as imidazole or pyridine derivatives.

EPR spectra were recorded at 77K for frozen solutions containing 10 mM of these copper complexes. Three pulse stimulated echo ESEEM's were observed for the solutions at 10-20 K. The obtained time domain ESEEM were analyzed by the LPQRD algorithm and transformed to the frequency domain spectra which were analogue of ENDOR spectra.

Pim and pbi take a restricted coordination structure with respect to the orientation of the imidazole plane by formation of the chelate structure and the imidazole ring becomes coplanar to the plane formed by the chelate bonds. Therefore, $[\text{Cu}(\text{pim})_2]^{2+}$ and $[\text{Cu}(\text{pbi})_2]^{2+}$ apparently take the planar structure (Fig. 1). The EPR spectra of these complexes can be well explained as having a planar structure coordinated by the four nitrogen atoms of the two chelate ligands (Fig. 2). Figure 3 is ESEEM's observed by setting the magnetic field on the extrema of g tensor of these EPR spectra. These ESEEM's show appreciable magnetic field dependency as a result of orientation selection in the ESEEM measurements. From this orientation selective ESEEM measurements, we determined the direction of the ^{14}N quadrupole coupling tensor for the far nitrogen atoms of the imidazole groups.

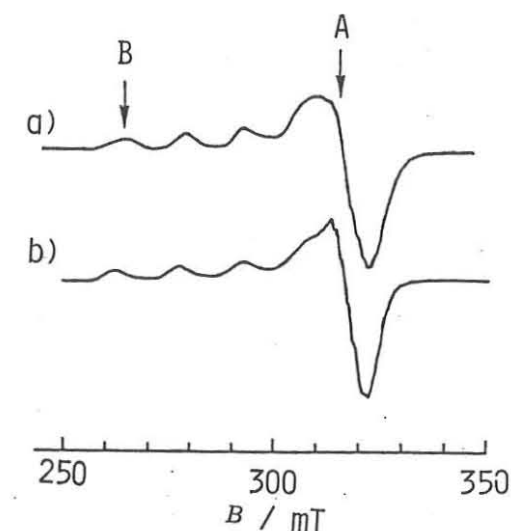


Figure 2. EPR spectra of (a) $[\text{Cu}(\text{pim})_2](\text{NO}_3)_2$ in $\text{DMF}/\text{CH}_3\text{NO}_2$ and (b) $[\text{Cu}(\text{pbi})_2](\text{NO}_3)_2$ in DMF/EtOH frozen solutions at 77K. The arrows indicate the magnetic field settings used for ESEEM measurements.

In the case of the six coordination species, $[\text{Cu}(\text{pim})_2\text{B}_2]^{2+}$, $[\text{Cu}(\text{pbi})_2\text{B}_2]^{2+}$, there are three possible structures (Fig. 4). One of the possible structures is that where the two chelate ligands constitute the tetragonal plane and form stronger coordination bonds than the added bases, B. Hence the unpaired spin orbital lie in the plane. In this case, the imidazole rings are coplanar with the unpaired spin orbital. The second possible structure is that where the two additional bases and the imidazole groups of the chelate ligands constitute the tetragonal plane containing the unpaired electron orbital.

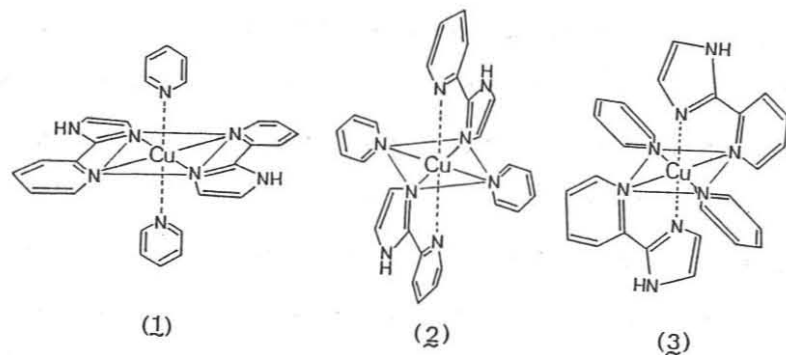


Figure 4. Three possible structures of $[\text{Cu}(\text{pim})_2\text{B}_2]^{2+}$, B: pyridine.

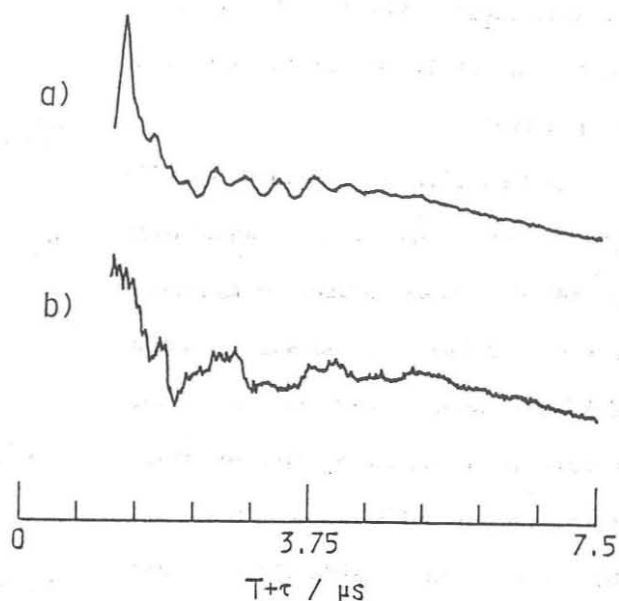


Figure 3. ESEEM of $[\text{Cu}(\text{pim})_2(\text{NO}_3)_2]$ in DMF/EtOH frozen solution at 20K. The ESEEM (a) is measured by setting magnetic field at A in Fig. 2 and (b) at B.

The third is the case in which the two N bases and the pyridyl groups of the chelate ligands make stronger coordination bonds than the imidazole groups and form the tetragonal plane. EPR spectroscopy can not distinguish these three structures. In our previous paper²⁾, we have shown that the ^{14}N -ENDOR can distinguish the type of nitrogen, sp^2 or sp^3 , in the tetragonal plane in the copper(II) complexes. However, in the present case, all the nitrogens are of the sp^2 type, and hence it is impossible to apply the method to distinguish the structures.

It is notable that in the first structure the relative orientation of the quadrupole tensor of the far nitrogens to the tetragonal plane of the unpaired spin orbital is different from that in the second and the third structures. On the other hand, the hyperfine interactions of the far nitrogens are expected to have appreciable magnitude for the first and the second, but they may be almost zero in the third case. Therefore for the first and the second structures strong ESEEM effects by the far nitrogens of the imidazole groups must be observed but their magnetic field dependence must be different for these two cases. In the third structure the ESEEM effects must be small because of the hyperfine interaction of the far nitrogens are too small. Based on these considerations, the ESEEM of the far nitrogens can be used to determine the coordination structure of the six coordination complexes. By using these criterion, we determined the structure of $[\text{Cu}(\text{pim})_2\text{B}_2]^{2+}$ to be the second, and that of $[\text{Cu}(\text{pbi})_2\text{B}_2]^{2+}$ to be the third.

References

- 1) F. Jiang, et al., J. Am. Chem. Soc., 112, 9035(1990).
- 2) M. Iwaizumi et al., Inorg. Chem., 25, 1546(1986).

maximum ODES signal would be equal with each other, if the same spin relaxation parameters are postulated. This means that with increasing the pyrene concentration the charge hopping rate increases and thus the recombination time decreases. Since the ODES spectrum for the system with the pyrene concentration higher than 1.0 wt% consists of mainly those of pyrene ion signals, the charges reside mainly on the doped molecules and thus hop only between pyrenes.

The fluorescence spectrum of this system consists of monomer and excimer peaks. The relative height of the latter is considerably higher for the X-ray excited system than that for UV-irradiated system, especially at high solute concentrations and at high observation temperatures. This excess excimer fluorescence in X-ray excited system can be explained only with hole hopping from a pyrene to a cluster of pyrenes which stabilizes the hole resulting a oligomer cation. This is

neutralized later by recombination with the electron and the excimer is preferentially formed. From the present results, together with the former study on EP-rubber[3], we deduced the charge recombination mechanism shown in Figure 1 for the polyolefin system doped with aromatic molecules.

3-2. Polystyrene

Figure 3 shows the magnetic field dependence of the recombination fluorescence in polystyrene doped with pyrene at 0.1, 1.0, and 8.9 wt%. The

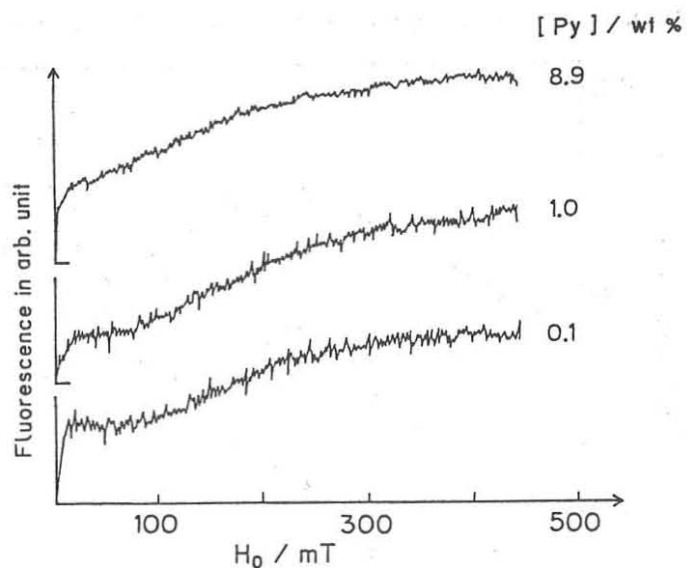


Figure 3. Magnetic field dependent fluorescence yield in X-ray irradiated polystyrene doped with pyrene at three different concentrations. Observations are made at room temperature.

magnetic field dependence is apparently composed of two parts, one is a sharp increase of the fluorescence which saturates over the magnetic field of about 50 mT and the other is a broad dip at around 60 mT followed by the gradual increase which does not saturate even over 500 mT. The cause of this dip is attributed to the level crossing between a triplet sublevel and the singlet level of the geminate pair. Zero field splitting of 60 mT corresponds to a separation of about 3-5 Å. We tentatively assign this metastable state as an excited state like exciton, which needs some energy to recombine to yield the excited pyrene. This interesting phenomenon must be due to a small difference in the ionization potentials (or electron affinities) between the matrix and the solute, which allows the charges delocalize in some wider region.

The ODES amplitude as the function of pyrene concentration showed a minimum at the concentration of about 1.0 wt%. This dependence was very much different from that in poly-olefins. We consider that this phenomenon is the result of competition between the two processes, charge hopping between the solute pyrenes and the formation of exciton-like excited state.

4. Conclusion

The charge recombination in a polyolefin doped with aromatic molecules proceeds through charge hopping between the solute molecules. On the other hand, in polystyrene which contains aromatics in the polymer itself the charge recombines through an exciton-like excited state. In the latter case, charges may hop between the aromatic groups including those in the polymer chain.

5. Reference

- [1] M. Okazaki, K. Nunome, K. Matsuura, and K. Toriyama, *Bull. Chem. Soc. Jpn.*, **63**, 1396 (1990).
- [2] M. Okazaki, Y. Tai, R. Nakagaki, K. Nunome, and K. Toriyama, *Chem. Phys. Lett.*, **166**, 227 (1990).
- [3] M. Okazaki, K. Toriyama, Y. Tai, and K. Nunome, *Appl. Magn. Reson.*, **1**, 213 (1990).
- [4] N.N. Lukzen, V.O. Saik, O.A. Anisimov, and Yu.N. Molin, *Chem. Phys. Lett.*, **118**, 125 (1985).

B12
20:00
~22:00

EPR and ODMR Studies of the Phosphorescent States
of trans-2,2'-Bipyridine, Metal-Free cis-2,2'-
Bipyridine and $[\text{Zn}(\text{bpy})]^{2+}$

Mikio Yagi

Department of Physical Chemistry, Faculty of
Engineering, Yokohama National University,
Tokiwadai, Hodogaya-ku, Yokohama 240, Japan

Bruce D. Schlyer and August H. Maki

Department of Chemistry, University of
California, Davis, CA 95616, USA

The lowest excited triplet (T_1) states of organometallic complexes of nd^{10} configuration, such as Zn^{2+} and Cd^{2+} with 2,2'-bipyridine (bpy) are believed to be $^3\pi\pi^*$ in character. The nature of the T_1 state of $[\text{Zn}(\text{bpy})]^{2+}$ may usually be explained by a small perturbation of bpy by Zn^{2+} . During the course of the time-resolved EPR studies, however, a remarkable change in the anisotropy of the triplet sublevel populating rates has been observed for $[\text{Zn}(\text{bpy})]^{2+}$ [1].

The trans and cis conformations are possible in bpy, as shown in Fig. 1. The bpy T_1 state has been considered for many years to have the trans conformation in ethanol [2], in Shpol'skii matrices [3] and in a single crystal of durene [4] at low temperatures. On the other hand, the stable conformation of bpy in its metal complexes is apparently cis. It is difficult to determine whether the observed changes in the sublevel populating rates are due to the intrinsic effect of the coordination to Zn^{2+} or the effect of the conformational change. The lack of data on

the metal-free cis-bpy leaves the question open.

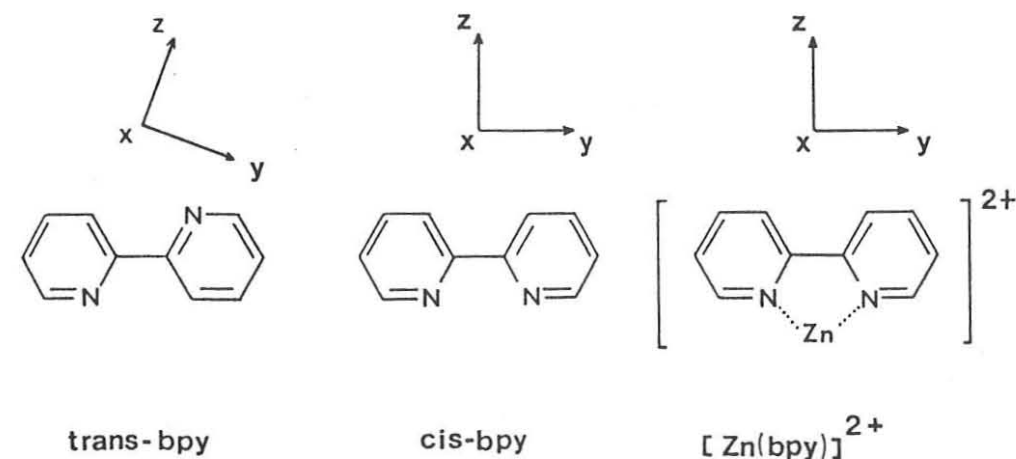


Fig. 1. Molecular structures and coordinate systems chosen for trans-bpy, cis-bpy and $[\text{Zn}(\text{bpy})]^{2+}$.

Recently, the T_1 state EPR spectra of a metal-free cis-bpy have been observed in mixtures of water with various alcohols at 77 K [5]. In the present work, we have observed the EPR and optically detected magnetic resonance (ODMR) signals from bpy using a 2-propanol-water (i-PrOH- H_2O) mixture as a host. We have been able to observe EPR and ODMR signals of the T_1 states of trans-bpy, cis-bpy and $[\text{Zn}(\text{bpy})]^{2+}$ in these solvent mixtures. Thus the separate effects of conformation and Zn^{2+} coordination on the zero-field splitting (ZFS) parameters and sublevel kinetics of bpy could be evaluated.

The EPR spectra of the T_1 state of bpy were measured in i-PrOH- H_2O and a stretched poly(vinyl alcohol) (PVA) film at 77 K. The EPR signals observed in i-PrOH- H_2O (3:2, v/v) are different from those observed in i-PrOH- H_2O (2:3, v/v). The former signals

can be reasonably assigned to the trans conformer, because their resonance fields are almost the same as those for the trans conformer observed in the stretched PVA film. On the other hand, from the similarity of the resonance fields between bpy in *i*-PrOH-H₂O (2:3, v/v) and the cis conformer observed in the stretched PVA film, bpy is expected to have the cis conformation in *i*-PrOH-H₂O (2:3, v/v) at 77 K.

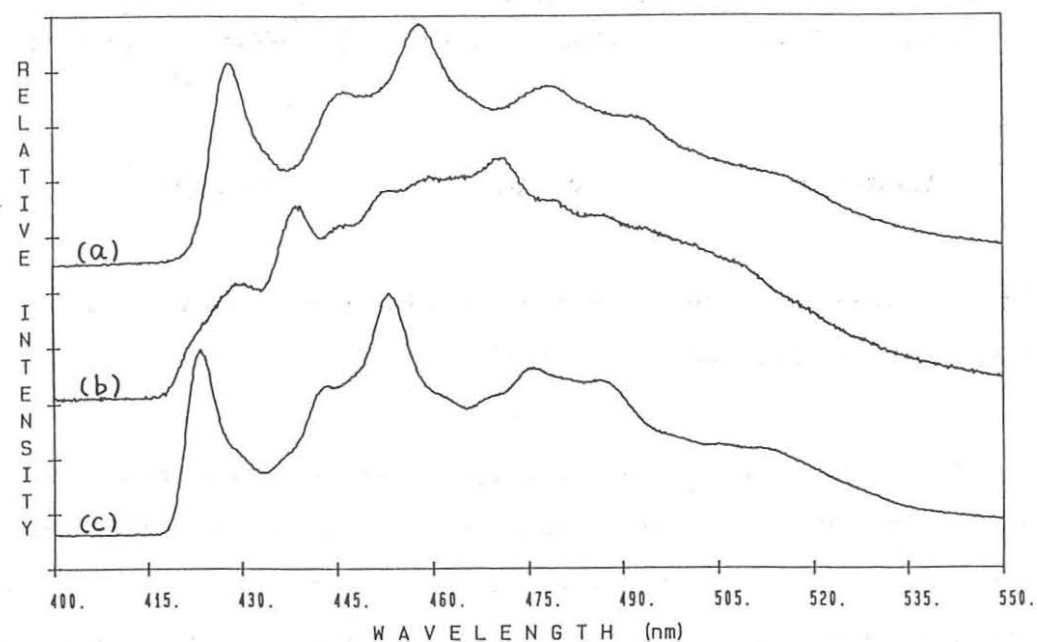


Fig. 2. Phosphorescence spectra of (a) trans-bpy in *i*-PrOH-H₂O (3:2, v/v), (b) cis-bpy in *i*-PrOH-H₂O (2:3, v/v) and (c) [Zn(bpy)]²⁺ in *i*-PrOH-H₂O (2:3, v/v) at 4.2 K.

The phosphorescence spectra of bpy and the [Zn(bpy)]²⁺ complex were measured at 4.2 K and are shown in Fig. 2. Each ODMR measurement was made by monitoring the apex of the first band of the phosphorescence (428 nm for trans-bpy, 429 nm for cis-bpy and 423 nm for [Zn(bpy)]²⁺). The kinetic properties obtained are

Table 1

ZFS parameters (in GHz) and kinetic properties observed at 1.2 K. k_i , decay rate constant (in s⁻¹); P_i , relative populating rate.

Molecule ^a	D ^b	E ^c	k_x	k_y	k_z	k^d	P_x	P_y	P_z
trans-bpy	3.32	0.36	0.48	1.2	1.4	0.97	$P_z > P_y > P_x$		
cis-bpy	3.36	0.16	0.32	1.4	1.1	0.93	0.16	1	0.56
[Zn(bpy)] ²⁺	3.33	0.17	0.48	0.77	1.2	0.77	0.48	1	0.65

^a trans-bpy is in *i*-PrOH-H₂O (3:2, v/v). cis-bpy and [Zn(bpy)]²⁺ are in *i*-PrOH-H₂O (2:3, v/v).

^b $D = (-3/2)X$.

^c $E = (1/2)(Z - Y)$.

^d Obtained from the phosphorescence decay at 4.2 K.

listed in Table 1. We can see from this table that the ZFS E parameter is sensitive only to the conformational change of bpy, while the triplet sublevel kinetics are sensitive to both the conformational change and to metal complex formation with Zn²⁺.

References

- [1] M. Yagi, H. Shirai, J. Ohta, and J. Higuchi, Chem. Phys. Lett., 160 (1989) 13.
- [2] Y. Gondo and A. H. Maki, J. Phys. Chem., 72 (1968) 3215.
- [3] K. Vinodgopal and W.R. Leenstra, J. Phys. Chem., 89(1985)3824.
- [4] N. Okabe, T. Ikeyama, and T. Azumi, Chem. Phys. Lett., 165 (1990) 24.
- [5] M. Yagi, K. Makiguchi, A. Ohnuki, K. Suzuki, J. Higuchi, and S. Nagase, Bull. Chem. Soc. Jpn., 58 (1985) 252.

We-1

9:00

~9:30

Spin Dependent Phenomena in Radical Spur Recombination

Oleg A. Anisimov

Institute of Chemical Kinetics and Combustion, Novosibirsk
630090 (USSR)

Radical ion pairs are produced in liquids and solids under ionizing irradiation (γ - and β -particles, X-rays, vacuum ultraviolet light). The products of radical ion pair recombination are usually electronically excited molecules. Many of them fluoresce. This circumstance is very favorable for the observation of spin-dependent phenomena in radical-ion geminate recombination because the intensity of recombination fluorescence is proportional to the number of pairs which recombine to a singlet state. The primary spin state of a recombining radical ion-pair can be altered for different reasons (hyperfine interaction of radical ion spins with magnetic nuclei, difference of g -factors of radical anion and radical cation, external magnetic and microwave fields). These interactions are responsible for spin dependent phenomena such as quantum beats, magnetic field effects, and optically detected electron spin resonance (OD ESR) of radical ion pairs [1].

Dilute solutions of aromatic molecules are a popular object of investigation of the primary processes of radiation chemistry and photochemistry. In this case after the primary ionization and excitation of solvent molecules the secondary aromatic radical ion pairs are formed. Their recombination fluorescence is also spin-dependent and their initial spin state the same as that of the primary pair since the process of secondary pair formation is fast and spin-correlation is preserved.

In the present communication we will show how spin-dependent phenomena give evidence for a novel mechanism of secondary radical ion pair formation in dilute hydrocarbon solutions.

The conventional mechanism for secondary radical ion formation includes the charge transfer reactions (2) and (3):



or



Here S is the solvent molecule, D and A are holes and electron acceptors, respectively. According to this scheme spin evolution of cation radicals includes two stages. During the first stage the unpaired electron interacts with magnetic nuclei of the solvent radical cation, S^+ , and then, after the charge transfer reaction, it interacts with magnetic nuclei of the aromatic radical cation, D^+ . If hyperfine interactions are significantly stronger for S^+ compared to D^+ (for example if D is deuterated) then the spin evolution is significantly faster for the first stage than for the second. This circumstance should be reflected in a time development of magnetic field effects. One would expect a fast increase in the magnetic field effect for short times and then a slower increase. This, in fact, takes place for branched hydrocarbon solvents like isooctane or 3-methylpentane. But for normal hydrocarbons, and, especially, for cyclic hydrocarbons, like cyclo-hexane and decalin, there is no evidence for the first stage; only a slow increase of the magnetic field effect is observed.

We obtained a confirmation of this result from quantum beat experiments. Para-terphenyl- d_{14} and diphenylsulfide- d_{10} were chosen as A and D , respectively, to provide strong quantum beats for the pair (diphenylsulfide- d_{10}^+ /p-terphenyl- d_{14}^-) via the Δg -mechanism [2]. According to theoretical calculations there should be a particular shift in the phase of quantum beats if the upper-mentioned first stage of spin evolution takes place. It should be dependent on the viscosity of the solvent and the concentration of the solute D . We could not find any shift in the quantum beats curve for such solvents as n -pentadecane, cis-decalin and trans-decalin even at low temperatures and at low concentrations of diphenylsulfide- d_{10} .

A possible explanation is that a significant part of the secondary aromatic radical cations in normal and cyclic hydrocarbon dilute solutions are formed by a mechanism that does not include the charge transfer reaction (2). We propose that an energy transfer process is involved. If the energy that transfers from solvent to an aromatic molecule is sufficient to ionize it, the secondary radical ion pairs D^+/e^- and D^+/A^- can be formed. The singlet state, $^1S^*$, of the solvent cannot be responsible for this energy transfer process because it is known that the energy transfer process for this state is diffusion controlled [3]. It should provide a significant shift in the quantum beats curves that contradict the experimental results. Accordingly, it would appear that there is some other excited state of the solvent that can provide the appropriate transfer efficiency. The existence of such a state could explain not only the spin-dependent results but also, an unusually high efficiency of energy transfer for dilute solutions of aromatic molecules in hydrocarbons which was observed by the Lipsky group [4].

This mechanism can explain the difference between the spin-dependent effect in branched and in non-branched solvents. It is known that for many branched hydrocarbons, like isooctane, energy transfer processes do not take place. So only the conventional mechanism is possible for these hydrocarbons.

Some support of an ionization mechanism via energy transfer has been found in our experiments on the spur-density dependence of the magnetic field effect. For the conventional mechanism, eqs. (1)–(5), one can expect a significant decrease in the magnetic field effect for X-ray irradiation compared to MeV-electrons because in a dense spur created by X-rays the probability of non-spin-sensitive cross-recombination is higher. For a 10^{-3} M p-terphenyl- d_{14} solution in isooctane (where the conventional mechanism is expected), the time-resolved magnetic field effect decreases 2.8 times for 20–30 KeV X-rays, compared to the β^- spectrum from a ^{90}Sr radioactive source. But for normal and cyclic hydrocarbons, only a small decrease (ca. 30%) takes place. One can expect this behavior for an energy transfer ionization mechanism because in this case, the secondary radical ion pairs can be formed outside of a spur.

Additional support for the above mechanism comes from the result of the Strasburg group [5] who observed time-resolved magnetic field effects in 10^{-3} M p-terphenyl in cyclohexane under synchrotron irradiation even at photon energies of 6.5 eV. This is lower than the ionization potential of cyclohexane in the liquid state. For 10^{-3} M p-terphenyl in isooctane (a recent result that was obtained in collaboration with the Lipsky group), the threshold for the magnetic field effect is at ~ 8.8 eV.

References

- [1] O. A. Anisimov, *J. of Industr. Irradiation Techn.*, 2 (1984) 271.
- [2] A. V. Veselov, V. I. Melekhov, O. A. Anisimov and Yu. N. Molin, *Chem. Phys. Letters*, 136 (1987) 263.
- [3] G. Orlandi, L. Flamingi, *Rad. Phys. Chem.*, 21 (1983) 113.
- [4] F. Hirayama and S. Lipsky, "Organic Scintillations and Liquid Scintillation Counting" (Edited by D. L. Horoché and C. T. Peng), p. 205, Academic Press, London, 1971.
- [5] J. Klein, private communication.

We-2
9:45
~10:15

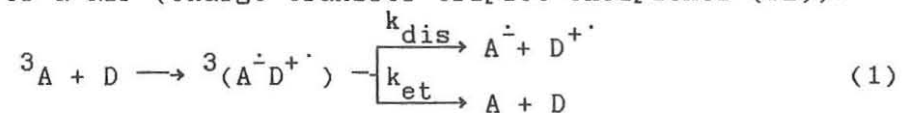
Magnetic Field Effects on the Decay Kinetics of Triplet Radical Pairs in Homogeneous and Organized Systems

Peter P. Levin and Vladimir A. Kuzmin

Institute of Chemical Physics, Academy of Sciences of the USSR, 117334 Moscow, USSR

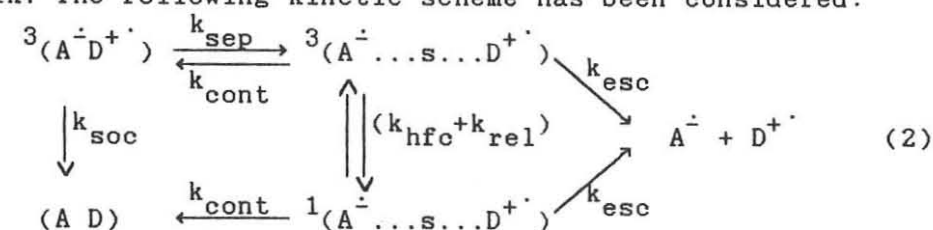
The magnetic field effects on the decay kinetics of triplet-derived radical ion pairs (RIP) and radical pairs (RP) formed by electron or hydrogen atom transfer from aromatic amines or phenols (D), to the quinones and the ketones (A) in solvents of middle polarity [1], in viscous solvents [2], in micellar solutions [3] and on the surface of porous glass [4], have been studied by transient absorption measurements using the laser flash technique. The time scale of RIPs and RPs decay is of the order of 0.01-10 μ s.

The photoexcitation of A in the presence of tertiary aromatic amines results in an electron transfer (et) from D to 3A and to the appearance of a RIP (charge transfer triplet exciplexes (TE)):



In nonpolar solvents ($\epsilon \leq 5$), the only RIP decay route is intersystem crossing to the ground state (spin inverted backward et induced by spin-orbit coupling (SOC) in a contact state of the RIP. There is no magnetic field effect. In moderately polar solvents ($5 \leq \epsilon \leq 15$), partial dissociation takes place and there is a reversible stage of formation of the distance-separated RIP ($A^{\cdot-} \dots s \dots D^{\cdot+}$), where the spin exchange interaction is small and the hyperfine coupling (hfc) mechanism of S - T evolution is

active. Application of a magnetic field leads to the inhibition of the RIP decay and to an increase of the yield of radical ions in the bulk. The following kinetic scheme has been considered:

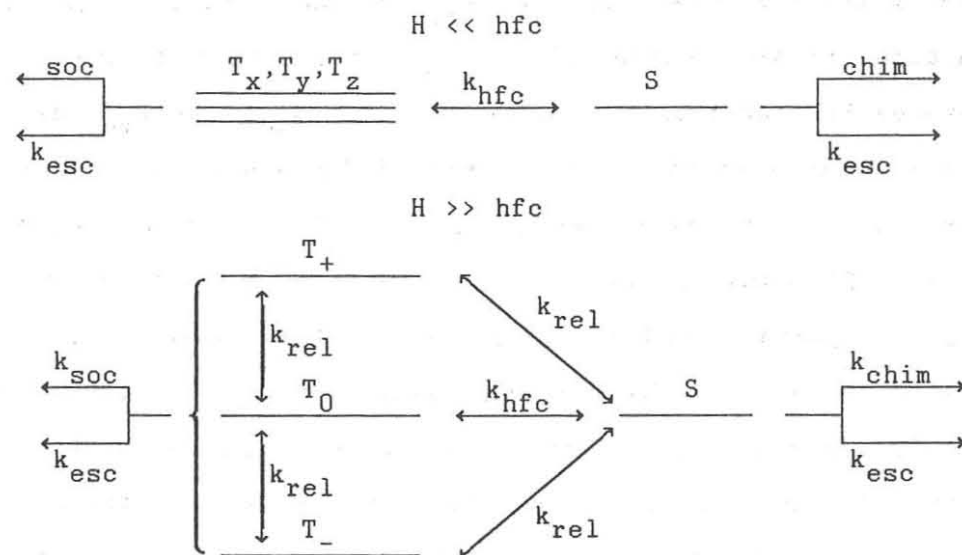


where k_{soc} is the rate constant for spin-inverted et in the contact state of the RIP caused by SOC, k_{sep} is the rate constant for the separation of the contact RIP, k_{cont} is the rate constant of the separated RIP junction to the contact RIP, k_{hfc} and k_{rel} are those for T - S transitions in the separated RIP due to the hfc and the relaxation mechanisms respectively, k_{esc} is the rate constant for separated RIP dissociation into the radicals in the bulk. There are several important solvent-dependent factors which control the competition between the two different routes of backward et in RIPs. The rate of SOC-induced intersystem et in the contact state of the RIP is determined by the position of a system on the bell-shaped energy gap dependence and by the parameters leading to this dependence. The probability of the magnetosensitive process goes through a maximum with increase in ϵ . The highest magnetic field effects (up to 50%) have been observed at $\epsilon = 8 - 15$.

In homogeneous solvents of the viscosity $\eta \geq 1$ P, it is possible to record the microsecond kinetics of the geminate recombination of the triplet RP without coulomb attraction between the radicals. In the case of triplet exciplexes as well, the most important pathway of the RP decay in viscous solvents is the intersystem recombination induced by SOC in the contact RPs. At the same time, the contribution of the magnetosensitive process is

sufficient to observe the magnetic field effects up to 100%. This contribution goes through a maximum with an increase in η .

The decay kinetics of geminate triplet-derived RP in micellar solutions depend drastically on the external magnetic field (retardation up to 25 times) due to the very large contribution of the magnetosensitive pathway. The observed structural, additive and magnetic field effects are satisfactorily described in terms of a simple kinetic scheme of the first order processes:



which includes the singlet-triplet transitions in the separated states of RP due to the isotropic hfc (k_{hfc}) and relaxation (k_{rel}), the RP recombination in the singlet state (k_{chim}), the escape of the radicals from the micelle (k_{esc}) and the intersystem recombination process due to the SOC (k_{soc}) in the contact state of the RP. The magnetic field dependence at $0.03 < H < 0.1$ T is conditioned by the decrease in the rate of paramagnetic relaxation, which is mainly due to the anisotropy of the hyperfine interaction. Intersystem recombination is the most important route of the decay of micellized RPs produced in T_{\pm} states in very high magnetic

fields. The model gives a possibility to determine the relaxation parameters from the magnetic field dependences.

The behavior of the geminate RP and RIP adsorbed onto the surface of silicate porous glass has similarities with that in the homogeneous as well as in the micellar solutions. Magnetic field effects up to 100% have been observed, which is the result of a significant contribution of the recombination route through the separated RP. The pronounced internal heavy atom effect of the same order of magnitude as that for the triplet exciplexes, the RP in viscous solvents and the RP in micelles in high magnetic field, evidences the important role of intersystem recombination or intersystem electron transfer.

References

- [1] P.P.Levin and V.A.Kuzmin, Bull.Acad.Sci.USSR,Div.Chem.Sci., 36 (1987)2426; P.P.Levin, P.F.Pluzhnikov and V.A.Kuzmin, Chem. Phys., 137(1989)331; P.P.Levin, P.K.N.Raghavan and V.A.Kuzmin, Chem.Phys.Letters, 167(1990)67.
- [2] P.P.Levin, I.V.Khudyakov and V.A.Kuzmin, Bull.Acad.Sci.USSR, Div.Chem.Sci., 35(1986)479; 36(1987)395,918; 37(1988)432; 38(1989)18; Dokl.Phys.Chem., 288(1986)440; Kinet.Katal., 29(1988)326; Khim.Fiz., 8(1989)902; J.Phys.Chem., 93(1989)208.
- [3] P.P.Levin and V.A.Kuzmin, Bull.Acad.Sci.USSR,Div.Chem.Sci., 35 (1986)430; 36(1987)691,923; 37(1988)224; Dokl.Phys.Chem., 292(1987)26; Khim.Fiz., 7(1988)909; 8(1989)1034; Chem.Phys. Letters, 165(1990)302.
- [4] P.P.Levin, I.V.Katalnikov and V.A.Kuzmin, Bull.Acad.Sci.USSR, Div.Chem.Sci., 38(1989)1095; Khim.Fiz., 8(1989)1604; Chem. Phys. Letters, 167(1990)73; Chem.Phys. (accepted).

We-3

10:30

~11:00

MAGNETIC FIELD EFFECT ON EXCIPLEX LUMINESCENCE

Mihir Chowdhury, Rina Dutta, Samita Basu and

Debnarayan Nath

Department of Physical Chemistry,

Indian Association for the Cultivation of

Science, Jadavpur, Calcutta 700032, India.

The magnetic field effect (MFE) on radical pair (RP) recombination is as much a function of the environment as the RP system itself. The influence of the environment on the complex interplay between spin evolution, diffusional excursion and chemical recombination has been studied by us through MFE on exciplex luminescence. Photogenerated solvent-separated-ion pairs (SSIP), initially in the singlet state, combine to form luminescent contact ion pairs (CIP). An externally applied field suppresses the hyperfine interaction (HFI) induced rate of the competing $^1\text{SSIP} \rightleftharpoons ^3\text{SSIP}$ process and thus increases the CIP yield. The luminescence from the CIP can therefore be used as an indirect means for monitoring the spin evolution process of such RP systems. This presentation will review some of our work concerning the dependence of MFE on the nature of molecules surrounding the CIP/SSIP.

MFE on the following systems have been studied :- (a) unlinked exciplex systems of Pyrene (Py) / Dimethylaniline (DMA), trans-Anethole (TA) / Cyanophenanthrene (CNP) and Anthracene (An) / Octafluoronaphthalene (OFN), in presence and in absence of other paramagnetic species ; (b) unlinked luminescent exciplex system of diphenyl-hexatriene (DPH) / DMA and diphenyl-butadiene (DPB) / DMA — in presence of viscous polymeric medium ; (c) linked Py/DMA system consisting of a polystyrene chain with Py as one end group and DMA as the other. Our results are summarised below.

(a) The effect of solvent medium on all the unlinked systems are strikingly similar. If non-alcoholic solvent mixtures are chosen, the MFE

peaks at a dielectric constant of $\approx 16 - 18$, falling off rapidly below the ϵ_{max} and relatively slowly after the ϵ_{max} . We have tried to model the system quantitatively [1], assuming Smoluchowski's equation for diffusion and a linear time dependence of spin-evolution upto a limiting time t' . The time dependence [2] of the MFE is also consistent with the proposed model.

If however, alcoholic solvents are chosen as one of the components comprising the solvent mixture, the peak MFE decreases by about four times and the ϵ at which $(\Delta\phi/\phi)_{\text{max}}$ peaks shifts to 28. This peculiar behaviour of alcoholic solvents points towards modification of the potential energy curve at short distances through specific interaction. The quenching of MFE in alcoholic media has been interpreted by us [3] as arising from fluctuations in local magnetic fields which in turn are caused by hopping of hydrogen.

The effect of spin exchangeable species, other than the RIP, such as Ln^{3+} -acetylacetonates on the exciplex luminescence has been reported by us [4]. The MFE quenching efficiency, measured from the slope of the plot of $(\Delta\phi/\phi)$ against Ln-complex concentration, correlates well with the root of the de Gennes factor. The implication of this correlation will be discussed.

(b) The MFE on luminescent exciplex systems has also been looked into. The effect of the viscosity of the medium on the MFE of exciplex luminescence is not perceptible until it is very high. In highly viscous medium of poly-vinyl acetate in THF/DMF mixture, the MFE on exciplex luminescence from DPH/DMA [5] and DPB/DMA was found to be dependent on the direction of the magnetic field. The experimental situation is shown in Fig. 1. When the molecules oriented parallel to the magnetic field are chosen by exciting with light polarised in the direction of the field, the $(\Delta\phi/\phi)$ value was 3.2 % (± 0.2 %) On the other hand, when the exciting light was perpendicular to the field, the $(\Delta\phi/\phi)$ value reduced to 2.7 % (± 0.2 %). Similar results were obtained when the polariser was placed on the emission side instead of in the excitation beam. The anisotropy of the MFE disappears if solvent viscosity

is reduced, or if other exciplex systems such as Py/DMA or An/DMA are excited in the same medium. The novel anisotropic effects are probably a consequence of the elongated shape of the DPH/DPB molecule and the preservation of the spatial relationship between the radical partners during their lifetime. The most probable explanation seems to be anisotropic dipolar interaction between the two radical ions.

(c) The response of Py-PS-DMA polymer ($M_n = 4770$) to an externally applied magnetic field is closer (as regards $(\Delta\phi/\phi)_{max}$, $B_{1/2}$, solvent effect etc.) to that of unlinked system than to those of methylene chain linked systems, although the lifetimes of the polymer linked and the unlinked systems differ widely [6]. Qualitatively, the lack of sensitivity of MFE on the formation and decay rates of the exciplex can be understood if one assumes that the triplet probability saturates out after several nano-seconds. The time-resolved MFE curves show that not only the growth of the exciplex is affected by 20 % by magnetic field, the decay is also affected to the same extent. This indicates that there is reversible SSIP \leftrightarrow CIP transformation. Although the dielectric constant effect is similar to unlinked system, a closer look shows interesting dependence on the nature of the solvent mixture. In pure acetone $(\Delta\phi/\phi)$ is higher than that in mixed solvent (THF/DMF) of same ϵ . On adding a small amount of benzene or cyclohexane to acetone, the $(\Delta\phi/\phi)$ drops considerably. Acetone is known to be a bad solvent for polystyrene. The considerable deviation of acetone from the unlinked system can be explained on the basis of the fact that it assumes a coiled conformation in this solvent. Consequently, the immediate environment of the exciplex becomes a mixture of acetone and phenyl groups, the latter being provided by the polymer itself. The effective dielectric constant therefore becomes less than 20, somewhere around ϵ_{max} corresponding to free Py-DMA and the $(\Delta\phi/\phi)$ increases. If any other solvent (good or poor) is added, the polymer uncoils and gets extended, the degree of extension being dependent on the nature of the solvent. The

influence of coil extension on the MFE and the ϵ - effect compete with each other resulting in different behaviour depending on the nature of the solvent mixture.

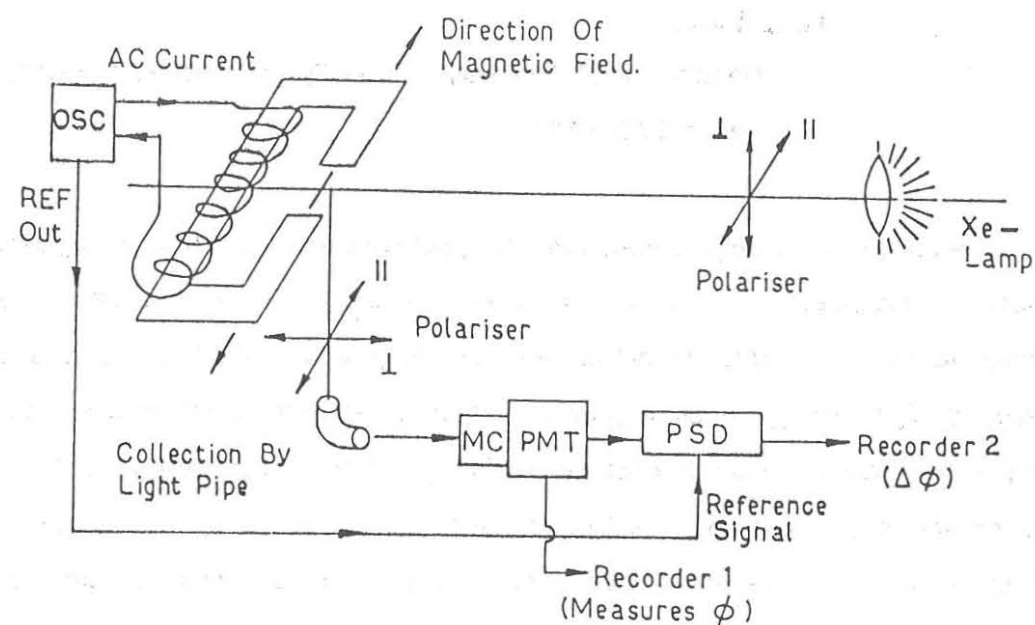


Fig 1. Schematic diagram of phase sensitive detection system with modification for inclusion of polarisers. Only one beam (excitation or emission) was polarised in one particular set of experiments. Osc — Oscillator ; MC — Monochromator ; PMT — Photomultiplier ; PSD — Phase sensitive detector.

References

- [1] D.N.Nath and M.Chowdhury, *Pramāna - J.Phys.*, 34 (1989) 51.
- [2] S.Basu, D.N.Nath and M.Chowdhury, *Chem.Phys.Lett.*, 161 (1989) 449.
- [3] D.N.Nath, S.Basu and M.Chowdhury, *J.Chem.Phys.*, 91 (1989) 5857.
- [4] S.Basu, L.Kundu and M.Chowdhury, *Chem.Phys.Lett.*, 141 (1987) 115.
- [5] R.Dutta, S.Basu and M.Chowdhury, *Chem.Phys.Lett.*, 1991 (in press).
- [6] S.Basu, D.N.Nath, M.Chowdhury and M.A.Winnik, *J.Phys.Chem.*, (communicated)

Th-1
9:00
~9:30

Applications of Electron Spin Echo Spectroscopy To Location
Control of Electron Donors in Photoinduced Charge Separation
Across Vesicle, Micelle and Reverse Micelle Interfaces

Larry Kevan

Department of Chemistry, University of Houston, Houston,
Texas 77204-5641

Photoinduced charge separation of photoionizable solutes in organized molecular assemblies such as micelles, vesicles, reverse micelles and microemulsions is a currently active area of study with a goal to optimize the storage of light energy. Such a goal is a type of artificial photosynthesis and in many ways parallels natural photosynthesis, in which a chlorophyll solute in a lipid bilayer is photoionized, resulting in electron transfer to a chain of electron acceptors which causes net charge separation and ultimate chemical conversion of this stored light energy into chemical energy.

In general, the net charge separation across surfactant interfaces depends upon the following factors.

- (1) The solute location within the micellar or vesicular assembly is a control factor for net charge separation. It is almost always found that the electron donor is asymmetrically located within the surfactant assembly and is relatively near to the interface.
- (2) Another control factor is the micelle or vesicle size. In general a smaller size, as controlled by the length of the alkyl chain of the surfactant molecule, leads to higher photoionization efficiency although the size cannot be too small.
- (3) A major control factor is the interface charge. In frozen systems it is found that a positive interface charge is generally better because it

assists the electron escape across the interface whereas a negative surface or interface charge tends to impede the electron from traversing the interface.

- (4) Likewise the interface charge density is a control factor in which a more positive or less negative charge density enhances the photoionization efficiency.
- (5) The ionic strength of the interface is another control factor. It can be varied by added salts and by specific complexation of counterions by crown ethers. The ionic strength effect depends on the charge of the interface such that increased ionic strength can lead to either greater or less photoionization efficiency depending on the charge of the interface.
- (6) Finally, when a specific molecular electron acceptor is present, the relative locations of the electron donor and acceptor are major control factors for the photoionization efficiency. For efficient charge separation the acceptors should be close but not too close or back electron transfer will be too facile.

Achievement and assessment of location control of donors and acceptors in surfactant assemblies by the addition of pendant alkyl chains to donors and acceptors is shown to be achievable.¹ The net photoionization efficiency can be measured by electron spin resonance of radical ions in frozen surfactant solutions. Assessment of relative locations of radical ions with respect to a surfactant interface has been achieved by analysis of electron spin-echo modulation from deuterium in deuterated water at the interface.

Results for a series of negatively charged alkylphenothiazine sulfonates in vesicle², micelle³ and reverse micelle⁴ surfactant assemblies of different interface charge will be discussed and compared with results on neutral alkylphenothia-

zines and positively charged alkylphenothiazine trimethylammonium bromides. Controlling factors involve the alkyl chain length of the electron donors, the relative charge of the surfactant assembly interface versus that of the electron donor derivative, and the degree of molecular order in the interface.

References

- [1] L. Kevan, Intl. Rev. Phys. Chem., 9 (1990) 307.
- [2] M. Sakaguchi, M. Hu and L. Kevan, J. Phys. Chem., 94 (1990) 870.
- [3] P. Baglioni, M. Hu and L. Kevan, J. Phys. Chem., 94 (1990) 2586.
- [4] M. Hu and L. Kevan, J. Phys. Chem., 94 (1990) 5348.

[Faint, illegible text, likely bleed-through from the reverse side of the page]

Th-2
9:45
~10:15

New Aspects of Photo-induced Chemical Reactions Studied by FT-EPR

Klaus-Peter Dinse, G. Kroll, and M. Plüschau

Institute of Physics, University Dortmund,
D-4600 Dortmund 50, Otto-Hahn-Strasse, Germany

Fourier-transform EPR (FT-EPR) has recently been proven to be a powerful tool for the investigation of photo-induced chemical reactions in solution [1-3]. Single pulse FT-EPR is a perfect stroboscopic method, combining time resolution of approximately 10 ns with frequency resolution, only limited by T_2 of the radicals under investigation. This unique combination enables the observation of intensity/time profiles of individual hyperfine components (hfcs) with unprecedented time resolution even in the case of overlapping spectra originating from different reaction products.

In addition, the phase of the EPR lines derived from the Fourier-transformed Free Induction Decay (FID) carries information about the non-directly observed radical pair (RP) precursor. Projecting the complex EPR spectrum on the rotating frame determined by the microwave field, the time profile of the collinear ("dispersion") signal can be used to determine the kinetics of the spin-correlated radical pair and its interaction potential [4]. This report is focussed on the complete reconstruction of a sequential electron/proton transfer reaction and on the analysis of the spin-correlated RP dissociation under the condition of virtual jitter-free synchronization of laser- and microwave pulses even for arbitrary short delay times.

Except for simple chemical systems, which have first been used for a verification of conventional CIDEP processes, no single reaction channel can be expected in general. For instance, the triplet quenching reaction of anthraquinone (AQ) by di-tert.-butylphenol (DTBPH) in 2-propanol resulted in anthraquinone radical ions ($AQ^{\cdot-}$) and also in protonated neutral hydroxy-anthroxyl radicals (AQH^{\cdot}) both showing a completely different intensity/time profile. As is shown in fig. 1, the resulting spectrum is quite complicated. However, an unambiguous assignment was possible, leading to the identification of at least

one hyperfine line of each radical, completely unperturbed by lines of the other one. (The di-tert.-butylphenoxyl radical (DTBP \cdot) is separated from most $AQ^{\cdot-}$ and AQH^{\cdot} lines and could easily be identified.)

The polarization pattern of both radicals was dominated by the triplet mechanism (TM), therefore a single hfc intensity/time plot was sufficient for a description of the polarization kinetics. From comparison with the results of laser photolysis of similar systems, a fast diffusion-controlled electron transfer from DTBP to the photo-excited AQ triplet can be expected [5]. However, the predominance of AQH^{\cdot} radicals at short delay times clearly proves that this first step is followed by a proton transfer before the RP dissociates. The appearance of $AQ^{\cdot-}$ radicals with the same rise time as observed for the AQH^{\cdot} radicals actually proves that the photo-reduction of AQ to AQH^{\cdot} has to be described as a sequential two-step process. This is only possible, if $AQ^{\cdot-}$ radicals escape DTBP \cdot with a finite probability. On the long time scale ($t \geq 1 \mu s$) we observe a proton abstraction reaction, leading to an interconversion of AQH^{\cdot} to $AQ^{\cdot-}$.

In fig. 2 the time/intensity profile of both radicals is depicted. In addition the result of a simulation for both radical polarizations is shown, taking into account the following reaction scheme: a) charge transfer: $AQ^T + DTBPH \xrightarrow{k_q} (AQ^{\cdot-} + DTBPH^{\cdot+})$; b) proton transfer: $(AQ^{\cdot-} + DTBPH^{\cdot+}) \xrightarrow{k_H} (AQH^{\cdot} + DTBP^{\cdot})$; c) radical-pair separation: $(AQH^{\cdot} + DTBP^{\cdot}) \xrightarrow{k_s} AQH^{\cdot} + DTBP^{\cdot}$; d) proton abstraction: $AQH^{\cdot} \xrightarrow{k_a} AQ^{\cdot-} + H^+$.

As a result, the charge transfer rate k_q , the proton abstraction rate k_a in 2-propanol and the ratio k_s/k_H of radical-pair separation and proton transfer rate constants from oxidized DTBPH to $AQ^{\cdot-}$ could be determined. In addition, the spin-lattice relaxation rates of the triplet precursor and of $AQ^{\cdot-}$ and AQH^{\cdot} radicals could be measured. From the signal analysis clear evidence for a two-step sequential electron/proton transfer could be deduced, determining with high precision the escape probability of the primary reaction product $AQ^{\cdot-}$ from its Coulomb-coupled reaction partner. It should be noted that the proton abstraction reaction with the solvent alcohol is spin-conserving, as expected.

As a second example, the spin-correlated radical pair separation kinetics was studied with increased time resolution. Our first experiments investigating the build-up and decay

kinetics of the dispersive signal component showed relatively large fluctuations of the signal amplitude for short delay times ($\Delta t < 200$ ns) [4]. This resulted from the fact that because of unavoidable trigger and set-up delays the pulse programmer could not be triggered by the light pulse but rather the electronic discharge trigger of the excimer laser had to be used. Because of a noticeable jitter between this trigger and the actual light pulse, the EPR signal build-up was seriously affected. Using a new synchronization method, time zero can now be defined within 8 ns, thus virtually eliminating this error source. With the finally reached time resolution, the identity of the rise time of the dispersive signal component with the electron transfer rate could be demonstrated for Zn-tetraphenyltetraporphyrin(ZnTPP)/duroquinone (DQ) in two different solvents.

Close collaboration with D. Beckert (Leipzig) and H. van Willigen (Boston) is gratefully acknowledged. This work was supported by a grant of the Deutsche Forschungsgemeinschaft and a NATO travel grant.

References

- [1] T. Prisner, O. Dobbert, K.P. Dinse and H. van Willigen, *J. Am. Chem. Soc.* 110 (1988) 1622
- [2] M. Plüschau, A. Zahl, K.P. Dinse and H. van Willigen, *J. Chem. Phys.* 90 (1989) 3153
- [3] M.K. Bowman, M. Toporowics, J.R. Norris, T.J. Michalski, A. Angerhofer and H. Levanon, *Israel J. Chem.* 28 (1988) 215
- [4] G. Kroll, M. Plüschau, K.P. Dinse and H. van Willigen, *J. Chem. Phys.* 93 (1990) 8709
- [5] D. Beckert and G. Schneider, *Chem. Phys.* 116 (1987) 421

Figure captions

Fig. 1 EPR signals obtained 10 μ s after the photo-reduction of AQ in 2-propanol with 0.1 M DTBPH as triplet scavenger at room temperature. Lines indicated were used for a selective observation of AQ⁻ and AQH[•] signal intensities.

Fig. 2 EPR intensities in the coupled AQH[•]/AQ⁻ system. Most of the AQ⁻ signal intensity visible in this figure results from the comparatively slow proton equilibrium reaction with the solvent.

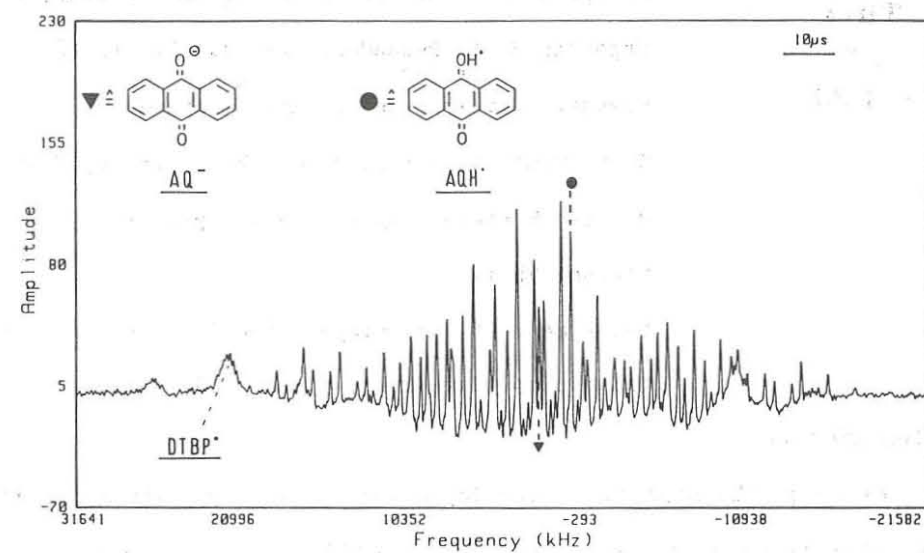


Figure 1

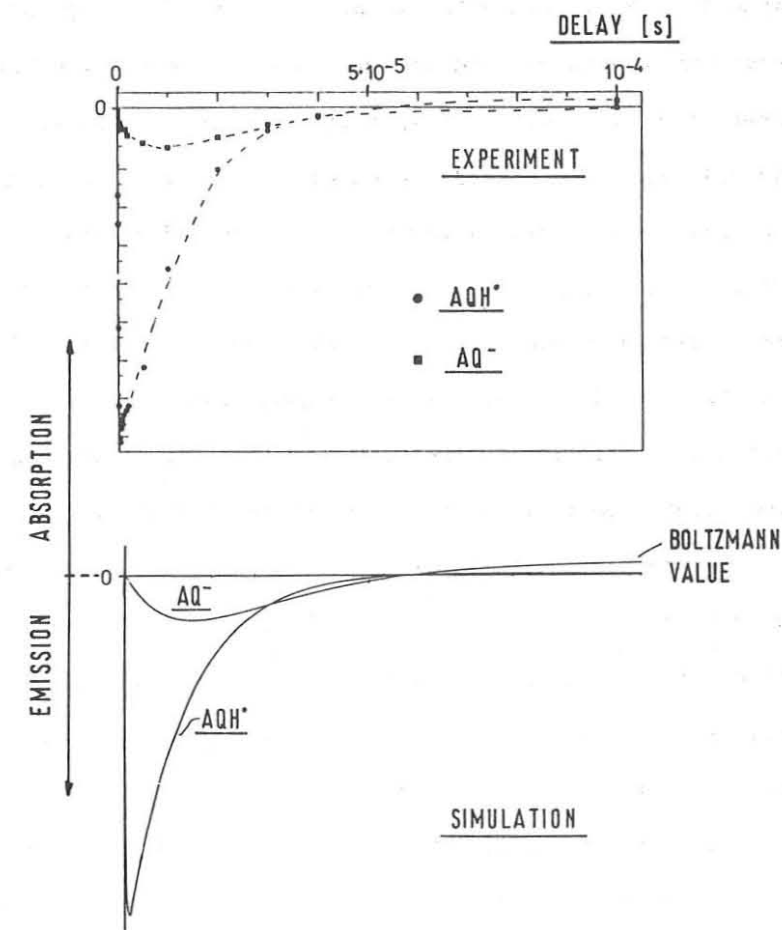


Figure 2

Th-4
11:00
~11:20

An Application of Spin Trapping to the Study of
Magnetic Field Dependent Chemical Reactions.

Masaharu Okazaki* and Kazumi Toriyama

Government Industrial Research Institute, Nagoya,
Hirate, Kita-ku, Nagoya, 462, Japan.

Takeshi Shiga

Department of Physiology, School of Medicine, Osaka
University, Yamadaoka, Suita, 565, Japan.

1. Introduction

Although the magnetic field dependent yield of a chemical reaction has been interpreted with the radical pair model[1,2], it is rare that both the component radicals of the pair were detected as the functions of the external magnetic field. Since the magnetic field effect appears strongly in photo-reduction of quinones and ketones in the micellar solutions[3,4], we tried to detect the SDS radical by spin trapping whose counter part, the semiquinone radical, had been already detected as the function of magnetic field[5]. As the result[6], a very large magnetic field effect was detected on the yield of SDS radical escaped from the micelle. To confirm the radical pair mechanism and to get into details of the phenomenon, however, only the observation of both the transient radicals as the functions of magnetic field is still insufficient. A detailed theoretical curve fitting of the magnetic field effect or some direct confirmation should be needed for that.

In the present talk, we would like to show our recent results as well as our previous studies[6,7] which we believe is the most clear and direct evidence for the radical pair mechanism of the magnetic field dependent chemical reaction. We recently constructed a new apparatus for this method, which we call "product yield detected ESR" where ESR transitions of the transient radical pair are detected through measuring the spin adduct yield. We observed about 40 % decrease in the yield of the spin adduct of SDS radical by irradiating the ESR transition of anthrasemiquinone radical simultaneously with the

photo-irradiation for an anthraquinone solution of SDS micelle.

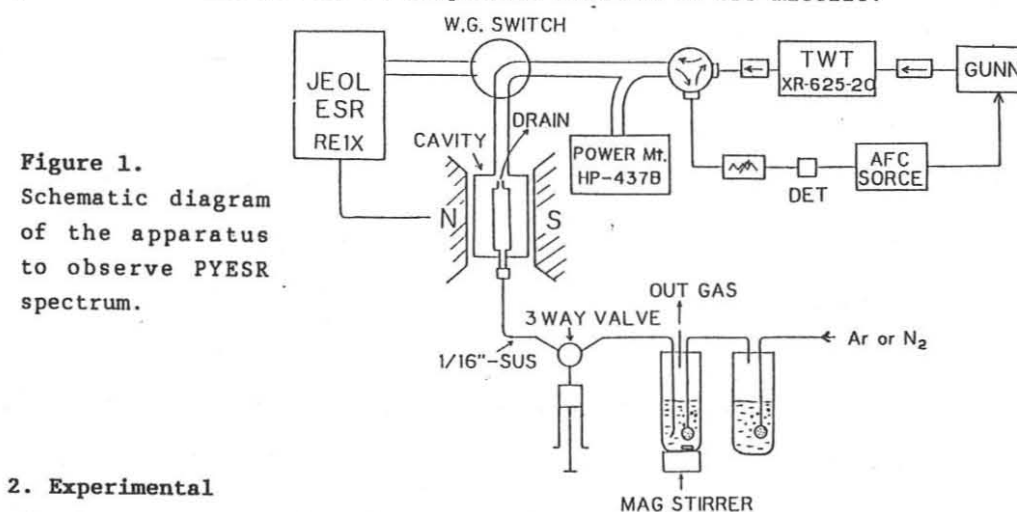


Figure 1.
Schematic diagram
of the apparatus
to observe PYESR
spectrum.

2. Experimental

Figure 1 shows a schematic diagram of our apparatus. Well deoxygenated sample solution is charged into a quartz flat cell with a flow system and is irradiated with an ultra-high pressure mercury lamp. The sample solution is irradiated with microwave from a TWT amplifier simultaneously with photoirradiation at various magnetic fields. The spin adduct yield is measured by the conventional ESR method after switching the connection of the cavity from the TWT amplifier to the original ESR system.

Anthraquinone was obtained from Tokyo Kasei Kogyo and recrystallized from ethanol. Sodium dodecyl sulfate and 3,5-dibromo-4-nitrosobenzene sulfonate (a spin trap) were used as supplied from Nakarai Chemicals and Sigma Chemical Company, respectively. Experiments were performed at ambient temperatures.

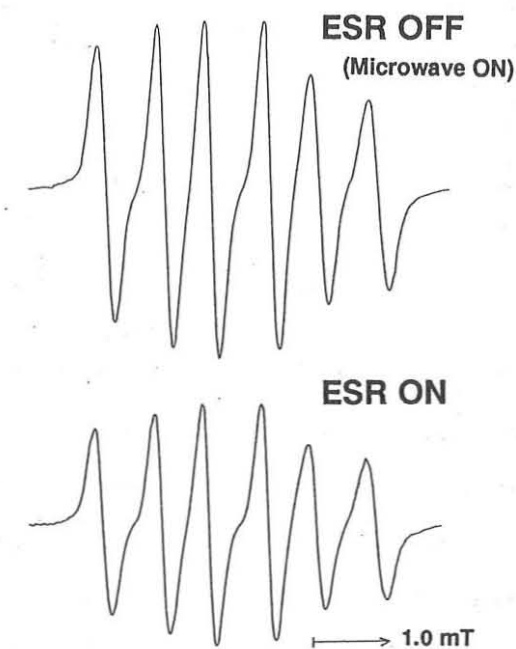


Figure 2. Effect of the ESR transition of anthra-semiquinone on ESR spectrum of the spin adduct of SDS radical.

The sample solution was buffered with 50 mM sodium phosphate at pH 6.0.

3. Results and Discussion

Figure 2 shows the ESR spectra of an UV-irradiated SDS (0.2 M) micellar solution of anthraquinone (0.1 mM) with simultaneous irradiation of microwave at 9.39 GHz at the resonance magnetic field for the semiquinone radical (334.7 mT; lower) and at a magnetic field (330 mT; upper) off-resonant for both the intermediate radicals. The microwave power was about 0.5 W. Since the ESR spectrum of the spin adduct indicates that the radical trapped has one alpha-proton ($a_H=0.76\text{mT}$), thus it is safely assigned to the SDS radical as in the previous study[7]. The observed reduction in the spin adduct yield is about 40 % which is the maximum resonant-microwave effect ever observed. Figure 3

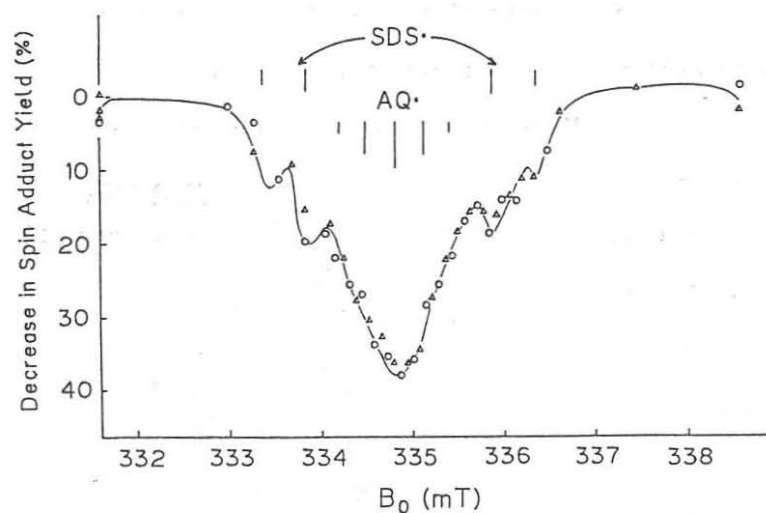


Figure 3.
PYESR spectrum for UV-irradiated 0.1 mM anthraquinone solution of 0.2 M SDS micellar solution.

shows reduction in the spin adduct yield due to microwave irradiation as the function of the magnetic field. The stick diagram shows the expected ESR resonance lines from both the SDS radical and the semiquinone radical. As mentioned in the previous studies, this coincidence of the stick diagram with the observed "PY-ESR spectrum" indicates that microwave-induced spin-flip of one of the component radicals of the transient radical pair induces the change in the spin state of the radical pair from the initial triplet state to the singlet state from which the cage product is efficiently formed (thus the spin adduct decreases). This indicates that the yield of escaped SDS radical

accumulated as the spin adduct decreases by the spin-flip of either the SDS radical or the semiquinone radical. This is the direct evidence for the radical pair theory of this kind of magnetic field dependent chemical reactions. As an extension of this technique, isotope enrichment was demonstrated by selective induction of one of the ESR transitions of the intermediate SDS(D) and SDS(H) radicals in the same type of reaction [8].

This phenomenon may be classified as one of the "RYDMR" experiments, where fluorescence from a transient species is monitored[9]. In the present experiment, on the contrary, the yield of the final stable product is measured. Therefore our experiment represents the first reaction control by the ESR transitions of the intermediate radical pair. In addition the ESR spectrum of the spin adduct has information about the structure of the transient free radical. We are now improving the apparatus by introducing a laser and pulsed microwave to reduce the dielectric heating of the sample which prevent us to perform the experiment with the microwave power more than a few watts.

4. References

- (1) P.W. Atkins and T.P. Lambert, *Ann. Rep. Prog. Chem.*, **72A**, 67 (1975).
- (2) R.Z. Sagdeev, Yu.N. Molin, K.M. Salikhov, V. Leshina, M.A. Kamha, and S.M. Shein, *Org. Magn. Reson.*, **5**, 603 (1973).
- (3) N.J. Turro and B. Kraeutler *Acc. Chem. Res.* **13**, 369 (1980).
- (4) Y. Sakaguchi and H. Hayashi, *J. Phys. Chem.*, **88**, 1437 (1984).
- (5) M. Okazaki, S. Sakata, R. Konaka, and T. Shiga, *J. Am. Chem. Soc.*, **107**, 7214 (1985).
- (6) M. Okazaki and T. Shiga, *Nature* **323**, 240 (1986).
- (7) M. Okazaki, S. Sakata, R. Konaka, and T. Shiga, *J. Chem. Phys.*, **86**, 6792 (1987).
- (8) M. Okazaki, T. Shiga, S. Sakata, R. Konaka, and K. Toriyama, *J. Phys. Chem.*, **92**, 1402 (1988).
- (9) A.I. Grant, K.A. McLauchlan, and S.R. Nattrass, *Mol. Phys.* **55**, 557 (1985).

Th-5
13:30
~13:50

**Electron Spin Echo Study of Cross Relaxation in Free Radicals
with CIDEP**

P. P. Borbat, A. D. Milov, and Yu. N. Molin

Institute of Chemical Kinetics and Combustion,
630090, Novosibirsk, USSR

The published data on photolysis of acetone in 2-propanol at different temperatures shows that at temperatures below 220K initial EA polarization of acetone ketyl radicals transforms to A*E one at $\sim 10\mu\text{s}$ after laser flash. This behavior has been explained by existence of sufficiently high multiplet nuclear spin polarization in radical which is transformed into electron spin multiplet polarization by cross-relaxation due to scalar mechanism.

We studied CIDEP of *t*-butyl radical which is known to show also unusual CIDEP behavior at times up to $100\mu\text{s}$. Radicals were produced in laser photolysis of di-*t*-butyl ketone solutions in toluene and 2-propanol in wide temperature region. Radical concentration was changed by means of laser flux attenuating and solution diluting. To test if cross-relaxation mechanism is responsible for observed CIDEP behavior we used spin echo technique with extra pumping microwave pulse. This pulse rotates magnetization of detected component on desired angle and then the magnetization evolves prior detection.

In the spin-echo experiments without pumping pulse for 2-propanol at 160K kinetics of magnetization of *t*-butyl radical components corresponding $M_z = \pm 3/2$ cross at $10\mu\text{s}$ thus indicating transformation of EA to A*E polarization.

In toluene close to room temperature we find CIDEP after 90° pumping pulse to originate mainly from F-pairs. At lowering temperature F-pairs contribution as follows from concentration dependence of recovery curves gets smaller thus allowing investigation of cross relaxation effects. At temperature 233K at $50\mu\text{s}$ spectrum appears to be A*E but at some lower temperatures, at any case below 170K spectrum appears as EA* up to $150\mu\text{s}$. Experiments with pumping pulse strongly

support existence of considerable cross-relaxation feature below 170K in toluene and below 220K in 2-propanol.

Th-7
15:00
~15:20

CIDEP Studies on the Photoinduced Electron
Transfer Reactions from Metalloporphyrins
to Quinone

Seigo Yamauchi, Toru Ueda, Minoru Satoh, Kimio
Akiyama, Shozo Tero-Kubota, Yusaku Ikegami and
Masamoto Iwaizumi

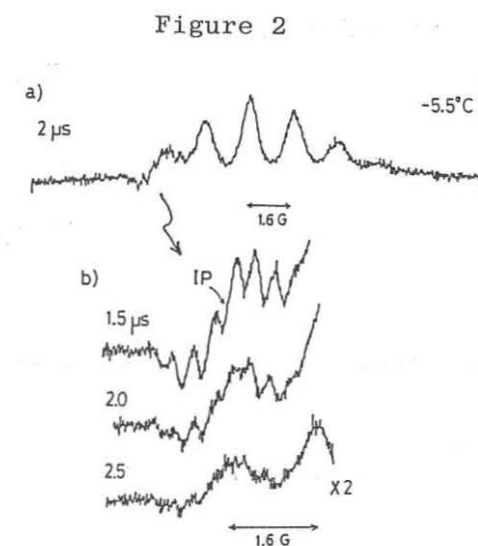
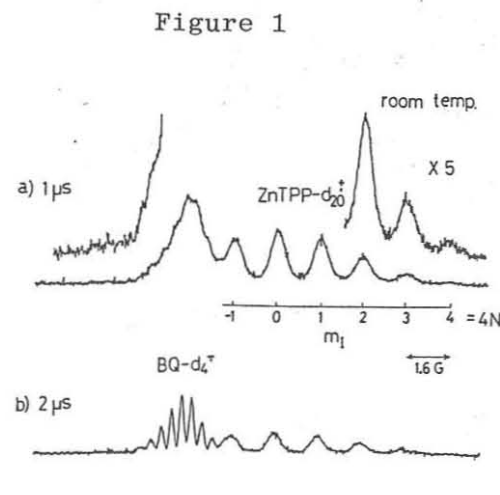
Institute for Chemical Reaction Science,
Tohoku University, Sendai 980, Japan.

The photoinduced electron transfer reactions in the systems of Zn and Mg tetraphenylporphyrins (TPP) and 1,4-benzoquinone (BQ) were investigated by means of a time-resolved EPR (TREPR) technique and deuteration of the compounds. Three kinds of reaction intermediates, the porphyrin cation, the quinone anion and their ion pair were definitely assigned with the EPR parameters. By observing these three species we examine effects of a solvent, a salt and an axial ligand on the reaction. We also investigate an effect of a central metal by comparing the results of the systems of ZnTPP-BQ and MgTPP-BQ.

TPP-d₂₀ was synthesized originally from toluene-d₈. BQ-d₄ was synthesized from phenol-d₆. The typical concentrations of the deaerated samples are 1 x 10⁻⁴M for ZnTPP and MgTPP, 1 x 10⁻²M for BQ, 0.1M for the salt, and 1~2M for the axial ligand in alcohol solutions. The S₁ states of metalloporphyrins were excited by using an excimer laser (Lumonics HE-420) pumped dye laser (Lumonics Hyper Dye 300) at 585 or 561nm. Transient EPR signals were detected with a boxcar integrator (NF EX531). Detailed descriptions of the TREPR system were reported previously [1].

The CIDEP spectra observed at room temperature in 2-butanol (BuOH) are shown in Figure 1. The nine peaks (g = 2.0025 and a_N = 1.60G) observed at 1μs after the laser pulse are definitely assigned to those of ZnTPP-d₂₀⁺. Another set of nine peaks (g = 2.0040, a_D = 0.36G) at 2μs is assigned to that of BQ-d₄⁻. The polarization of the spectra shows an absorption (A) of the microwave and is dominated by the triplet mechanism (TM). At -5.5°C the contribution of the radical pair mechanism (RPM) appears and the peak of the ion pair is observed as shown in Figure 2. From an analysis of the splitting of the E and A peaks the ion pair is assigned to the solvent separated ion pair (SSIP) [2]. The contact ion pair (CIP) is not observed by TREPR.

The peak of the pair decays faster (<0.5μs) than those (2~5μs) of the isolated ions. The decay rate of the deuterated ion pair is very similar to that of the hydrated ion pair (ZnTPP⁺...BQ⁻). This fact indicates that the decay of the ion pair is not mostly controlled by a spin-lattice relaxation process but by a dynamics of the pair [3].



TREPR Spectra of ZnTPP-d₂₀⁺-BQ-d₄⁻ in BuOH

Th-8

16:00

~16:30

ELECTRON SPIN POLARIZATION IN PHOTOSYNTHETIC BACTERIA

P. J. Hore, D. A. Hunter, D. J. Riley and J. J. Semlyen

Physical Chemistry Laboratory, Oxford University, United Kingdom

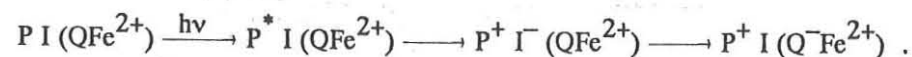
F. G. H. van Wijk and T. J. Schaafsma

Department of Molecular Physics, Wageningen Agricultural University, The Netherlands

P. Gast and A. J. Hoff

Department of Biophysics, University of Leiden, The Netherlands

The primary steps of bacterial photosynthesis take place in a pigment-protein complex known as the reaction centre, and may be summarized as follows:



The photo-excited electronic singlet state (P^*) of the primary donor (a bacteriochlorophyll dimer) undergoes rapid electron transfer (~ 3 ps) to the primary acceptor I (a bacteriopheophytin) which in turn transfers an electron (in about 200 ps) to the secondary acceptor, an iron-quinone complex (QFe^{2+}).

In pre-reduced (i.e. $Q \longrightarrow Q^-$) reaction centres, electron transfer to (QFe^{2+}) is blocked, and different decay channels for the primary radical pair [P^+I^-] become possible, Fig. 1. Formed from P^* in a spin-correlated singlet configuration, $^1[P^+I^-]$ can undergo charge recombination to give the primary donor in its ground (P) or excited singlet (P^*) state. At the same time, $^1[P^+I^-]$ is converted coherently by Zeeman, hyperfine, exchange and dipolar interactions into the triplet radical pair, $^3[P^+I^-]$, which may collapse with conservation of spin angular momentum, to give 3P , an excited triplet state of the primary donor, which in turn reverts slowly ($\sim 100 \mu s$) to P.

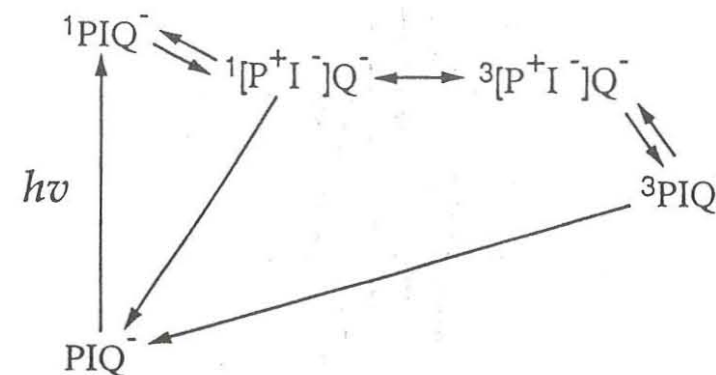


Fig. 1 Reaction scheme for pre-reduced photosynthetic reaction centres.

The presence of a third electron spin (Q^-), affects the singlet-triplet interconversion of the primary radical pair, by facilitating both ST_{+1} and ST_{-1} mixing in addition to the usual ST_0 process. When coupled with the anisotropy of the magnetic interactions in the reaction centre, this leads to some interesting electron spin polarization (ESP) behaviour. ESP can be observed in pre-reduced reaction centres for both 3P and, if the Fe^{2+} -quinone complex is disrupted, in the semiquinone Q^- (see Refs 1 and 2 for reviews). Both cases will be discussed.

The appearance of the EPR spectrum of 3P is dominated by the anisotropic zero-field splitting, Fig. 2A. Under conditions of continuous illumination at low temperature, a polarized spectrum is observed, Fig. 2B with a AEEAAE pattern. This observation is easily understood within the framework of the ST_0 radical pair mechanism, which populates only the central triplet sub-level. Thus the $|-1\rangle \leftarrow |0\rangle$ transitions are absorptively polarized while the $|0\rangle \rightarrow |+1\rangle$ transitions are emissive. However at temperatures above about 20 K, the spectrum for *Rhodospseudomonas viridis* changes to AEAEAE, Fig. 2C. That is, the polarization of the Y peaks is inverted implying that for certain orientations of the magnetic field with respect to the zero-field splitting tensor, the $|+1\rangle$ and $|-1\rangle$ states of 3P are more heavily populated than is $|0\rangle$. This anisotropic polarization is only seen when the (Q^-Fe^{2+}) complex is intact and when there is a large exchange interaction between I^- and Q^- . It will be shown that this behaviour may be understood by considering rapid spin-lattice relaxation of the iron-quinone complex together with the anisotropy of the EPR frequency of (Q^-Fe^{2+}) [3].

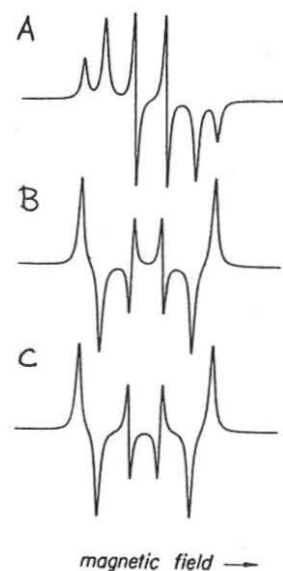


Fig. 2 Schematic, first derivative, EPR spectra of the donor triplet state, 3P , in *Rps. viridis*. (A) Unpolarized spectrum. (B) Low temperature polarized spectrum. (C) High temperature polarized spectrum.

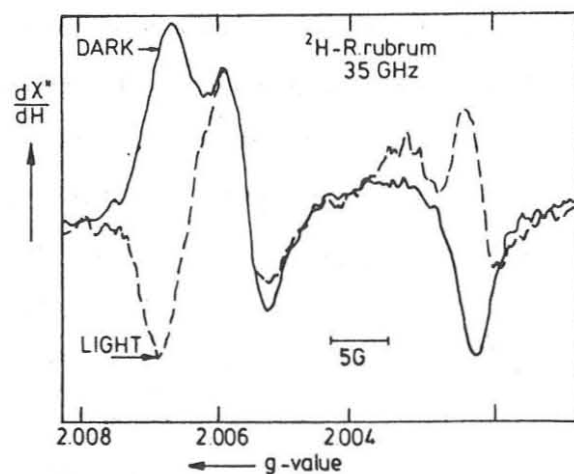


Fig. 3 Light and dark, first derivative, 35 GHz EPR spectra of Q^- in pre-reduced, perdeuterated cells of *Rhodospirillum rubrum* at 80 K. [Adapted from Ref. 5]

The EPR pattern of Q^- in reaction centres which lack the iron-semiquinone coupling also show anisotropic polarization, Fig. 3. Emission is observed for $g \approx g_{xx}$ and $g \approx g_{zz}$ while for $g \approx g_{yy}$ very little polarization is found. It will be shown that this observation can be rationalized by considering the anisotropy of the dipolar coupling of I^- with Q^- , which is the interaction principally responsible for singlet-triplet interconversion in the primary radical pair [4].

References

- [1] A. J. Hoff, *Q. Rev. Biophys.*, 17 (1984) 153.
- [2] P. J. Hore in A. J. Hoff (ed.), *Advanced EPR. Applications in Biology and Biochemistry*, Elsevier, Amsterdam, 1989, p. 405.
- [3] P. J. Hore, D. A. Hunter, F. G. H. van Wijk, T. J. Schaafsma and A. J. Hoff, *Biochim. Biophys. Acta*, 936 (1988) 249.
- [4] P. J. Hore, D. J. Riley, J. J. Semlyen, and A. J. Hoff, *Biochim. Biophys. Acta*, submitted.
- [5] P. Gast, A. de Groot and A. J. Hoff, *Biochim. Biophys. Acta*, 723 (1983) 52.

2F

Hotel New Oji
Second Floor

Wakakusa
Oral Presentation
Poster Session

Lobby
Coffee Break

Botan
Banquet

(中美会場)
桔梗の間

WC-WC

Cloak

Escalator

エレベーター

菊の間

Aoi
Reception

蘭の間

藤の間

300 : 1

Hotel New Oji
Omotemachi 2-1-30, Tomakomai,
Hokkaido 053, Japan
TEL 0144-33-6121
FAX 0144-36-6502

Th-9
16:45
~17:15

The Role of Spin Chemistry in the Primary Events of
Photosynthesis*

Gerd Kothe and Stefan Weber

Institut für Physikalische Chemie, Universität

Stuttgart, D-7000 Stuttgart 80, Germany

James R. Norris**, Seth S. Snyder, Jau Tang and

Marion C. Thurnauer

Chemistry Division, Argonne National Laboratory,

Argonne, Illinois, 60439

Andrea L. Morris, Richard R. Rustandi and Zhiyu Wang

**Department of Chemistry, The University of

Chicago, Chicago, Illinois, 60637

The primary electron transfer process in many natural and artificial photosynthetic systems proceeds via a radical pair mechanism. We have developed theoretical treatments and have performed various transient experiments such as RYDMR (reaction yield detected magnetic resonance) [1] and FT-CIDEP (Fourier transform-chemically induced dynamic electron spin polarization) [2] to understand the role that spin chemistry may play in photosynthesis. In addition, understanding the mechanism and the dynamics

* This work was supported by the U.S. Department of Energy, Office of Basic Energy Sciences, Division of Chemical Sciences under contract W-31-109-Eng-38.

for the unpaired electron spin system permits the characterization of the structure and function of natural and artificial photoreaction centers.

Previously, we presented a general description of electron spin polarization for interacting radical pairs and formulated a simple vector model as an aid to visualizing CIDEP [3]. In this current paper, we have extended our vector model to include the Redfield density matrix formalism in order to accommodate explicitly the processes of sequential electron transfer, relaxation and coherence. Even with the additional complications of relaxation and coherence, visualizing CIDEP with a vector diagram is straightforward. Such visualization is often crucial for planning and interpreting new experiments.

The formal calculations [4] will be illustrated using radical pairs occurring in photosynthetic reaction centers, including oscillations attributable to coherent spin dynamics. Quantum beats, as shown in Figure 1, have been observed as predicted for radical pairs in fully deuterated algae using ultrahigh time resolution CW EPR [4,5]. Time domain simulations provide information on T_1 , T_2 , and the lifetime of the radical pair.

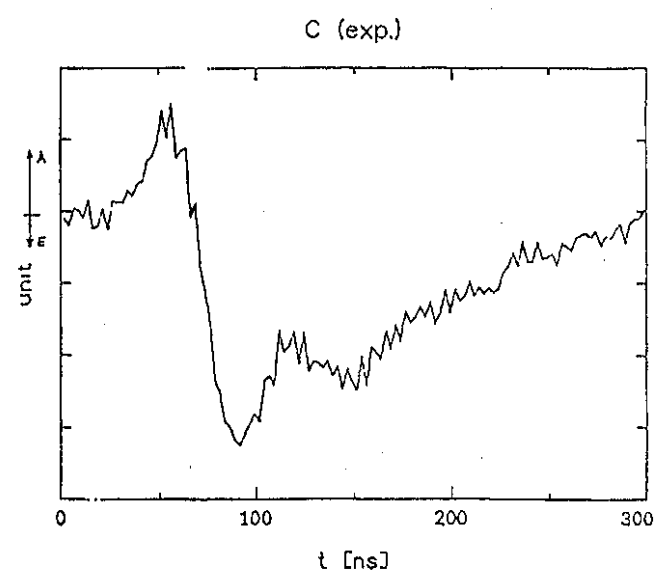


Figure 1. Time domain profiles observed using a 600 ps nitrogen laser (1.6mJ pulse energy) for excitation of a sample of fully deuterated (99.7%) whole cells of *Synechococcus lividus* at room temperature.

References

- [1] J. R. Norris, M. K. Bowman, D. E. Budil, J. Tang, C. A. Wraight and G. L. Closs, Proc. Natl. Acad. Sci., 79 (1982) 5532.
- [2] K. Hasharoni, H. Levanon, J. Tang, M. K. Bowman, J. R. Norris, D. Gust, T. A. Moore and A. L. Moore, J. Am. Chem. Soc., 112 (1990) 6477.
- [3] J. R. Norris, A. L. Morris, M. C. Thurnauer and J. Tang, J. Chem. Phys., 92 (1990) 4239.
- [4] R. Bittl and G. Kothe, Chem. Phys. Lett., 177 (1991) 547.
- [5] K. M. Salikhov, C. H. Bock and D. Stehlik, Appl. Magn. Reson., 1 (1990) 195.

Tu-2
10:00
~10:30

Quantum Beating of EPR Line Intensity of Spin
Correlated Radical Pairs

Kev M. Salikhov

Zavoisky Physical-Technical Institute
of the USSR Academy of Sciences, Kazan,
USSR

In photosynthetic reaction center ion-radical pairs start out in a singlet state, that is in correlated spin pair configuration. Two electron systems can be characterized by dipolar (linear in spin operators) and quadrupolar (bilinear in spin operators) ordering of spins. Spin-correlated radical pairs initially have non-zero quadrupolar ordering and zero dipolar ordering. But dipolar order is exactly what can be observed directly in EPR experiment. Spin evolution transforms initial quadrupolar ordering to observable. It happens that observable has to show quantum beats under circumstances outlined. In fact a zero quantum coherence which initially exists in radical pairs is transferred into one-quantum coherence detected in EPR experiments. This process reveals itself as beatings of EPR line intensities during time resolved continuous wave experiments and electron spin echo signals.

References

/I/ K.M.Salikhov, C.H.Bock, D.Stehlik, Appl.Magn.Res.,
I (1990) I95.

Th-3

10:30

~10:50

Pulsed ESR Study on Electron Spin Relaxation of Free Radical Intermediates in Photoreduction

Hidetada Tokioka, Naruhiko Sone, Hisao Murai, and

Keiji Kuwata

Department of Chemistry, Faculty of Science, Osaka University, Toyonaka, Osaka, 560 Japan

Electron spin relaxation times of free radical intermediates in photoreduction were investigated in relation to CIDEP spectra.

The hyperfine structure (hfs) of CIDEP spectrum for the negative ion of 2,6-di-tert-butyl p-benzoquinone (2,6-DBQ) in the mixture of 2-propanol and triethylamine was composed of three emissive lines with intensity ratio of nearly 1 : 3 : 1. The ratio changed from 1 : 3.2 : 1 to 1 : 2.5 : 1 as the concentration of quinone decreased from 0.05 to 0.005 mol dm⁻³ as shown in Figure 1.

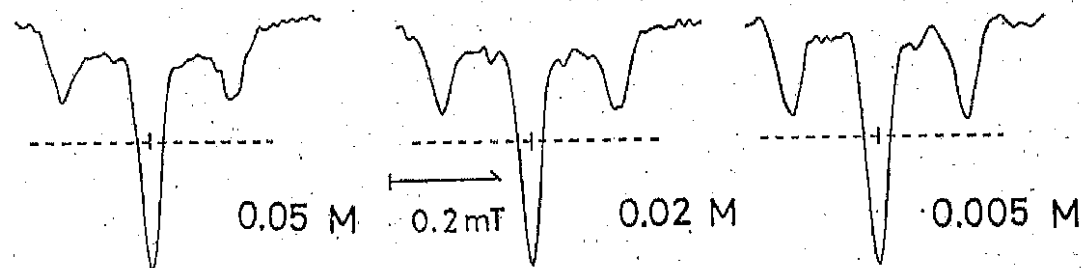


Figure 1. CIDEP spectra of negative ion of 2,6-DBQ

The spin-spin relaxation time T_2 of the negative ion in the system of electron transfer between the negative ion and the neutral molecule is dependent on the concentration of the neutral molecule. The effective spin-spin relaxation time T_{2i} for i -th line is given by ¹⁾

$$T_{2i}^{-1} = T_2^{-1} + (1 - D_i/E D_i) \tau^{-1} \quad (1)$$

where D_i is the degeneracy of i -th line and τ is the life time of electron transfer. The life time τ is given by the bimolecular rate constant k_{tr}

$$\tau^{-1} = k_{tr} [Q], \quad Q^- + Q \xrightarrow{k_{tr}} Q + Q^- \quad (2)$$

where $[Q]$ is the concentration of quinone. Then T_{2i} is given by

$$T_{2i}^{-1} = T_2^{-1} + (1 - D_i/E D_i) k_{tr} [Q], \quad (3)$$

where $k_{tr} [Q]$ replaces τ^{-1} .

The values of T_{2i} for the $M_I = 0$ line at the different concentrations of quinone were determined by the observation of free induction decay (FID) of the line using a pulsed ESR spectrometer for laser photolysis. The values obtained are listed in Table 1.

Table 1. Values of T_{2i}

$[Q] / \text{mol dm}^{-3}$	T_{2i} / ns
5×10^{-3}	330 ± 20
2×10^{-2}	280 ± 20
5×10^{-2}	170 ± 20

According to Eq. (3) T_{2i} was plotted vs. $[Q]$ as shown in Figure 2.

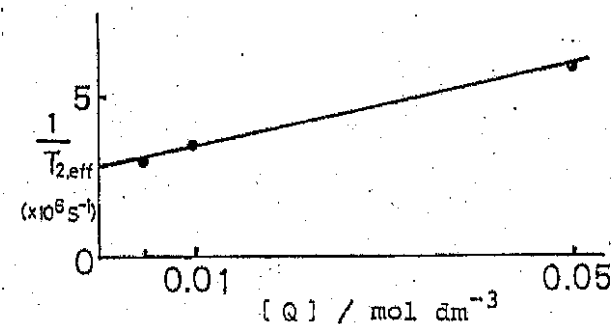


Figure 2. Plot of T_{2i} vs. $[Q]$

From the intercept and slope of the plot T_2 and k_{tr} were evaluated to be 340 ns and $6 \times 10^7 \text{ mol}^{-1} \text{ dm}^3 \text{ s}^{-1}$, respectively.

At the concentration of $5 \times 10^{-3} \text{ mol dm}^{-3}$, T_{2i} is close to T_2 and this fact shows minor contribution of electron transfer to T_{2i} . The difference between the intensity ratio of 1 : 2.5 : 1 at this concentration and the ultimate ratio of 1 : 2 : 1 shows that the contribution of electron transfer yet remained to small

extent or some other origin of this difference may exist.

As shown in Figure 3 the time profile of the decay of CIDEP was also dependent on the concentration of quinone.

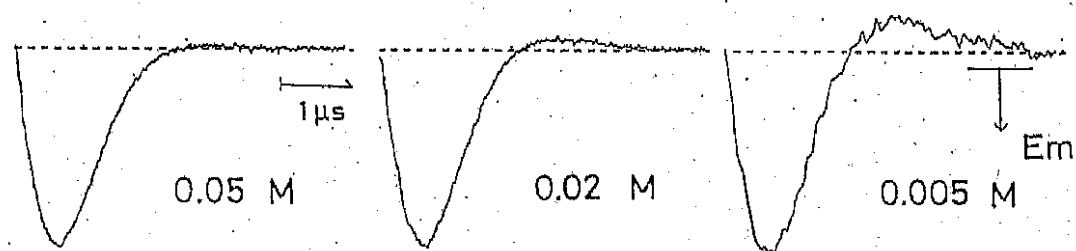


Figure 3. Time profile of decay of CIDEP

At low concentration the Torrey oscillation appeared due to the decrease in T_{2i} ²⁾. The decays of CIDEP were reproduced by the calculation using the modified Bloch equations³⁾ as shown in Figure 4.

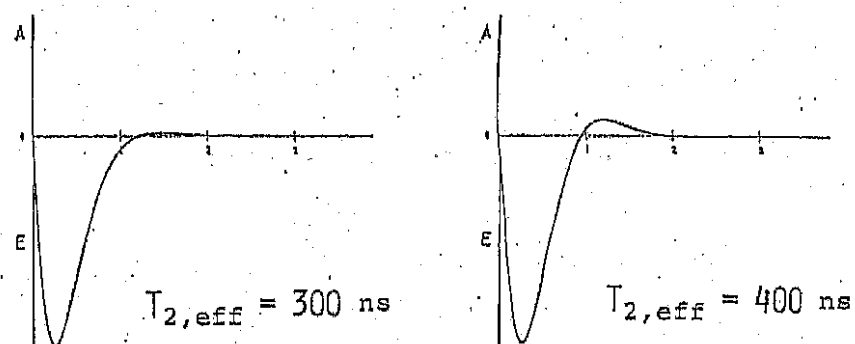


Figure 4. Time profile of decay of CIDEP (calculated)

The Heisenberg spin exchange between the negative ions is an origin of the change in T_{2i} . Thus, T_{2i} is dependent on the concentration of the negative ion⁴⁾. The concentration of the negative ion is probably determined by the intensity of the laser light provided the complete absorption of the laser light by the sample solution. To decrease the concentration of the negative ion the laser light was weakened to 40 % by inserting a mesh in the light path, however, no change in the time profile was found. The result shows the absence of the contribution of spin exchange to T_{2i} .

In the photolysis of other quinones and carbonyl compounds T_{2i} of the free

radical intermediates including alcohol radicals were similar to that of 2,6-DBQ and much smaller than the effective spin-lattice relaxation time $T_{1,eff}$. In the case of photolysis spatial distribution of free radical intermediates may be not uniform as compared to the solution of the negative ions prepared chemically. The effect of spatial distribution on T_{2i} , however, was found to be much small as was shown in the experiment to check the effect of light intensity on the CIDEP spectrum.

References

- [1] P.J.Hore and K.A.McLauchlan, *Mol.Phys.*, 42 (1981) 1009.
- [2] P.J.Hore and K.A.McLauchlan, *J.Magn.Reson.*, 36 (1979) 129.
- [3] R.W.Fessenden, *J.Chem.Phys.*, 58 (1973) 2489; J.B.Pedersen, *ibid.*, 59 (1973) 2656.
- [4] J.H.Freed, *J.Phys.Chem.*, 71 (1967) 38.

Magnetic Field Effects on Dynamic Behavior
of Excited Molecules - Studies in Japan

S. NAGAKURA

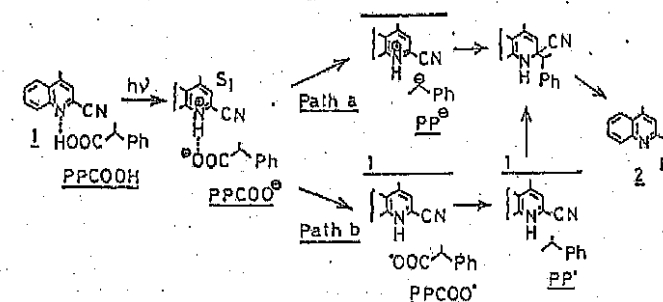
Graduate University for Advanced Studies

During recent 17 years, magnetic field effects (MFE) on dynamic behavior of excited molecules have been extensively studied in Japan. Studies made hitherto in Japan are mainly concerned with MFE on various kinds of photochemical reactions in solutions and MFE on photophysical and photochemical phenomena in the gaseous state.

The main studies made hitherto in Japan on MFE on photochemical reactions in solutions are listed in Table 1. The studies in Japan started in 1976 when MFE on photodecomposition of dibenzoyl peroxide in toluene and also on photoisomerization of isoquinoline N-oxide in ethanol were studied by Tanimoto et al. and by Hata, respectively. From the theoretical and experimental consideration of magnetic dependence of quenching, the former reaction was found to be due to the Δg mechanism, namely the singlet-triplet mixing of a radical pair caused by the difference in the g value between two component radicals. The photoisomerization of isoquinoline N-oxide in ethanol shows a characteristic magnetic field dependence that the magnetic quenching sharply occurs at ~ 1 T. This is due to the combination of the hyperfine coupling and level crossing caused by the Zeeman shift ($hfc-J$).

Quite recently Hata studied MFE on the photochemical reaction of 4-methyl-2-quinolinecarbonitrile with (S)-or(R)-2-phenylpropionic acid in benzene and found that magnetic fields increase the reaction yield (hfc mechanism) for the case of reaction with the (R) acid, while no effect for the case of reaction with the (S) acid. This strongly supports that the former reaction proceeds through a radical-pair

and the latter through an ion-pair.



Hata found that the product of the reaction with (S)-acid in the presence of $H \sim 0.04$ T is optically active. To my knowledge this is the first observation of magnetically induced asymmetric synthesis and may be a new type of MFE on photochemical reactions which cannot be interpreted in terms of the radical pair model. It is desirable to elucidate the mechanism of this reaction.

At the beginning of 1970's MFE studies on photochemical reactions in solutions were hidden in a veil of secret. They are now almost systematically interpreted in terms of the radical-pair theory considering the singlet-triplet mixing due to the hfc , electronic Zeeman interaction, level crossing, and relaxation mechanism. It may be essential for the future development of this field to find such new phenomena as magnetically induced asymmetric synthesis found by Hata, MFE on photochromic reactions and photocatalytic reactions, MFE on biological phenomena and others.

Let us turn to MFE on dynamic behavior of gaseous excited molecules. Since 1974 when fluorescence from the 1A_2 state of CS_2 was found to be magnetically quenched, MFE on emission from nonmagnetic excited singlet state has been extensively studied from both theoretical and experimental points of view. Works on this subject made in Japan are listed in Table 2. From the results shown in this table, MFE on fluorescence and photochemical reactions in the gaseous state can be classified as shown in Tables 3 and 4.

Table 1

Magnetic Field Effects on Photochemical Reactions
in Solution ----- Main Works in Japan

Subject	Author and Reference*	Remark
photodecomposition of dibenzoyl peroxide	Tanimoto, Hayashi, Nagakura, Sakuragi, Tokumaru; CPL 41(1976)267. Sakaguchi, Hayashi, Nagakura, BCSJ 53(1980)39	Δg classification
photoisomerization of isoquinoline N-Oxides	Hata; CL (1976)547, BCSJ 58(1985)1088. BCSJ 59(1986)2723.	hfc-J
general theory	Itoh, Hayashi, Nagakura; MP 17(1969)561. Hayashi, Nagakura; BCSJ 51(1978)2862.	Hamiltonian reaction yield (Δg , hfc, mixed).
photosubstitution of quinolinecarbonitriles	Hata, Yamada; CL (1980)989. Hata, Hokawa; CL (1981)507. Hata, Nishida; BCSJ (1985)3423.	Δg , hfc-J.

* CPL, Chem. Phys. Lett. BCSJ, Bull. Chem. Soc. Japan.
CL, Chem. Lett. MP, Mol. Phys.

Table 1 (continued)

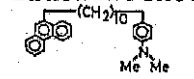
Subject	Author and Reference	Remark
photodecomposition of sulfur and phosphorus compounds	Hayashi, Sakaguchi, Tsunooka, Yanagi, Tanaka, CPL 136(1987)436. Hayashi, Sakaguchi, Kamachi, Schnabel, JPC 91(1987)3936. Hiramatsu, Nakagaki, Tanimoto, Mutai, Tukada, Nagakura, CPL 142(1987)413.	53% increase (1.2T) in the SO_2Ph yield. 8~9% decrease in the cage product yield (0.64T).
photoisomerization of olefin	Sakuragi, Nakagaki, Oguchi, Arai, Tokumaru, Nagakura, CPL 135(1987)325.	through ion radical pair.
photochemistry of bichromophonic chain compounds	Tanimoto, Okada, Itoh, Iwai, Sugioka, Takemura, Nakagaki, Nagakura, CPL 136(1987)42; JPC 93(1989)3586. Tanimoto, Takashima, Hasegawa, Itoh, CPL 137(1987)330. Nakagaki, Hiramatsu, Mutai, Tanimoto, Nagakura, CPL 134(1987)171. Nakagaki, Mutai, Nagakura, CPL 154(1989)581; 167(1990)439.	exciplex fluorescence  hydrogen abstraction. oxidation and reduction. switching of reaction path.

Table 1 (continued)

Subject	Author and Reference	Remark
Photo-Fries rearrangement of 1-naphthyl acetate	Nakagaki, Hiramatsu, Watanabe, Tanimoto, Nagakura; JPC 89(1985)3222.	hfc isotope effect.
photoinduced electron transfer	Tanimoto, Watanabe, Nakagaki, Hiramatsu, Nagakura; CPL 116(1985)341. Tanimoto, Takayama, Itoh, Nakagaki, Nagakura; CPL 139(1986)414. Nakamura, Uehata, Motonaga, Ogata, Matsuo; CL (1987)543. Uehata, Nakamura, Usui, Matsuo; JPC 93(1989)8197. Yonemura, Nakamura, Matsuo; CPL 155(1989)157.	TMPD in 2-propanol, 15% photocurrent increase 1-acetonaphthone and dipyeylamine in micelle. porphyrin-viologen, radical-pair decay rate reduced. phenothiazine-viologen-cyclodextrin.
photocrosslinking of polystyrene	Morita, Higayama, Yamaoka; CL (1986)963.	35% increase, hfc.
magnetically induced asymmetric synthesis	Hata; CL (1991)155.	

Table 1 (continued)

Subject	Author and Reference*	Remark
photoreduction of carbonyl compounds	Sakaguchi, Nagakura, Hayashi; CPL 72(1980)420. Sakaguchi, Hayashi, Nagakura; JPC 86(1982)3177. Tanimoto, Udagawa, Itoh; JPC 87(1983)724. Hayashi, Nagakura; BCSJ 57 (1984)322. Sakaguchi, Hayashi, Murai, Ihaya; CPL 110(1984)275.	benyophenone in micelle. isotope effect. T ₁ -S crossing. relaxation (theoretical). relaxation (CIDEP).
effect of paramagnetic (lanthanoid ions and copper complex)	Sakaguchi, Haysahi; CPL 106(1984)420. Tanimoto, Kita, Itoh, Okazaki, Nakagaki, Nagakura; CPL 165(1990)184.	enhance triplet radical pair recombination and biradical decay.
electrolytic oxidation and reduction	Watanabe, Tanimoto, Sakata, Nakagaki, Hiramatsu, Magalira; BCSJ 58(1987)1251. Watanabe, Tanimoto, Nakagaki, Hiramatsu, Nagakura; BCSJ 60(1987)4166.	reduction and oxidation of Fe ion. oxidation of phenylacetate ion.

*JPC, J. Phys. Chem.

Table 2

Magnetic Field Effects on Dynamic Behavior of
Gaseous Excited Molecules ---- Main Works in Japan

Subject	Author and Reference*	Remark
magnetic field effect (MFE) on fluorescence of gaseous CS ₂	Matsuzaki, Nagakura; CL (1974)675;BCSJ49(1976)359. HCA 61(1978)675. Orita, Morita, Nagakura; CPL 81(1981)29; 33. Imamura, Tamai, Fukuda, Yamazaki, Nagakura, Abe, Hayashi; CPL 135(1987)208. Ochi, Watanabe, Tsuchiya; CP 113(1987)271. Imamura, Nagakura, Abe, Fukuda, Hayashi; JPC 93(1989)69. Abe, Hayashi, Imamura, Nagakura; CP 137(1989)297.	fluorescence from ¹ A ₂ theoretical obs. of the fast component in p region magnetic quantum beat absorption and excitation spectra in N ₂ laser region fluorescence from ¹ B ₂ mechanism
MFE on fluorescence of gaseous glyoxal and methyl derivatives	Matsuzaki, Nagakura; CPL 37(1976)204. Hashimoto, Nagakura, Nakamura, Iwata; CPL 74(1980)228. Nakamura, Hashimoto, Nagakura; J. Luminescence 24/25(1981)763.	glyoxal methylglyoxal glyoxal, excitation energy dependence
MFE on fluorescence of gaseous D ₂ CO	Orita, Morita, Nagakura; CPL 81(1981)409; 86(1982)123.	collision induced magnetic quenching.

*HCA, Helv. Chim. Acta. CP, Chem. Phys.

Table 2 (continued)

Subject	Author and Reference*	Remark
MFE on emission intensity on OH in flames	Hayashi; CPL 87(1982)113.	10% increase (1.5T).
MFE on emission of radicals in flames	Wakayama, Ogasawara, Hayashi; CPL 105(1984)209. Wakayama, Ogasawara, Nishikawa, Ohyagi, Hayashi; CPL 107(1984)207. Fukuda, Abe, Hayashi, Imamura, Nagakura; CL (1986)777.	Na D line, intensity increase (3 times). HPO, SnH, intensity decrease. CH, intensity decrease by 5% (1.8T).
MFE on the D ₁ →a ³ Σ ⁺ emission and photodissociation of NaK	Katô; JCP 80(1984)3936.	intensity increase of Na D ₂ line.
population of sublevels at photodissociation	Katô; Faraday Discuss. 82(1986)1.	Na from NaK, Rb from Rb ₂ .
MFE on dynamics of CA ₂ excited to d ³ Π _u	Katô, Yokoyama, Baba, Tamai, Yamazaki, Nagakura; JCP 87(1987)1987.	emission intensity decrease, magnetic predissociation.
MFE on I ₂ emission	Baba, Kimura, Tsuboi, Katô, Nagakura; BCSJ 62(1989)17.	intensity decrease, magnetic predissociation.
MFE on dynamics of CA ₂ excited to C ¹ Π _u	Baba, Nakahori, Iida, Katô; JCP 93(1990)4637.	predissociation increase.
MFE on dynamics of CA ₂ excited to D ¹ Σ _u ⁺	Katô, Kobayashi, Chosa, Nakahori, Iida, Kasahara, Baba; JCP 94(1991)2600.	magnetic quenching, indirect magnetic predissociation.

*JCP, J. Chem. Phys.

Table 2 (continued)

Subject	Author and Reference	Remark
Zeeman quantum beat spectroscopy	Watanabe, Tsuchiya, Koda; JCP 82(1985)5310. Ochi, Tsuchiya; CPL 140(1987)20.	SO ₂ acetylene
MFE on the intensity of N+O afterglow.	Fukuda, Hayashi, Nagakura; CPL 119(1985)480. Sumitani, Abe, Nagakura; JCP 94(1991)1923.	NO β -band intensity decrease for $=0$ mixing of β^2 and a^4
MFE on the fluorescence polarization of pyrimidine	Ohta, Fujita, Baba; CPL 135(1987)330.	magnetic quantum beat.
MFE on fluorescence of pyrimidine	Ohta, Takemura, Fujita, Baba; JCP 88(1988)4197.	intensity decrease, spin decoupling.
MFE on fluorescence of pyrimidine-d ₄	Ohta; CPL 151(1988)93.	fluorescence enhancement, quantum beat frequency decrease.
MFE on fluorescence of Δ -triazine	Ohta, Takemura; JCP 93(1990)877.	spin decoupling.

Table 3

Magnetic Quenching of Fluorescence of Gaseous Molecules

- (1) Direct Mechanism ---- Electronic Zeeman Interaction of a Prepared Excited State with Quasi-Continuum States (Higher Rotation-Vibration Levels of the Ground State):
CS₂(¹A₂) under high magnetic fields.
Strong interaction between the Renner-Teller coupled rovibronic states:
CS₂(¹A₂)--CS₂(¹B₂)
Y. Fujimura, H. Hayashi and S. Nagakura, Chem. Phys., to be published.
- (2) Spin Decoupling:
pyrazine, pyrimidine, Δ -triazine,
CS₂ under low magnetic fields.
- (3) Magnetically Induced Predissociation:
(a) direct interaction with a repulsive state,
C₄H₂(C¹ π u);
(b) interaction with a repulsive state via intermediates,
C₄H₂(D¹ Σ u).
- (4) Collision Induced Magnetic Quenching:
D₂CO, glyoxal.
- (5) MFE on Excited State Formation Processes:
C₂, HPO, SnH, CN, CH.

Table 4

Magnetic Enhancement of Fluorescence

- (1) Magnetic Enhancement of Mixing through Rotational Perturbation:

CN(B-X 0-0) band, magnetically enhanced by mixing
of (B v'=0) with (A v'=10);

H. E. Badford and H. P. Broida, J. Chem. Phys., 38(1963)644.

- (2) Cancellation of Strong Hyperfine Interaction by an External
Magnetic Field:

Pyrimidine-d₄, S₀ ← S₁ fluorescence

- (3) Magnetic Enhancement of Excited State Formation Processes:

Fluorescence from NO (B²Π v'=2),

